DESIGN, SYNTHESES AND ANTI-MULTIDRUG RESISTANT BACTERIA ANALYSES OF DERIVED LUGDUNIN CYCLIC PEPTIDE

BY

MR. PAKONSIRI SONTISIRI

A THESIS SUBMITTED IN PARTIAL FULFILLMENT OF THE REQUIREMENTS FOR THE DEGREE OF
MASTER OF SCIENCE (CHEMISTRY)
DEPARTMENT OF CHEMISTRY
FACULTY OF SCIENCE AND TECHNOLOGY
THAMMASAT UNIVERSITY
ACADEMIC YEAR 2019

DESIGN, SYNTHESES AND ANTI-MULTIDRUG RESISTANT BACTERIA ANALYSES OF DERIVED LUGDUNIN CYCLIC PEPTIDE

BY

MR. PAKONSIRI SONTISIRI

A THESIS SUBMITTED IN PARTIAL FULFILLMENT OF THE REQUIREMENTS FOR THE DEGREE OF
MASTER OF SCIENCE (CHEMISTRY)
DEPARTMENT OF CHEMISTRY
FACULTY OF SCIENCE AND TECHNOLOGY
THAMMASAT UNIVERSITY
ACADEMIC YEAR 2019

THAMMASAT UNIVERSITY
FACULTY OF SCIENCE AND TECHNOLOGY

THESIS

BY

MR. PAKONSIRI SONTISIRI

ENTITLED

DESIGN, SYNTHESES AND ANTI-MULTIDRUG RESISTANT BACTERIA ANALYSES OF DERIVED LUGDUNIN CYCLIC PEPTIDE

was approved as partial fulfillment of the requirements for the degree of master of science (chemistry)

on October 21st, 2019

Chairman _____
(Jiraporn Arunpanichlert, Ph.D.)

Member and Advisor _____
(Assistant Professor Panumart Thongyoo, Ph.D.)

Member _____
(Peerada Yingyuad, Ph.D.)

Dean _____
(Assistant Professor Nuttanont Hongwarittorrn, Ph.D.)

Thesis Title	DESIGN, SYNTHESES AND ANTI-MULTIDRUG RESISTANT BACTERIA ANALYSES OF DERIVED LUGDUNIN CYCLIC PEPTIDE
Author	Mr. Pakonsiri Sontisiri
Degree	Master of Science (Chemistry)
Department/Faculty/University	Chemistry Faculty of Science and Technology Thammasat University
Thesis Advisor	Assistant Professor Panumart Thongyoo, Ph.D.
Academic Year	2019

ABSTRACT

Lugdunin is a novel thiazolidine containing antibiotic, isolated from *Staphylococcus lugdunensis*. Its structure is consisted of six amino acid residues, including a thiazolidine moiety. Lugdunin demonstrated a highly effective antibacterial activity against methicillin-resistant *Staphylococcus aureus* (MRSA). To this work, we designed and successfully synthesized the native and mutant lugdunins that were classified into three important parts; (1) the synthesis of a thiazolidine derivative, (2) an amino acid assembly and (3) a peptide cyclization. A mutant lugdunin was also synthesized by replacing a thiazolidine moiety with cysteine.

Keywords: Lugdunin, Antibiotic, Superbug, Cyclic peptide

ACKNOWLEDGEMENTS

The thesis was carried out at Department of Chemistry, Faculty of Science and Technology, Thammasat University under the supervision of Assistant Professor Dr. Panumart Thongyoo.

Firstly, I would sincerely like to thank my advisor, Assistant Professor Dr. Panumart Thongyoo, Department of Chemistry, Faculty of Science and Technology, Thammasat University for his professional suggestion and very excellent support.

I would like to thank Dr. Peerada Yingyuad, Department of Chemistry, Faculty of Science, Kasetsart University and Dr. Jariya Romsaiyud, Department of Chemistry, Faculty of Science, Ramkhamhaeng University for kindness in an NMR experiment.

I would like to thank Dr. Jiraporn Arunpanichlert, Department of Chemistry, Faculty of Science and Technology, Thammasat University and Dr. Peerada Yingyuad, Department of Chemistry, Faculty of Science, Kasetsart University for suggestions and generous advices.

I would like to thank Department of Chemistry, Faculty of Science and Technology and Center of Scientific Equipment for Advanced Research, Thammasat University for instrumental support.

I would like to thank all members of Medicinal Chemistry Research Unit, Thammasat University for their support and kindness.

This work was supported by National Research Council of Thailand "FY2018 Thesis Grant for master degree student". I would like to thank National Research Council of Thailand "FY2018 Thesis Grant for master degree student" for support.

Finally, I would like to thank my parents for their support, understanding, inspiration, patience, encouragement, and love.

Mr. Pakonsiri Sontisiri

TABLE OF CONTENTS

LIST OF TABLES

LIST OF FIGURES

LIST OF SCHEMES

LIST OF ABBREVIATIONS

Symbols/Abbreviations	Terms
α	Alpha
β	Beta
Abs.	Absorbance
Ac	Acetyl
AOP	(7-azabenzotriazol-1-yloxy)tris(di-methylamino)phosphonium hexafluorophosphate
Arg	Arginine
Boc	*tert*-butyltoxycarbonyl
BOP	(Benzotriazol-1-yloxy)tris(dimethylamino)phosphonium hexafluorophosphate
Bu^t	Tert-butyl
CDI	Carbonyldiimidazole
Cys	Cysteine
DCC	N,N-dicyclohexylcarbodiimide
DCM	Dichloromethane
DIBAL-H	Diisobutylaluminium hydride
DIC	N,N-diisopropylcarbodiimide
DIPEA	N, N-Diisopropylethylamine
DMAP	4-dimethylaminopyridine
DME	dimethylethane
DMF	Dimethylformamide
DMSB	borane-dimethyl sulfide complex
E.coli	*Escherichia coli*
EDC	1-ethyl-3-(3-dimethylaminopropyl) carbodiimide

ee	Enantiomeric excess
Et	ethyl
EtOAc	Ethyl acetate
Fmoc	9-fluorenylmethyloxycarbonyl
FTIR	Fourier-transform infrared spectroscopy
HATU	1-[Bis(dimethylamino)methylene]-1H-1,2,3-triazolo[4,5-b]pyridinium 3-oxide hexafluorophosphate
HBTU	2-(1H-benzotriazol-1-yl)-1,1,3,3-tetramethyluronium hexafluorophosphate
HCTU	O-(1H-6-Chlorobenzotriazole-1-yl)-1,1,3,3-tetramethyluronium hexafluorophosphate
HMPA	Hexamethylphosphorotriamide
HOAt	7-aza-1-hydroxybenzotriazole
HOBt	1-hydroxylbenzotriazole
HOSu	N-hydroxysuccinimide
HPLC	High-performance liquid chromatography
HR-ESI-MS	High-resolution electrospray ionisation mass spectrometry
IBX	2-iodoxybenzoic acid
Leu	Leucine
MALDI-TOF-MS	Matrix-assisted laser desorption/ionization Time-of-flight mass spectrometer
mCPBA	*meta*-Chloroperoxybenzoic acid
Me	methyl
MeCN	acetonitrile
MeOH	Methanol
mg	milligram

MIC	Minimum inhibitory concentration
MRSA	Methicillin-resistant *Staphylococcus aureus*
NMR	Nuclear magnetic resonance
Pbf	2,2,4,6,7-pentamethyldi hydrobenzofuran-5-sulfonyl
Ph	Phenyl
PyBOP	(benzotriazole-1-yloxy)tris(pyrrolidino)phosphonium hexafluorophosphate
PyAOP	(7-azabenzotriazol-1-yloxy)tris(pyrrolidino) phosphoniumhexafluorophosphate
SAR	Structure-activity relationship
SPPS	Solid phase peptide synthesis
TFA	Trifluoroacetic acid
THF	Tetrahydrofuran
TIPS	Triisopropylsilyl
Trp	Tryptophan
Trt	Trityl
UV	Ultraviolet
Val	Valine
VRE	Vancomycin-resistant *enterococci*

CHAPTER 1
INTRODUCTION

1.1 Antibiotic resistance

1.1.1 The history of antibiotic

Antibiotics have been widely known as effective therapeutic agents for the treatment and prevention of bacterial infection for over decades. Penicillin was the first example of antibiotic that was discovered by Sir Alexander Fleming in 1928. Penicillin possessed the ability to treat the bacterial infection (particularly *Staphylococcus* and *Streptococci*) and showed low toxicity to animal cell.[4] However, penicillin resistance was found and became to clinical problem in a few year after the invention. Presently, more than 95% of *Staphylococcus aureus* were resistance to penicillin. Back in the late 1940s to early 1950s, there were a number of discovered antibiotics which were introduced to eradicate the bacteria strain, namely Streptomycin, Chloramphenicol and Tetracycline. They were effective against gram-positive and gram-negative bacteria, intracellular parasites and *Tuberculosis bacillus*. However, the multiple drug resistance was also observed during *Shigella* outbreak in japan in 1953. The Dysentery bacillus stain was isolated, and found to be resistant to Chloramphenicol, Tetracycline, Streptomycin and Sulfanilamide. In order to cope with the bacteria resistance, the new beta-lactam antibiotic classes were discovered, and developed, for example the invention of methicillin, which was discovered in 1960. Unfortunately, the first methicillin resistant *Staphylococcus aureus* case was found in the same decade, in 1962 (in UK) and in 1968 (in US), and also in the late 1980s methicillin resistance *Staphylococcus aureus* became an important problem in many hospitals.[4, 5]

The antibiotic resistant bacteria could be developed to get resistant nearly all developed antibiotics. In 1972, Vancomycin was effectively used for treatment of disease caused by methicillin resistance *Staphylococcus aureus* and coagulase-negative *staphylococci*. However, the Vancomycin resistance cases were

reported in coagulase-negative *staphylococci* in a few years later (1979 and 1983). According to the discovery of penicillin in 1928 to early 1980s, many scientists attempted to explore and to develop a novel antibiotic for saving the human life from the antibiotic resistance problem. In the past 40 years, there have been only four classes of compounds which have been developed as effective antibiotic drugs. Importantly, a number of drug companies have ceased the development of novel antibiotic drugs to the market mainly due to the rapid bacterial resistant problem, and it is not economically worth of spending the budget for research and development with no return. While, the resistance of bacteria has now become the important crises globally, only a few new antibiotic drugs has been developed, and reached to the market. It was found that misconception, discontinuous and excessive uses of antibiotic drugs caused the bacterial resistance in human.[4-6]

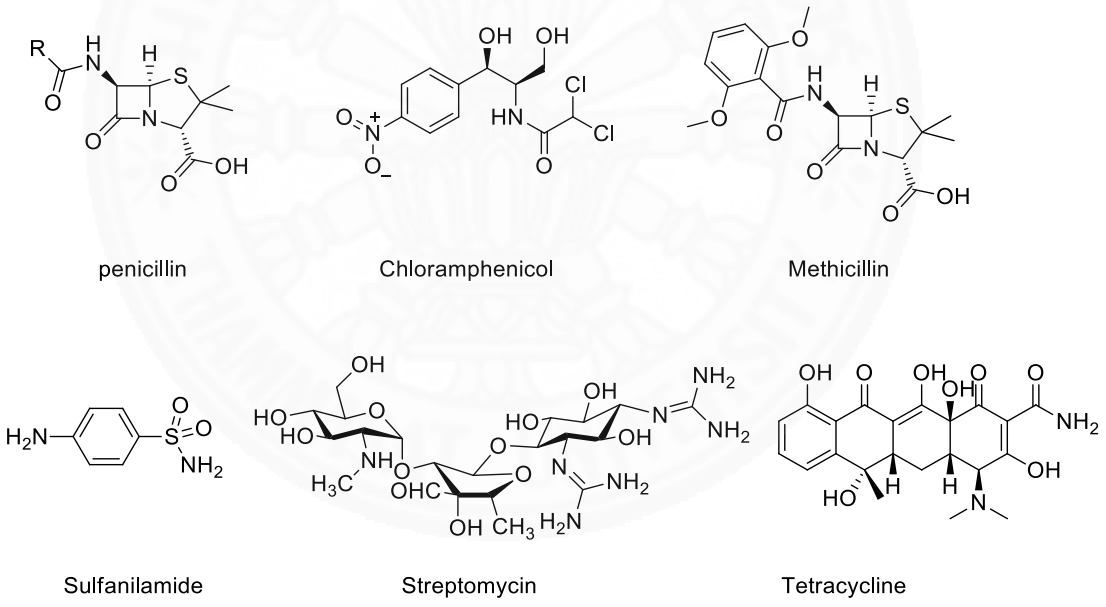

Scheme 1.1 Chemical structure of antibiotic drugs discovered in 1928 to early 1980s

1.1.2 The causes of antibiotic resistance

The causes of antibiotic resistance could be reasoned as follows. Firstly, the overuse of antibiotic drugs is the most important cause of antibiotic resistance. As clearly seen from 2000 to 2010, the antibiotic drug consumption was significantly increased by 35% (from 52,057,163,835 standard units in 2000 to 70,440,786,553 standard units in 2010) and 76% of this increase was attributed to the new emerging economy counties, namely Brazil, Russia, India, China, and South Africa.[1] Notably, the antibiotic drugs were found to be used without control in many other countries. Secondly, incorrectly antibiotic prescriptions were also found to be an important issue of antibiotic resistance. It was reported that the mistreatment of antibiotic in hospitals was increased between 30% to 50%. Additionally, a large number of antibiotics were used widely in agricultural industry, and became the major cause of the rapid antibiotic resistance. In USA, approximately 80% of antibiotic was used in animal farming for promoting growth and preventing the infection. These mentioned factors were of an important cause of the antibiotic resistance in present day. [1, 4, 5, 7]

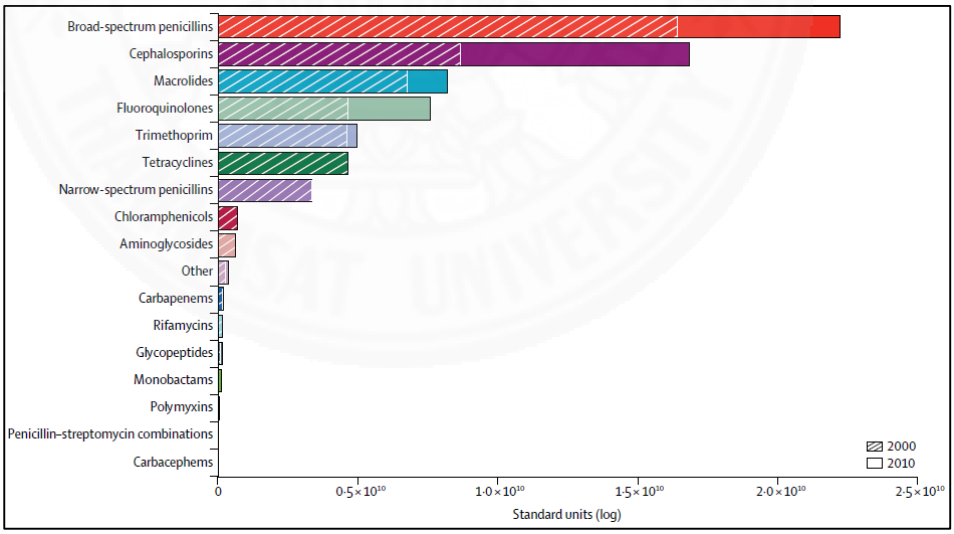

Figure 1.1 Global antibiotic consumption by class in 2000 and 2010[1]

1.1.3 Antibiotic resistance

Today, antibacterial resistance has caused patients to overstay in hospital, to pay higher medicine cost and to increase mortality. Recently, The Centers for Disease Control and Prevention in United States of American (CDC) reported at least 2 million people infection with bacteria that were resistance to antibiotic and at least 23,000 people died each year from this infection. This has concerned the people globally. In 2016, there was a report that American people died from new *E.coli* species infection called superbug which were resistant to Colistin, the last resort of antibiotic drugs used in human. The antibiotic resistance problem has now become one of the most catastrophic crises for humanity. This has led us to discover and to develop new antibiotic drugs which possesed the potentials to fight against a panel of superbugs.[8, 9]

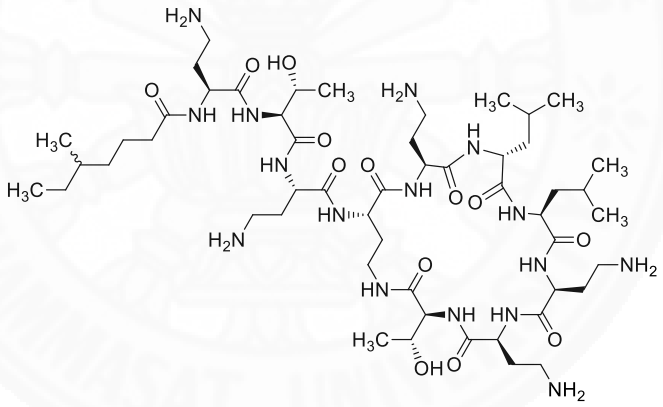

Scheme 1.2 Chemical structure of Colistin (PubChem search: Sept., 2019)

1.2 Lugdunin

In 2016, Alexander Zipperer and his research group discovered the macrocyclic thiazolidine peptide antibiotic known as “lugdunin” which was successfully isolated from *Staphylococcus lugdunensis* found in human nose. Lugdunin is a cyclic peptide containing a thiazolidine group, which is comprised of six amino acids with a head-to-tail cyclization. Lugdunin demonstrated a very effective antimicrobial activity against methicillin-resistant *S. aureus* (MIC = 1.9-15.3 μM). The mechanism of inhibition is believed that when bacterial cells were exposed by lugdunin, which resulted in the cease of incorporating caell-wall precursor, causing the death of bacteria almost simultaneously even at concentrations below the MIC. Additionally, lugdunin has led to the rapid breakdown of bacterial energy resources. However, the development of resistance is not observed in *Staphylococcus aureus*.[10]

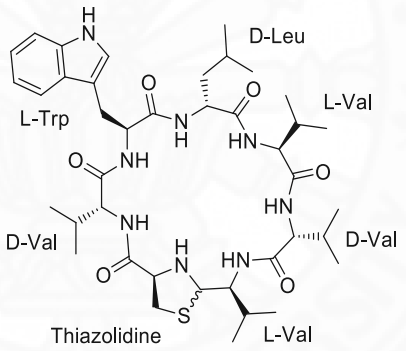

Scheme 1.3 A chemical structure of lugdunin

Recently, the chemical syntheses and structure-activity relationship (SAR) study of lugdunin has been reported by using an aldehyde-generating resin along with an amino acid assembly *via* solid phase peptide synthesis (SPPS). To the synthetic strategy, a linear peptide chain was assembled, which was subsequently cleaved to afford a linear peptide chain, comprising of an aldehyde functionality at C-terminus. Consequently, the thiazolidine ring was generated by an intramolecular cyclization of C-terminal aldehyde and N-terminal cysteine to afford a lugdunin. According to the structure-activity relationship (SAR) study, it clearly indicated that a thiazolidine ring, secondary amine of thiazolidine ring, tryptophan and leucine were highly essential for an activity of lugdunin. Additionally, the alternation between D- and L-amino acid (isomers of lugdunin) did not affect to the lugdunin activity.[(2)]

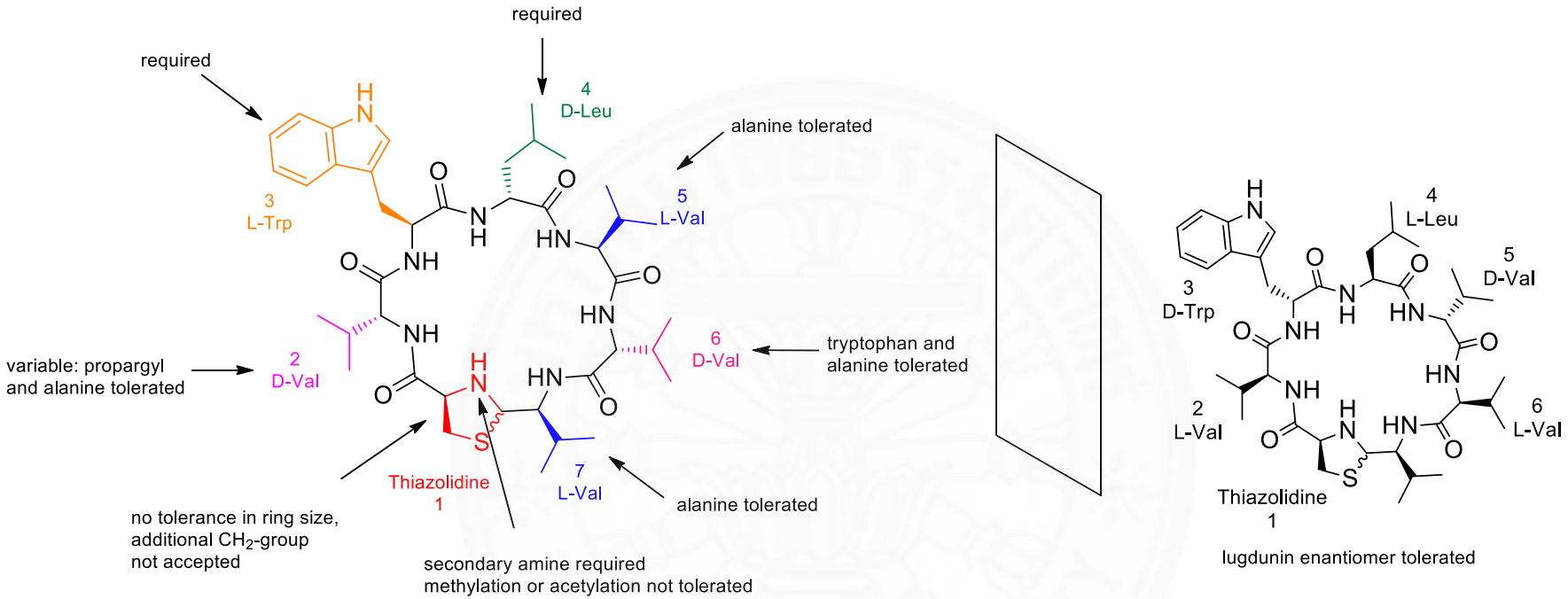

Figure 1.2 Structure-activity relationship study summary of lugdunin[2]

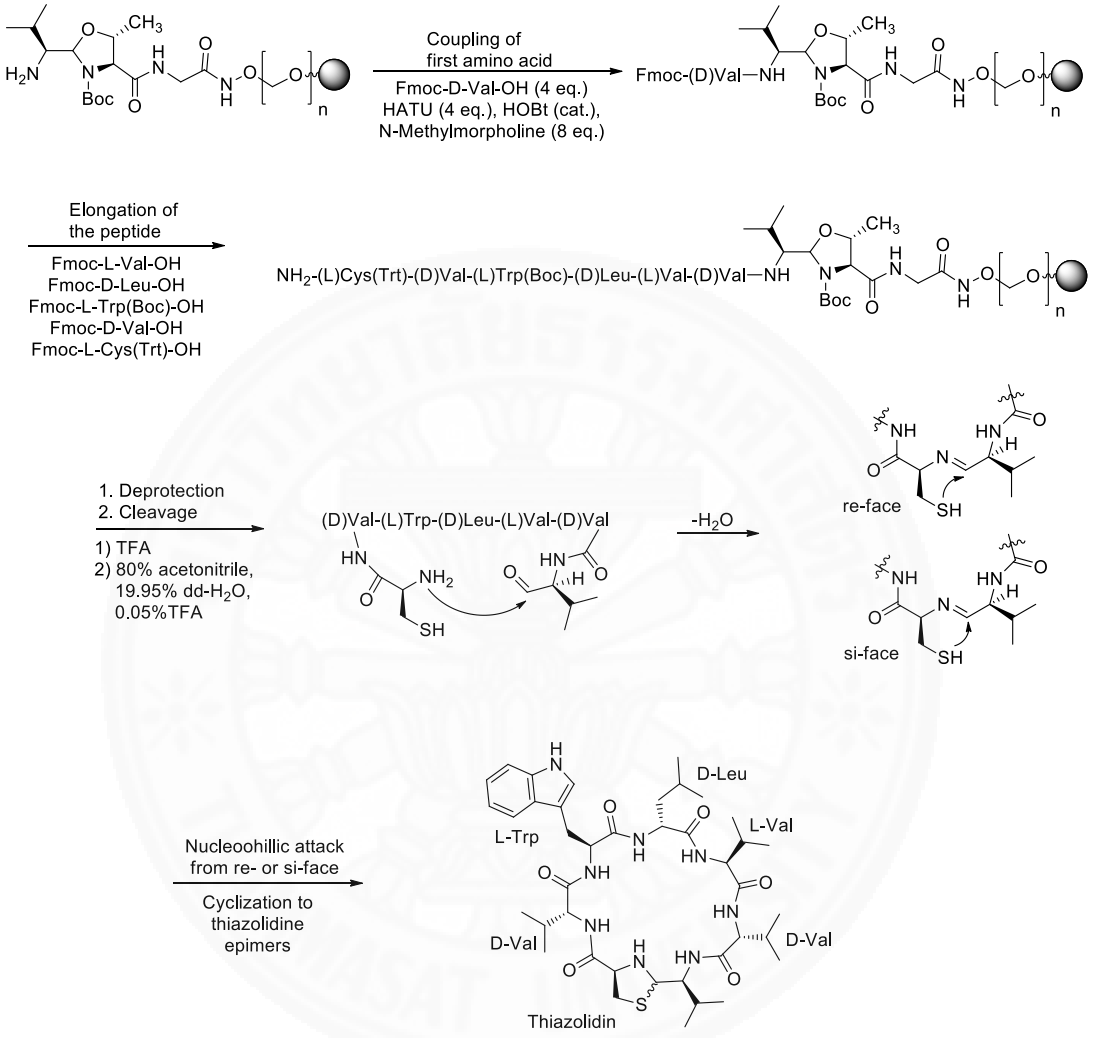

Scheme 1.4 The chemical syntheses of Lugdunin by using an intramolecular cyclization of C-terminal aldehyde and N-terminal cysteine[(2)]

1.3 Objectives

1. To explore and to implement the synthetic strategy of Fmoc-Val-thiazolidine-OH precursor.

2. To design and to synthesize native lugdunin and mutant lugdunins, namely mutant linear lugdunin, mutant linear lugdunin (cysteine) and mutant cyclic lugdunin (cysteine).

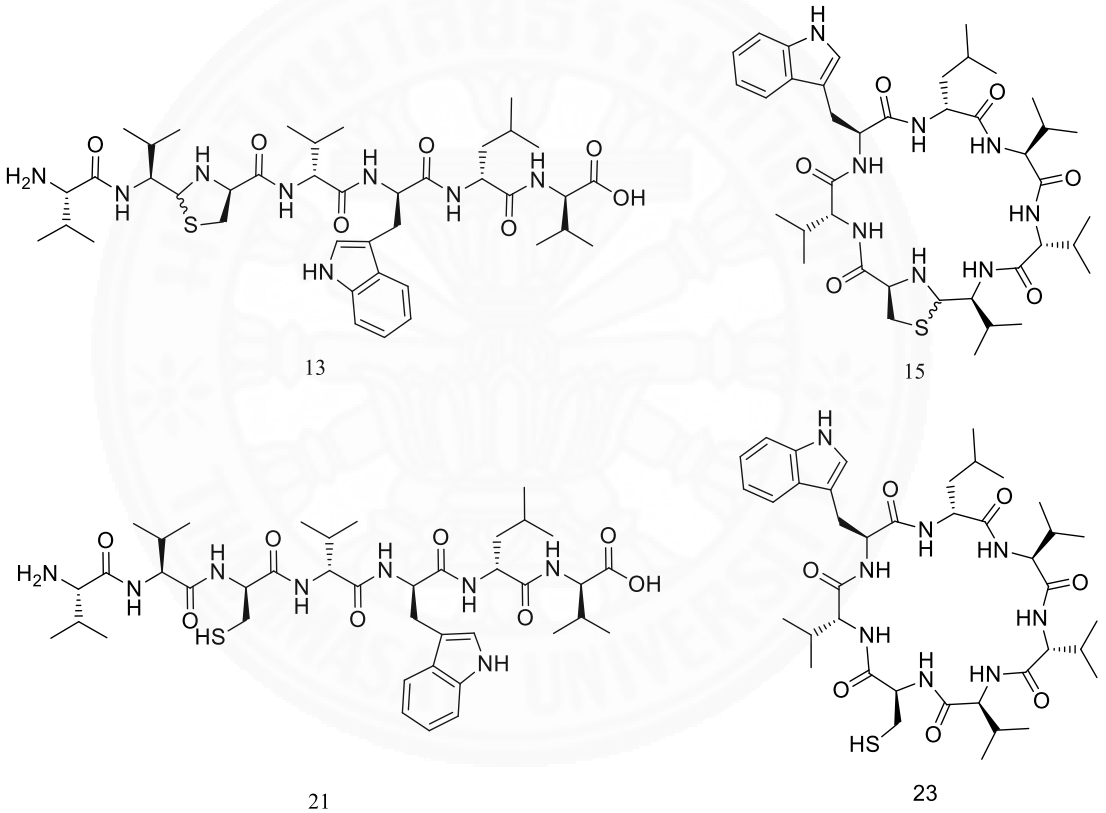

Figure 1.3 The chemical structure of synthetic compound: mutant linear lugdunin (13), synthetic native lugdunin (15), mutant linear lugdunin (cysteine) (21) and mutant cyclic lugdunin (cysteine) (23).

CHAPTER 2
REVIEW OF LITERATURE

2.1 Peptide synthesis

Peptide synthesis is a key approach for an amino acid assembly, consisting of multiple amino acid residues linked by amide/peptide bond. The amide/peptide bond formation is generated between two amino acid residues in which the activation of the carboxylic acid group must be firstly activated to increase the coupling efficacy. Secondly, a nucleophilic attack of N-amino terminus to an activated carboxyl group to afford an amino/peptide bond as shown in **Scheme 2.1**.[11]

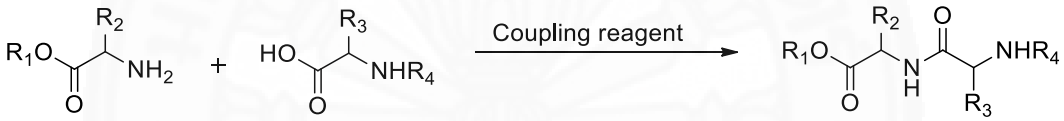

Scheme 2.1 The formation of peptide bond

2.1.1 Coupling reagent

The formation of peptide bond between two amino acid residues was slowly generated whreas the activation of a carboxylic acid by coupling agents is highly required to fasten the peptide bond formation. To date, a number of coupling reagents are commercially available, and can be classified in three important groups; (1) carbodiimides, (2) phosphonium salt and (3) aminium/uronium salt.[11-13]

2.1.1.1 Carbodiimides group

The carbodiimides have been extensively used from the past, and known as an effective coupling agent for an amide/ester bond formation. The mechanism of carbodiimides in the peptide bond formation is believed to proceed *via* a labile O-acylisourea, which subsequently reacts with a free amino group to afford an amino bond as shown in **Scheme 2.2**. The general coupling reagents in this group are shown as follows; (1) N,N-dicyclohexylcarbodiimide (DCC), (2) N,N-diisopropylcarbodiimide (DIC) and (3) 1-ethyl-3-(3-dimethylaminopropyl) carbodiimide (EDC) showed in **Figure 2.1**.

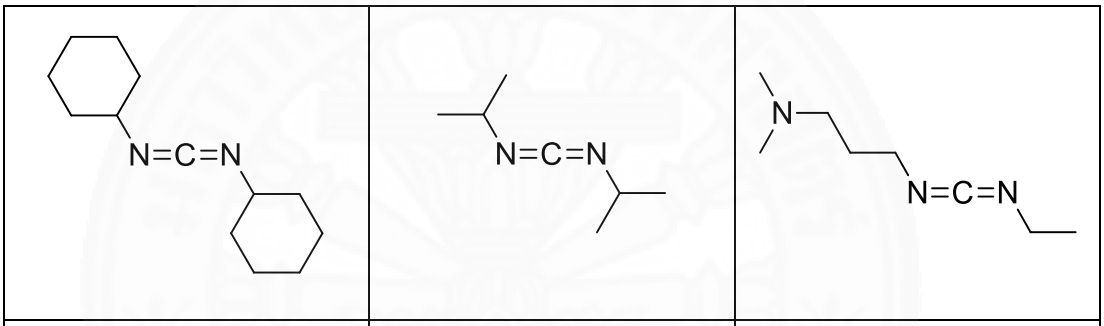

DCC	DIC	EDC

Figure 2.1 The structure of N,N-dicyclohexylcarbodiimide (DCC), N,N-diisopropylcarbodiimide (DIC) and 1-ethyl-3-(3-dimethylaminopropyl)carbodiimide (EDC)

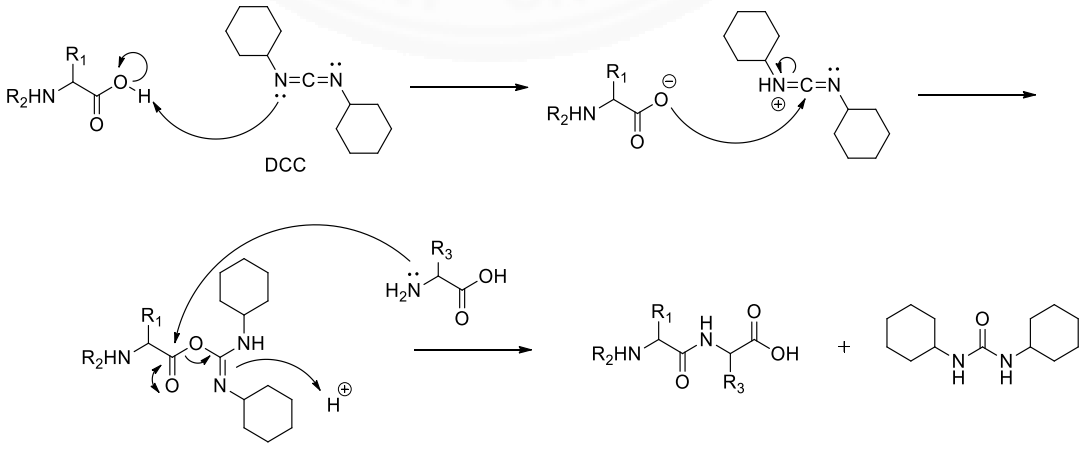

Scheme 2.2 The mechanism of DCC initiated a peptide bond formation.

2.1.1.2 Phosphonium salt group

(Benzotriazol-1-yloxy)tris(dimethylamino)phosphonium hexafluorophosphate (BOP) was classified as phosphonium based coupling reagents that commonly used for the peptide synthesis. It was used to increase the coupling efficacy. Unfortunately, the human carcinogenic "hexamethylphosphorotriamide (HMPA)" was obtained as the by-product from BOP. From this problem, (benzotriazole-1-yloxy)tris(pyrrolidino)phosphonium hexafluorophosphate (PyBOP) was used as a phosphonium based coupling agent instead of BOP. Other phosphonium based coupling reagents are shown in **Figure 2.2**, such as (7-azabenzotriazol-1-yloxy)tris(di-methylamino)phosphonium hexafluorophosphate (AOP) and (7-azabenzotriazol-1-yloxy)tris(pyrrolidino)phosphoniumhexafluorophosphate (PyAOP). The mechanism of BOP as an effective coupling agent is illustrated in **Figure 2.3**.

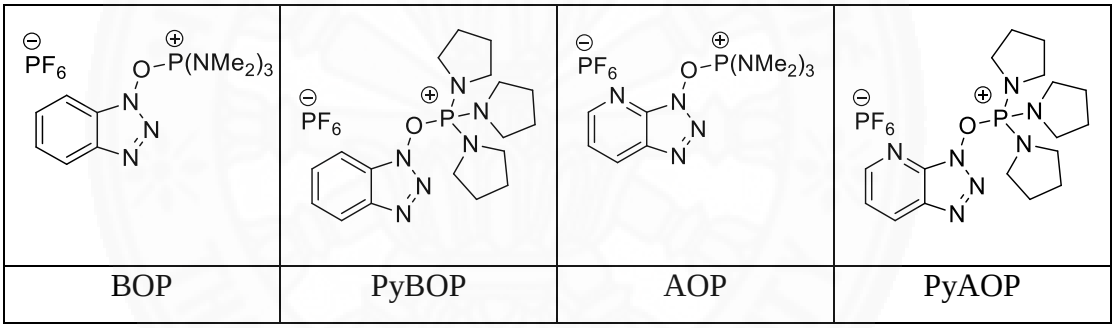

BOP	PyBOP	AOP	PyAOP

Figure 2.2 The structure of (Benzotriazol-1-yloxy)tris(dimethylamino)phosphonium hexafluorophosphate (BOP), (benzotriazole-1-yloxy)tris(pyrrolidino)phosphonium hexafluorophosphate (PyBOP), (7-azabenzotriazol-1-yloxy)tris(di-methylamino)phosphonium hexafluorophosphate (AOP) and (7-azabenzotriazol-1-yloxy)tris(pyrrolidino) phosphoniumhexafluorophosphate (PyAOP)

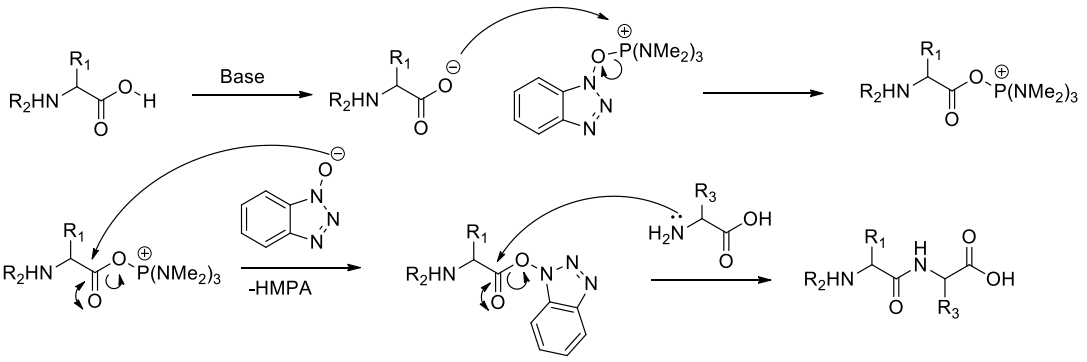

Scheme 2.3 Mechanism of BOP initiated a peptide bond formation.

2.1.1.3 Aminium/uronium salt

Aminium salt and uranium salt are presently known as highly effective coupling agents which show highly coupling efficacy, and extensively use for the peptide bond formation. Examples of coupling reagent in this group are 1-[Bis(dimethylamino)methylene]-1H-1,2,3-triazolo[4,5-b]pyridinium 3-oxid hexafluorophosphate (HATU), 2-(1H-benzotriazol-1-yl)-1,1,3,3-tetramethyluronium hexafluorophosphate (HBTU) and O-(1H-6-Chlorobenzotriazole-1-yl)-1,1,3,3-tetramethyluronium hexafluorophosphate (HCTU). The mechanism of BOP as an effective coupling agent is illustrated in **Scheme 2.4**.

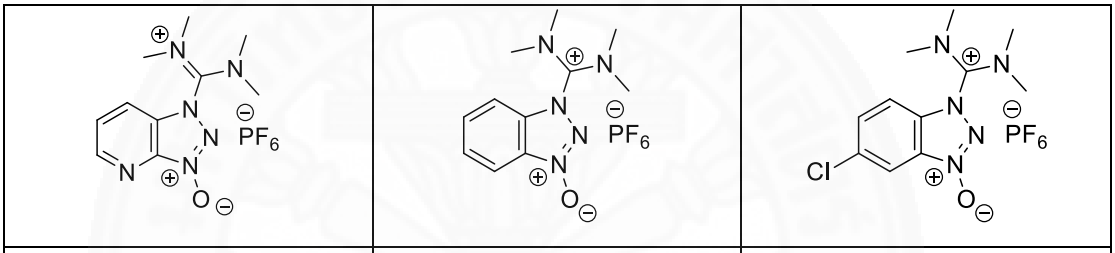

HATU	HBTU	HCTU

Figure 2.3 The structure of 1-[Bis(dimethylamino)methylene]-1H-1,2,3-triazolo[4,5-b]pyridinium 3-oxid hexafluorophosphate (HATU), 2-(1H-benzotriazol-1-yl)-1,1,3,3-tetramethyluronium hexafluorophosphate (HBTU) and O-(1H-6-Chlorobenzotriazole-1-yl)-1,1,3,3-tetramethyluronium hexafluorophosphate (HCTU)

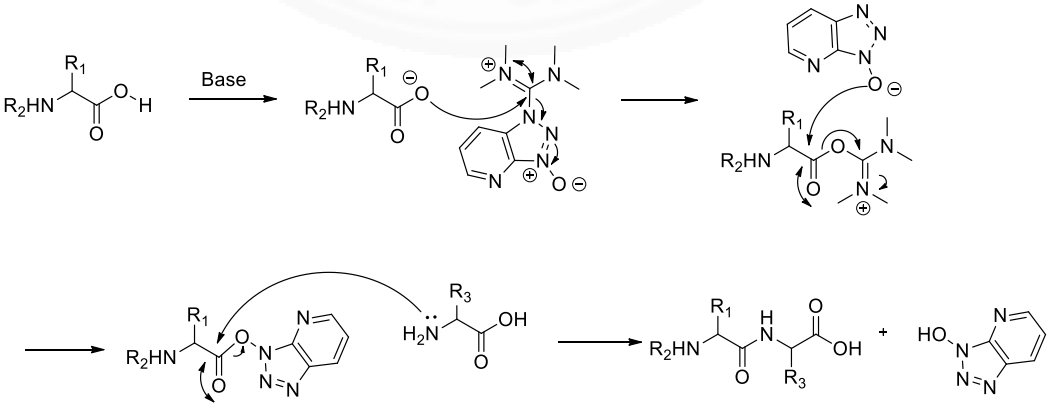

Scheme 2.4 Mechanism of HATU coupling reagent

Additionally, an additive was also added for the synthesis of peptide bond as an activator for increasing the coupling efficacy, and suppressing the racemization. Examples of additive activators are shown in **Figure 2.4**, such as N-hydroxysuccinimide (HOSu), 1-hydroxylbenzotriazole (HOBt), and 7-aza-1-hydroxybenzotriazole (HOAt). Importantly, 4-dimethylaminopyridine (DMAP) was used as a base in the synthesis of peptide along with coupling agents as shown in **Figure 2.4**.

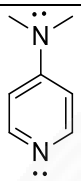	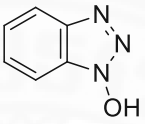	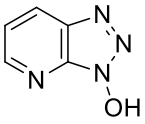
DMAP	HOBt	HOAt

Figure 2.4 The structure of 4-dimethylaminopyridine (DMAP), 1-hydroxylbenzotriazole (HOBt) and 7-aza-1-hydroxybenzotriazole (HOAt)

2.1.2 Solid phase peptide synthesis (SPPS)

Solid phase peptide synthesis (SPPS) is a general strategy for synthesizing the peptide chain, which was synthesized from the C-terminus (A carboxylic end) to the N-terminus (An amino acid end). Solid phase peptide synthesis (SPPS) approach is comprised of three main steps; (1) the first amino loading step, (2) an amino assembly and (3) the peptide chain cleavage.[14]

2.1.2.1 First amino loading step

The first amino loading has been the key step for the solid phase peptide synthesis (SPPS), which significantly affected to an obtained yield. In this step, the first amino acid residue is attached to 2-chlorotrityl linker as shown in **Scheme 2.5**.

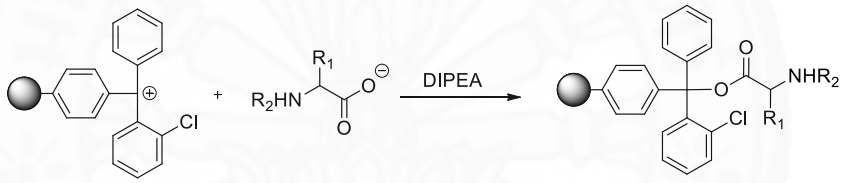

Scheme 2.5 The first amino attachment of 2-chlorotityl chloride resin

2.1.2.2 Peptide elongation step

To this step, the protecting group of first amino acid was orthogonally deprotected to afford free amino group (at N-terminus). Then, a free amino group was coupled with a carboxyl group of a second amino acid to afford the peptide bond attached to the resin. The process was repeatedly performed to afford the required peptide chain as shown in **Scheme 2.6**.

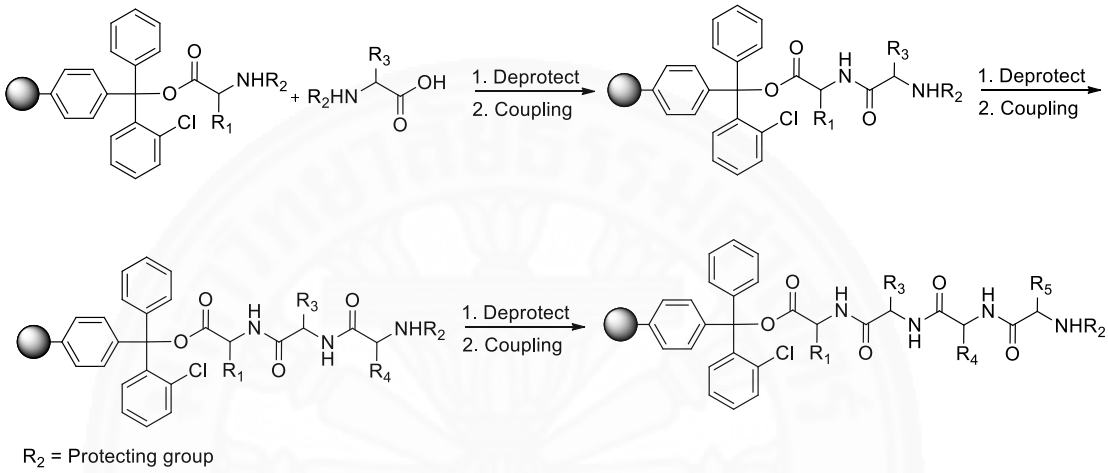

Scheme 2.6 The peptide elongation process

2.1.2.3 The peptide cleavage step

After the amino acid assembly was successfully completed, the peptide chain was then cleaved by using a required deprotection cocktail, which was specific of each resin. In this case, 2-chlorotrityl resin was allowed to cleave by using 1%TFA/CH_2Cl_2 in order to free the peptide carboxy terminus as shown in **Scheme 2.7**.

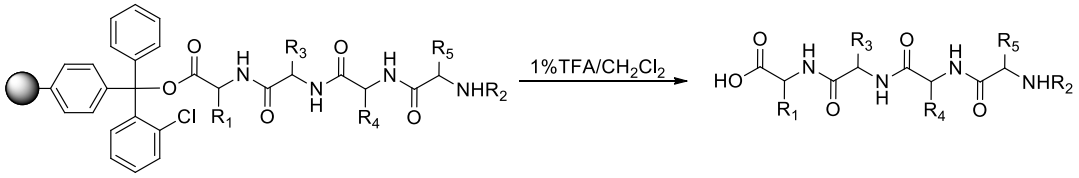

Scheme 2.7 The peptide cleavage of 2-chlorotrityl resin

2.1.2.4 The solid phase peptide synthesis strategy

The protecting group of amino acids was highly important in solid phase peptide synthesis as it prevented the side reactions between the peptide bond formations. The protecting groups used in solid phase peptide synthesis are generally classified into three important groups. Firstly, the protecting groups of amino acid side chain or orthogonal protecting groups were used to prevent side reactions at an amino side chain. For example, the acid fragile protecting groups were easily cleaved under acidic condition, and highly stable under basic condition; for examples Trt- in Cys, Boc- in Trp, Pbf- in Arg and etc. Secondly, the protecting groups at the C-terminus were used to protect the carboxylic acid group. The C-terminus protecting group was mostly used for the solid phase peptide synthesis from N-terminus to C-terminus. Finally, N-terminus protecting groups were used for N-terminus protection. The great examples of N-terminus protecting groups were fluoren-9-ylmethyloxycarbonyl (Fmoc-) and *tert*-butoxy-carbonyl (Boc-) groups that were named as Fmoc- and Boc- strategies. The Fmoc strategy was widely utilized relative to Boc strategy mainly because the Fmoc- group could easily be removed under mild condition.[15] The deprotection mechanism of Fmoc is shown in **Scheme 2.8**.

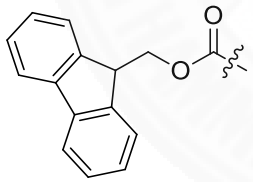	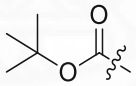	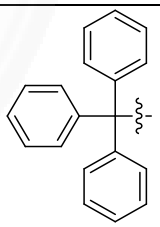
Fmoc-	Boc-	Trt-

Figure 2.5 The structures of Fmoc-, Boc- and Trt- protecting group

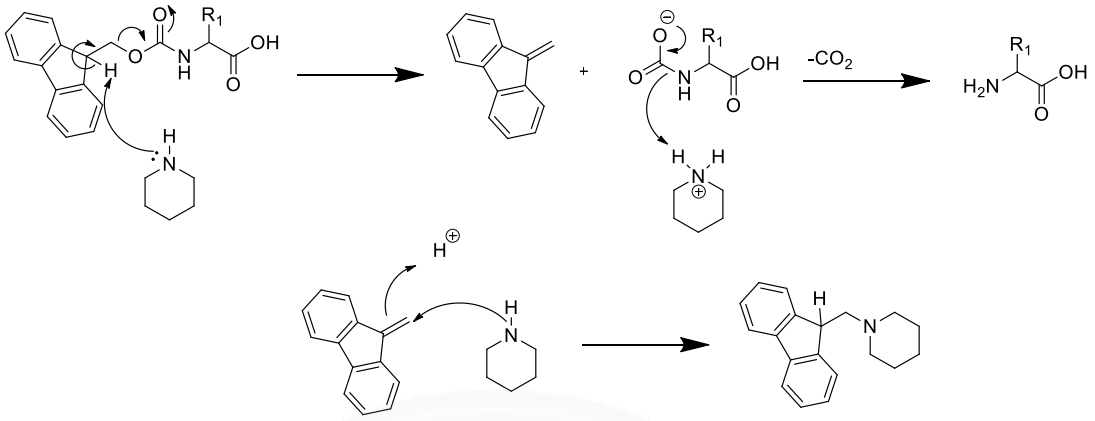

Scheme 2.8 The deprotection mechanism of Fmoc

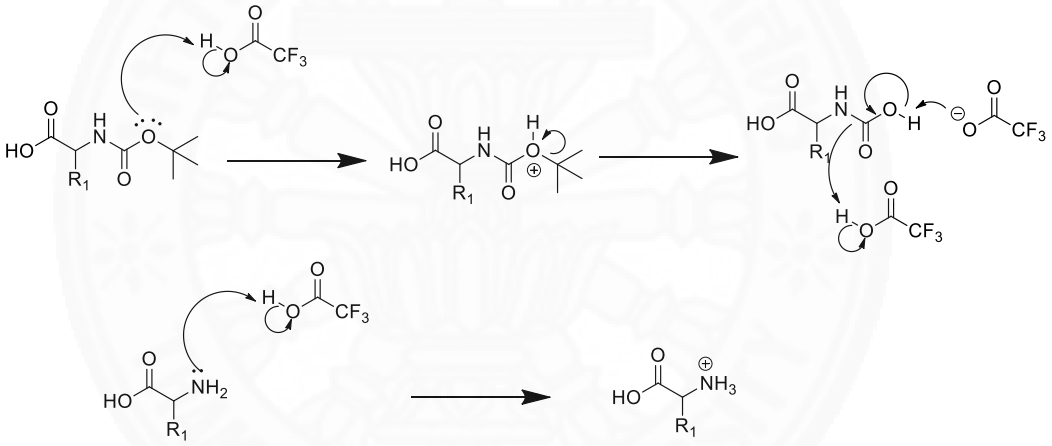

Scheme 2.9 The deprotection mechanism of Boc group.

The amide/peptide bond formation was an important reaction for syntheses of biologically active peptides. Additionally, some unusual amino acids were used as important building blocks for the syntheses of biologically active proteins, especially chiral α-amino aldehydes. The syntheses of N-protected chiral α-amino aldehydes were described in **Section 2.2**.

2.2 The synthesis of α-amino aldehyde

The chiral α-amino aldehydes have been regarded as an important building bock, widely used for biologically active molecule synthesis. The chiral α-amino aldehydes were often synthesized by following two routes as showed **Scheme 2.10**. In the first route, the carboxylic acid group of N-protected amino acid was converted to an activated carboxyl amino derivative C, namely an ester or Weinreb amide. Then, an activated carboxyl amino derivative C was directly reduced to an amino aldehyde (B). While, the second route, the N-protected amino acid was fully reduced to amino alcohol (D), following by a selective re-oxidation to yield an amino aldehyde (B).[3]

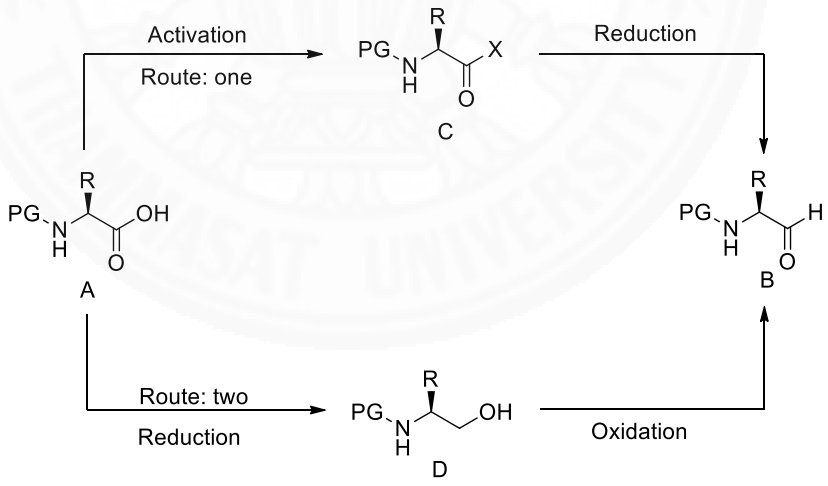

Scheme 2.10 The synthetic strategy of an amino aldehyde.[3]

Jay R. Luly and co-worker reported the synthesis of protected aminoalkyl epoxides from α-amino acid *via* α-amino aldehyde. The aminoalkyl epoxide was preliminary synthesized from N-protected amino acid *via* the carboxyl methylation followed by the reduction of methyl ester to afford N-protected amino aldehyde. The N-protected amino aldehyde was converted to an olefinated amino acid by using Wittig olefination, which was subsequently epoxidized by using 3-chloroper-oxybenzoic acid (mCPBA) to afford an aminoalkyl epoxide as seen in **Scheme 2.11**. To this research, the N-protected amino aldehyde was synthesized *via* the conversion of carboxylic acid group to an activated carboxyl amino derivative, and then followed by the selective reduction to N-protected amino aldehyde as presented in **Scheme 2.10** in the first route.[16]

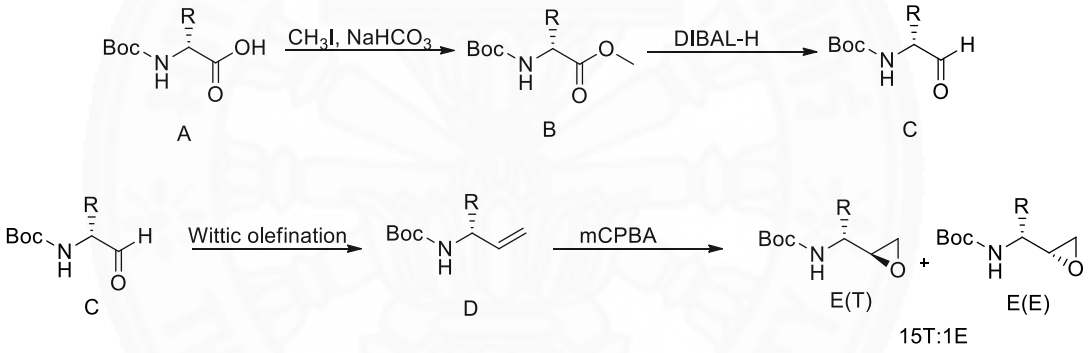

Scheme 2.11 The syntheses of aminoalkyl epoxides

Adam Golebiowski and his research group reported the total synthesis of 6-epi-D-purpurosamine B synthesized from L-alanine. To the synthetic approach, L-alanine was employed as a protected amino group with Boc protecting group, which followed by the esterification of a carboxylic group of N-protected amino acid. The resulting ester (C) was subsequently reduced by diisobutylaluminum hydride (DIBAL-H) to afford an amino aldehyde (D). Then, the N-protected amino aldehyde D was reacted with diene (F) *via* [4+2] cycloaddition to afford isomer (F) and (G) in a ratio of 2:1. The compound (F) was further reacted in multiple steps to afford 6-epi-D-purpurosamine B (H) as shown in **Scheme 2.12**. [17]

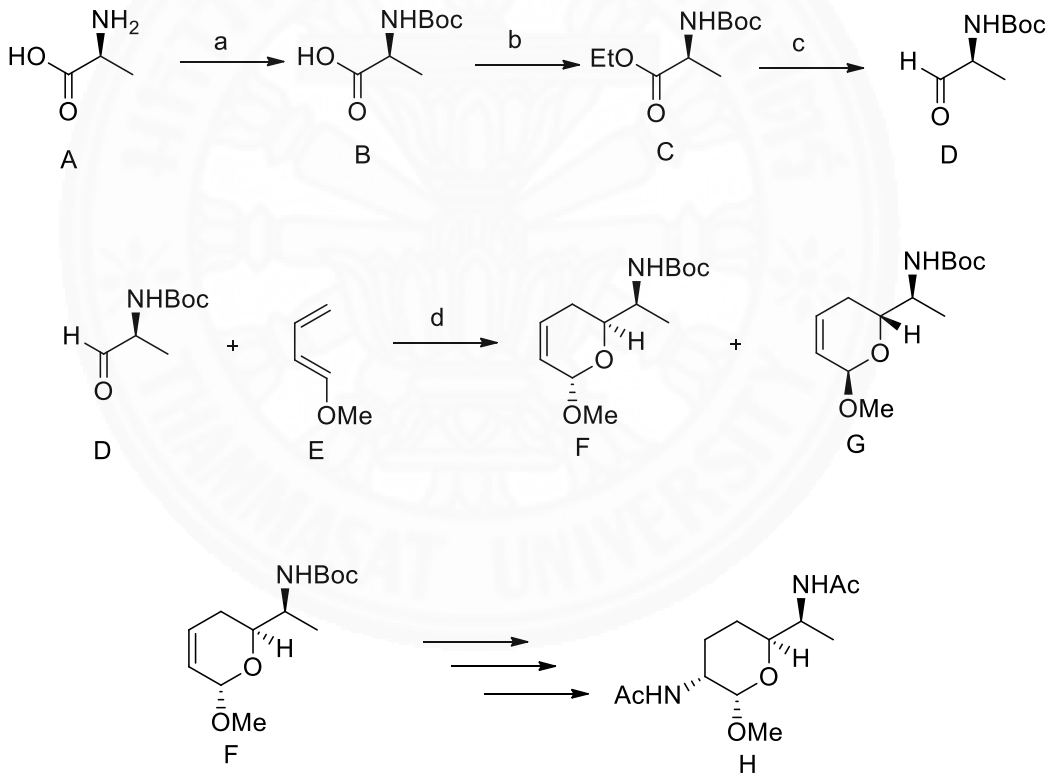

Scheme 2.12 The synthesis of 6-epi-D-purpurosamine B: (a) $(Boc)_2O$, Bu^tOH, H_2O, pH 8-9, RT, 16 h; (b) $ClCO_2Et$, Et_3N, DMAP, 0°C to RT, 0.5 h; (c) DIBAL, Et_2O, -78°C, 0.5 h; (d) i. 20 Kbar, 2% $Eu(fod)_3$, Et_2O, 50°C, 20 h; ii. PPTS, MeOH, RT, 24 h

Massimo Falorni and co-worker reported a simple strategy for the reduction of carboxylic acids to aldehydes using H_2 and Pd/C. The carboxylic acid (D) was initially treated with compound (C), synthesized by 2-chloro-4,6-dimethoxy[1,3,5]triazine (A) and N-methylmorpholine (B) in dimethylethane (DME) to afford an activated ester (E). Then, the compound E was directly treated by H_2, Pd/C to afford an aldehyde product (F) as seen in **Scheme 2.13**. [18]

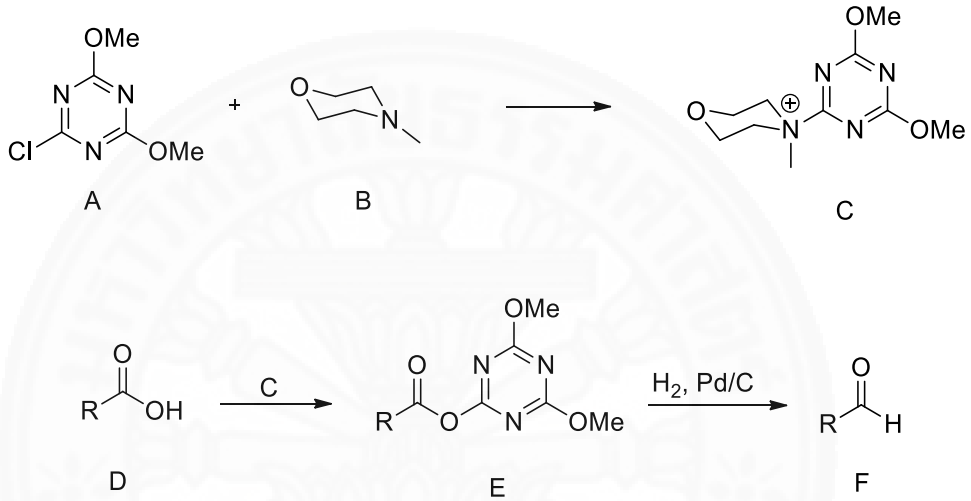

Scheme 2.13 The reduction of carboxylic acids to aldehydes using H_2 and Pd/C

Marta Ocejo and co-worker published a direct and efficient stereoconservative procedure for the selective oxidation of N-protected α-Amino alcohols. In this work, the N-protected amino aldehyde was synthesized *via a* selective oxidation of an amino alcohol. To synthetic approach, the N-protected amino aldehyde was allowed to reflux with 2-iodoxybenzoic acid (IBX) in ethyl acetate for 1-2 hour to afford a desired aldehyde with high yield and high % e.e. (≥ 92 ee%) as shown in Scheme 2.14.[19]

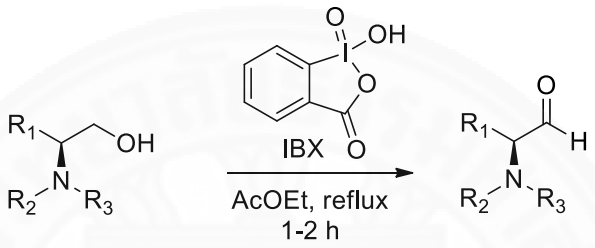

Scheme 2.14 The synthesis of an amino aldehyde using 2-iodoxybenzoic acid (IBX)

Maxim E. Sergeev and co-worker demonstrated the synthetic approach for the oxidation of β-amino alcohols to α-amino aldehydes. In this research, N-protected amino acid was converted to an amino aldehyde by treating with N-hydrosuccinimide and N, N'-Dicyclohexylcarbodiimide (DCC), which was subsequently reduced by using sodium borohydride ($NaBH_4$) to afford an amino alcohol. Finally, an amino alcohol was oxidized by using manganese (IV) oxide (MnO_2) to afford a desired N-protected amino aldehyde with high yield and high ee % as shown in **Scheme 2.15**.[20]

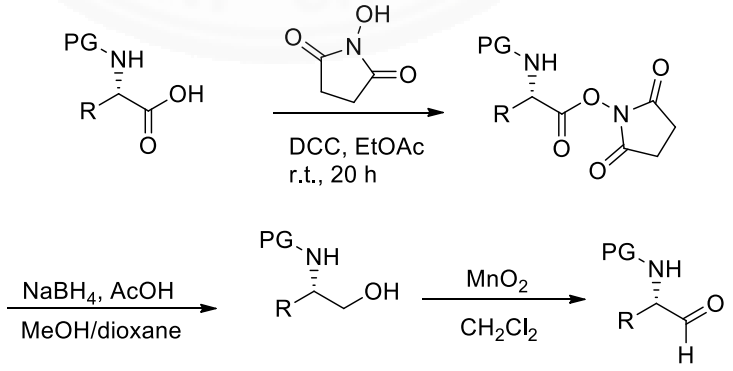

Scheme 2.15 The synthesis of an amino aldehyde by using MnO_2

Buddy Soto-Cairoli and his research group published the enantiomerically pure α-amino aldehydes from a silylated α-amino acid. To this work, triisopropylsilyl (TIPS) was used to activate a carboxylic acid. In the synthetic approach, the compound B was prepared from the silylation of an amino acid (A). Then, it was converted to a compound C by treating with borane-dimethyl sulfide complex (DMSB). Next, the compound C was hydrolyzed under a very mild condition to afford an aldehyde E as shown in **Scheme 2.16**. Interestingly, the racemization of an amino aldehyde was not observed in this method (≥ 98 % ee).[21]

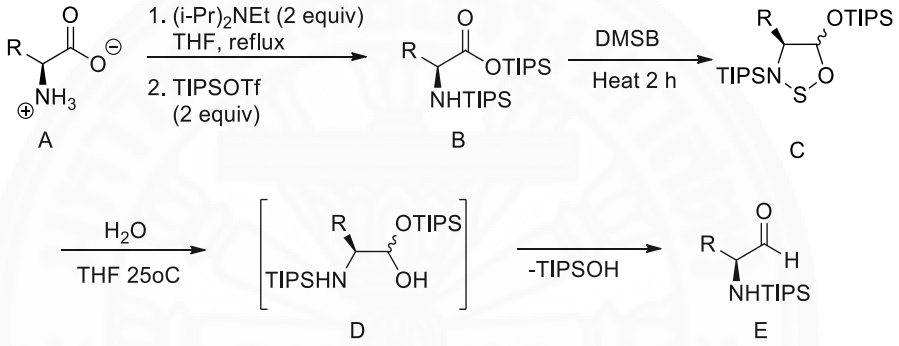

Scheme 2.16 The synthesis of an amino aldehyde by using triisopropylsilyl (TIPS)

In 2015, Jakov Ivkovic and co-worker published a rapid and efficient one-pot method for the reduction of N-protected α-amino acids to chiral α-amino aldehydes using CDI/DIBAL-H. This method is a quite simple and rapid for N-protected amino aldehyde synthesis. To this approach, the N-protected amino acid was activated using 1,1'-carbonyldiimidazole (CDI), which was then reduced by using diisobutylaluminium hydride (DIBAL-H) to afford a desired N-protected amino aldehyde with high yield and high % ee (≥ 97%) as shown in **Scheme 2.17**. [3]

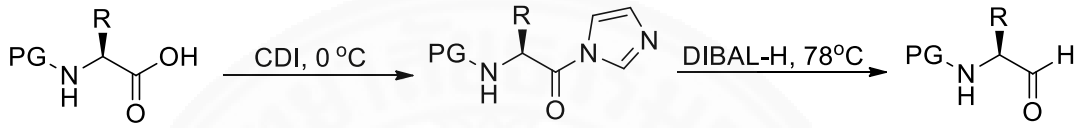

Scheme 2.17 The synthesis of an amino aldehyde by using CDI as an activator, and DIBAL as a reducing agent.

According to antibiotic resistance crises, the new antibiotic compounds were sought, isolated and developed to fight against the bacteria resistance. It was widely known that the thiazolidine containing compounds displayed a number of biological activities, particularly antibacterial and antiviral properties. Therefore, the syntheses of thiazolidine containing compounds were of great interest. The example of thiazolidine syntheses are described in **Section 2.3**.

2.3 The synthesis of thiazolidine

Thiazolidine ring is a five membered ring heterocycle organic compound, consisting of carbon, nitrogen and sulfur within the molecule. It is widely known that the thiazolidine containing compounds are significantly important in terms of biological activities, particularly anticancer, antibacterial and antiviral properties.[22] The preparation of a thiazolidine ring was firstly reported in 1937 by Sarah Ratner and co-work. It was successfully synthesized by using the condensation between cysteine and formaldehyde as shown in **Scheme 2.18**.[23]

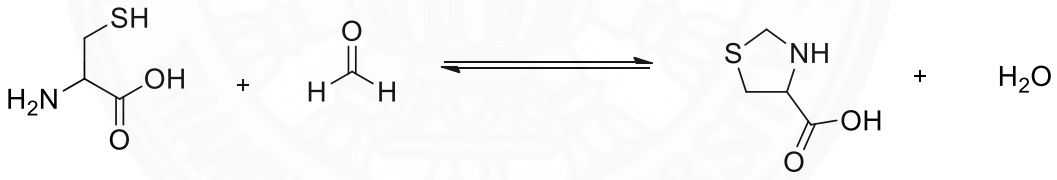

Scheme 2.18 The synthesis of a thiazolidine-4-carboxylic acid

In 2008, F. Esra Onen and co-worker reported the design, syntheses and the evaluation of potent thymidylate synthase X inhibitors. To this research, they demonstrated three series of thymidylate synthase X inhibitor syntheses base on a thiazolidine core. The thiazolidine core of thymidylate synthase X inhibitor can be synthesized by the acetylation of L-cysteine with benzaldehyde to afford compound 2, which was esterified by using thionyl chloride to afford the thiazolidine core as shown in Scheme 2.19.[24]

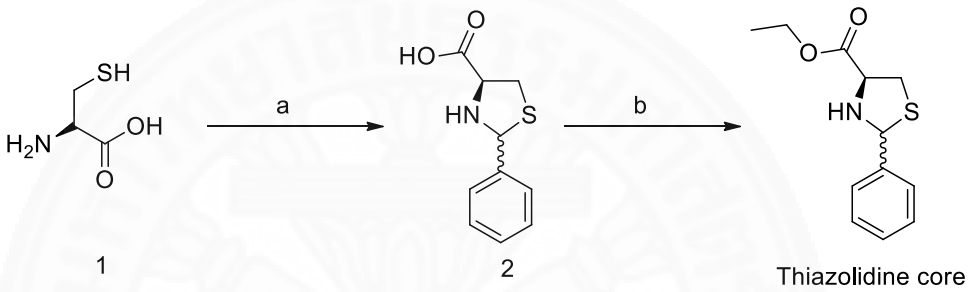

Scheme 2.19 The synthesis of a thiazolidine core: (a) benzaldehyde, EtOH/H_2O, 3 h, rt; (b) $SOCl_2$, anhydrous EtOH, 1 h, 0°C, then 18 h at room temperature.

In 2011, Yu Liu and his research group demonstrated the design, synthesis and the biological activity of thiazolidine-4-carboxylic acid derivatives as novel influenza neuraminidase inhibitors. To this work, they reported a series of thiazolidine-4-carboxylic acid derivative syntheses, which were subsequently tested against a neuraminidase (NA) of an influenza A virus, showing the great inhibition in a micromolar range. The core of a thiazolidine-4-carboxylic acid derivative was synthesized by coupling between an aldehyde precursor and L-cysteine hydrochloride in EtOH/H_2O 1:1 to afford the thiazolidine (1). Then, the thiazolidine (1) was further reacted with $ClCH_2COCl$ and $PhCH_2COCl$ to afford thiazolidine-4-carboxylic acid derivatives (3 and 4) as shown in **Scheme 2.20**.[25]

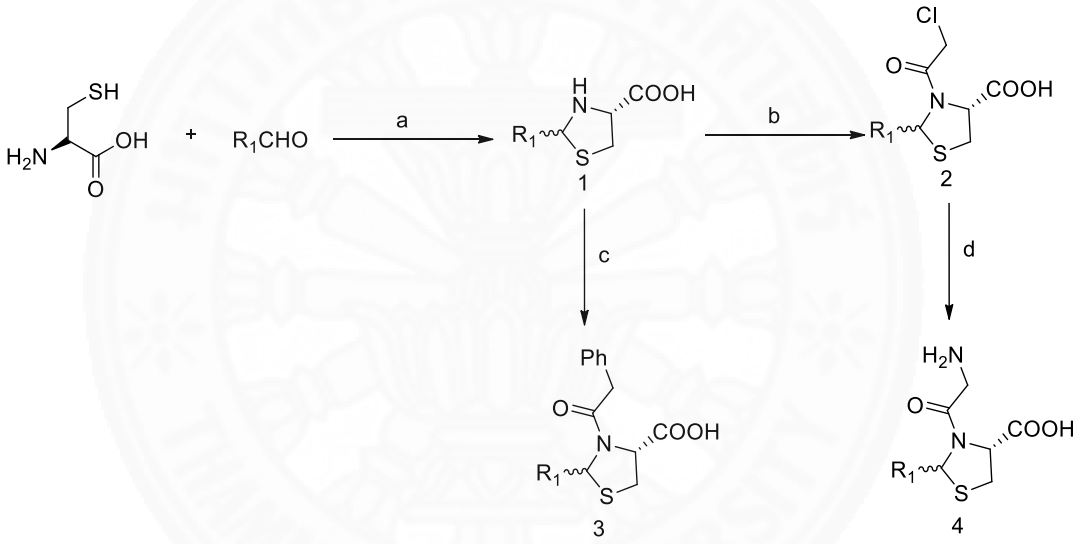

Scheme 2.20 The synthesis of thiazolidine-4-carboxylic acid derivatives (3) and (4): (a) $NaHCO_3$, EtOH/H_2O; (b) $ClCH_2COCl$, $NaHCO_3$/H_2O; (c) $PhCH_2COCl$, $NaHCO_3$/H_2O; (d) $NH_2{\cdot}H_2O$; BOC_2O, THF; HCl/EtOAc.

Additionally, F. Esra Onen-Bayram and co-work reported the synthesis of 3-propionyl-4-carboxylic acid ethyl ester. To this research, a thiazolidine could be synthesized by coupling cysteine with aldehyde precursors whereas the alkyl moieties were an aromatic aldehyde, and an aliphatic aldehyde as shown in **Scheme 2.21**.[26]

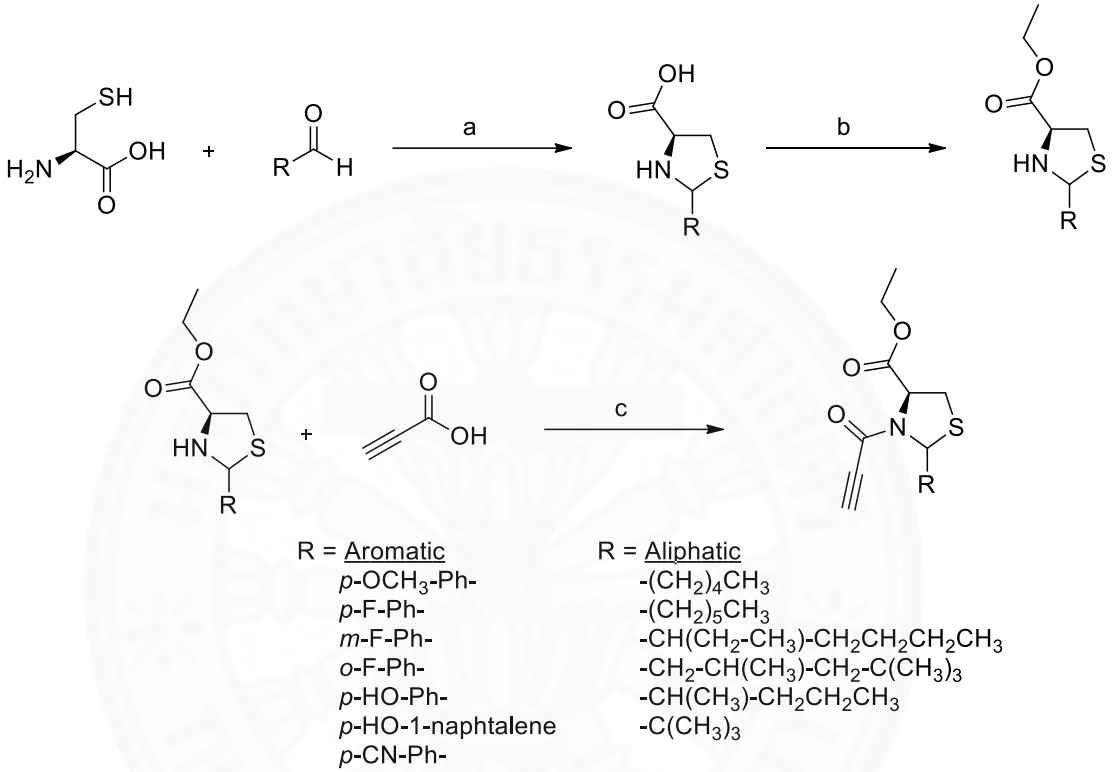

Scheme 2.21 The preparation of 3-propionyl-thiazolidine-4-carboxylic acid ethyl esters from a series of aliphatic and aromatic aldehydes. (a) NaOH in EtOH/H_2O (1/1); (b) $SOCl_2$ in absolute EtOH; (c) DCC in dry CH_2Cl_2.

The resistance of bacteria has now become the important crises globally. Therefore, the discovery and development of new antibiotic drugs to fight against a panel of superbugs have been of great importance. Interestingly, the peptides are the great source of discovering novel antibiotics. A thousands of antibiotic peptide molecules have continuously been discovered. The example of antibiotic peptides are shown in **Section 2.4**.

2.4 The antibiotic peptide

Chenguang Yuan and Robert M. Williams reported the synthesis of TAN-1057A-D, a dipeptide isolated from *Flexibacter* sp. PK-74 and PK-176. TAN-1057A and TAN-1057B are known as diastereomers, consisting of β-homoarginine and a unique heterocyclic amidinourea derivative. TAN-1057A-D demonstrated an effective anti-bacterial activity against methicillin-resistant *Staphylococcus aureus* (MRSA) with a mechanism of action by inhibiting protein biosynthesis as shown in **Figure 2.6**.[27]

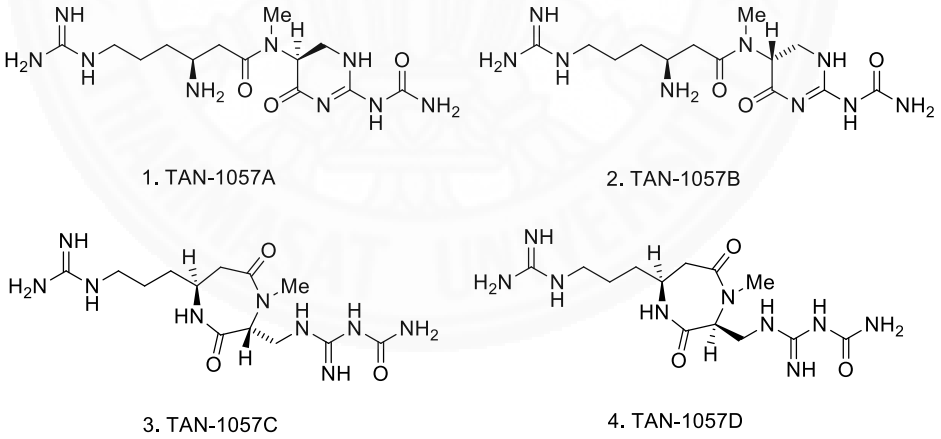

Figure 2.6 Chemical structure of TAN-1057A-D: The dipeptide isolated from *Flexibacter* sp. PK-74 and PK-176

E. K. S. Vijaya Kumar and his research group discovered methylsulfomycin I, a cyclic peptide isolated from the fermentation broth of a *Streptomyces* sp. HIL Y-9420704. Methylsulfomycin I was a cyclic peptide, consisting of deala, oxazole and thiazole which displayed an antibiotic ability against *Staphylococcus* and *Enterococcus* species in the range of 0.06-0.125 µg/mL. Additionally, Methylsulfomycin I was found to be more potent than vancomycin drug as shown in **Figure 2.7** .[28]

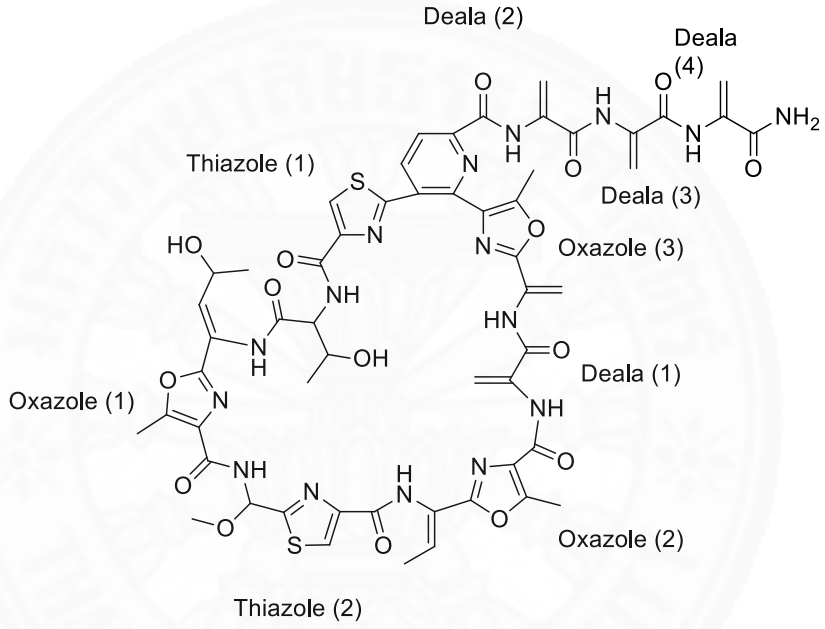

Figure 2.7 Chemical structure of Methylsulfomycin I, the cyclicpeptide isolated from the fermentation broth of a *Streptomyces* sp. HIL Y-9420704.

Todd Barsby and his research group confirmed the structure of Bogorol A, a linear peptide isolated from cultures of a marine *Bacillus* sp., which was collected in Papua New Guinea. Bogorol A was a linear peptide, consisting of a number of amino acid residues, ranging from tyrosine, valine, leucine, isoleucine, lysine to ornithine as shown in **Figure 2.8**. It showed a very effective antibacterial activity against methicillin- resistant *Staphylococcus aureus* (MRSA) and vancomycin- resistant *Enterococcus* with MIC = 2 µg/mL and 10 µg/mL, respectively.[29]

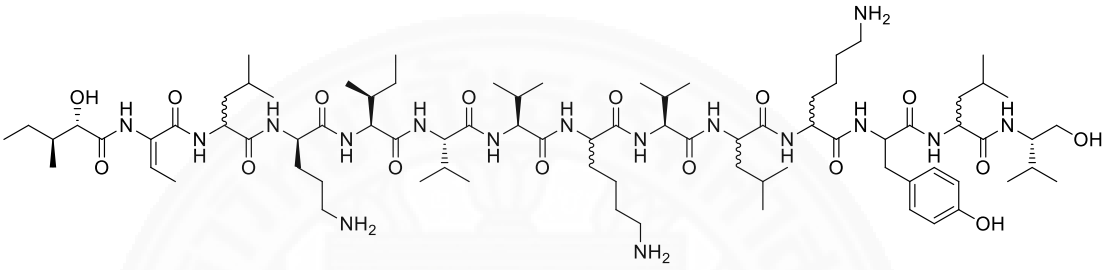

Figure 2.8 Chemical structure of Bogorol A

Rachael A. Hughes and his research group reported the synthesis of Amythiamicin D, which was a member of thiopeptide group. The structure of amythiamicin D was consisted of six thiazole rings, pyridine, methyl- asparagine and valine as shown in **Figure 2.9**. It showed the great antibacterial activity against methicillin-resistant *Staphylococcus aureus* (MRSA).[30]

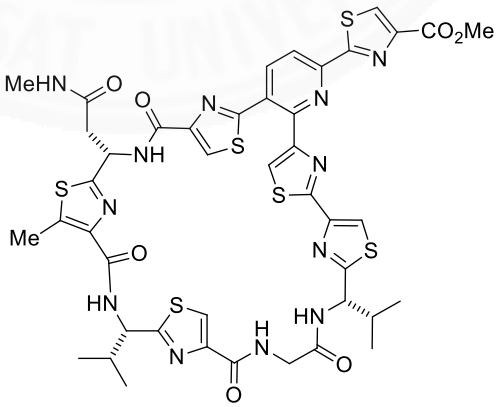

Figure 2.9 Chemical structure of Amythiamicin D

Aaron wohlrab and his research group showed the synthesis of Plusbacin A3, a cyclic peptide isolated from a fermentation broth of *Pseudomonas* sp. PB-6250 which was obtained from a soil sample collected in the Okinawa Prefecture, Japan. Plusbacin A_3 was a lipodepsipeptide consisted of 3-hydroxyisopentadecanoic acid, L-threo-β-hydroxyaspartic acid, D-threo-β-hydroxyaspartic acid D-allo-threonine and trans-3-hydroxy-L-proline as shown in **Figure 2.10**. Plusbacin A_3 demonstrated a very strong antibacterial activity against methicillin-resistant *Staphylococcus aureus* and Van A-type vancomycin-resistant *enterococci* with MIC values from 0.78-3.13 µg/mL. Additionally, Plusbacin A3 could inhibit the incorporation of N-acetylglucosamine into *staphylococcal* cell wall peptidoglycan.[31]

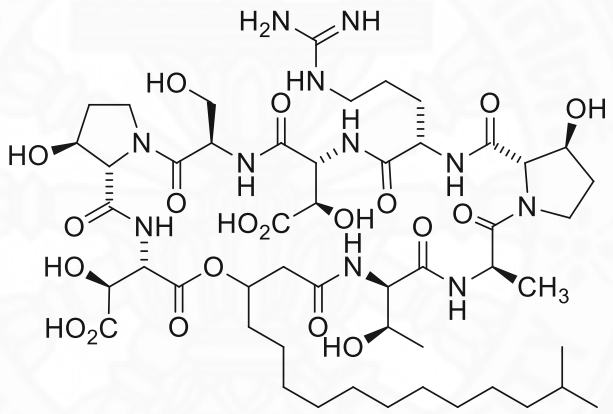

Figure 2.10 The chemical structure of Plusbacin A_3

Kelsey desjardine discovered the synthesis of Tauramamide, a lipopeptide isolated from *BreVibacillus laterosporus* PNG276. Tauramamide is well-known as a lipopeptide, consisting of L-arginine, D-tryptophan, D-isoleucine, D-serine, D-tyrosine and a lipid part as shown in **Figure 2.11**. Tauramamide showed a very potent and relatively selective activity against the important Gram-positive human pathogen *Enterococcus* sp. with MIC 0.1 µg/mL.[32]

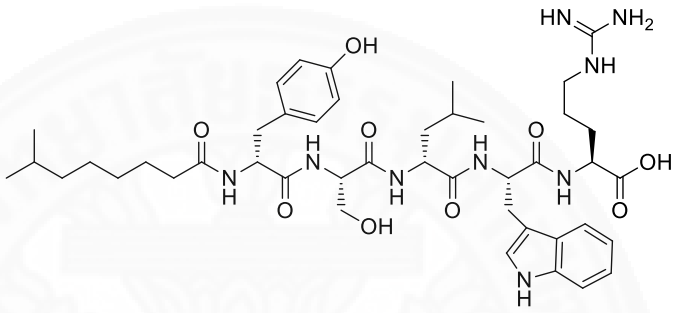

Figure 2.11 The chemical structure of Tauramamide

Honggang Hu and his research group reported the synthesis of Tyrocidine A and glycosylated derivative of Tyrocidine A, a cyclic peptide isolated from *Bacillus* bacteria. Tyrocidine A was a macrocyclic decapeptide, consisting of tyrosine, valine, ornithine, leucine, D-phenylanine, L-phenylanine, proline, asparagine and glutamine as shown in **Figure 2.12**. The bactericidal activity of Tyrocidine A was tested against gram-positive bacterium *Bacillus subtilis* (strain CMCC-B 63501) with a MIC value of 31 µg/mL.[33]

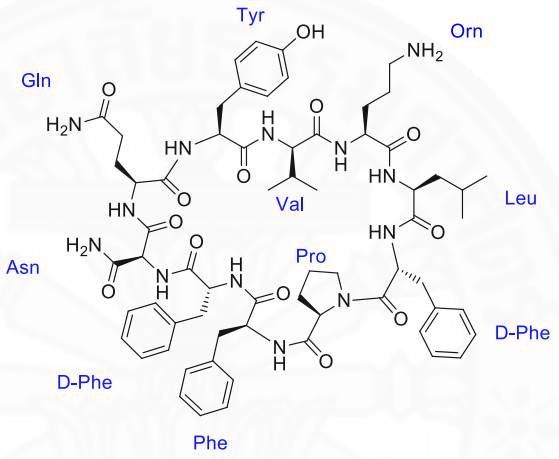

Figure 2.12 A chemical structure of Tyrocidine A

Chaowei Zhang and his research group isolated a new compound in a thiazomycins class, named as thiazomycin and thiazomycin A-D, a cyclic peptide isolated from *Amycolatopsis fastidiosa* MA7332. This compound was a thiazolyl peptide, consisting of a thiazole ring, serine, threonine and glutamic residues. The structure of Thiazomycin and thiazomycin A-D structure are different at three aryl positions as shown in **Figure 2.13**. Both Thiazomycin and thiazomycin A-D have shown a potent antibacterial activity against *Streptococcus spp.* with MIC values 0.004-0.03 μg/mL.[34]

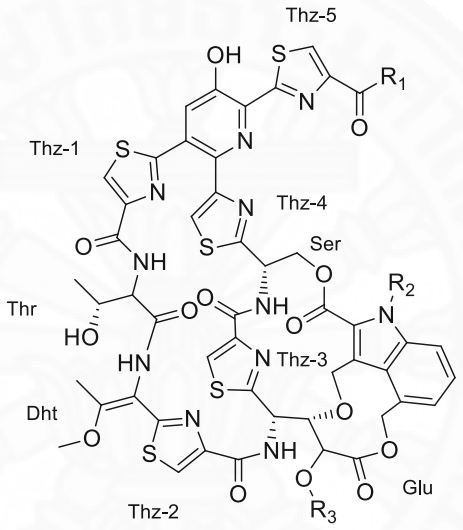

Figure 2.13 A chemical structure of thiazomycins core

Matthew J. LaMarche and his research group reported the chemical stability and physico-chemical properties of thiomuracin A. Thiomuracin A was an antibiotic sulfur-containing macrocyclic peptide as shown in **Figure 2.14**. It can bind to the elongation factor Tu and disrupts a prokaryotic protein synthesis. Thiomuracin A displayed a potent antibacterial activity against methicillin-resistant *staphylococci* (MRSA), vancomycin-resistant *enterococci* (VRE), group A *streptococci*, and the anaerobic gut pathogen *Clostridium difficile*, with minimum inhibitory concentrations (MIC) < 1 μg/mL. However, Thiomuracin A had poor physicochemical properties, such as poor organic solubility and low stability. Matthew J. LaMarche and his research group initiated to improve chemical stability and physicochemical properties by removing the C2−C7 side chain, by derivatizing the C84 epoxide region, and by altering the C44 hydroxyphenylalanine motif. The Thiomuracin A derivative was found to improve an organic solubility and high stability.[35]

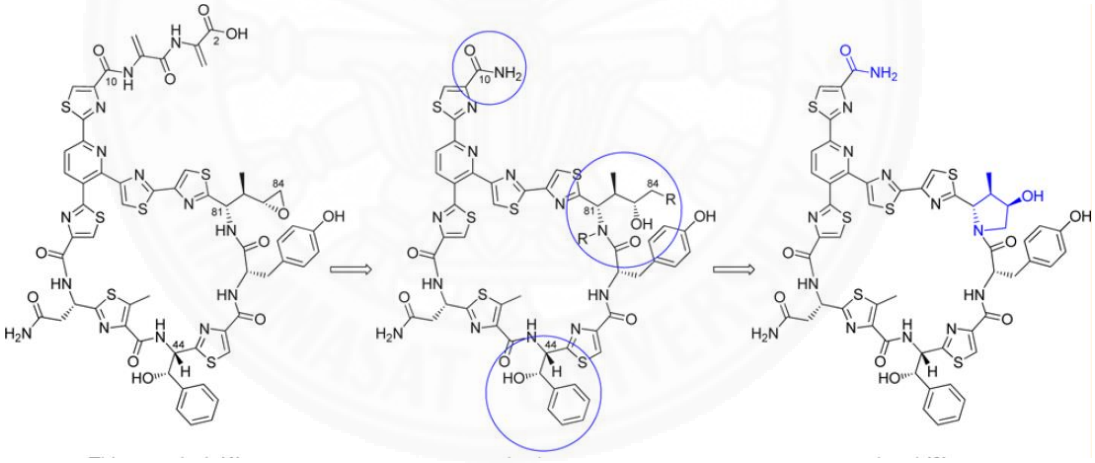

1 2 3

Figure 2.14 Chemical structures of thiomuracin A (1), improved position of thiomuracin A (2) and thiomuracin A derivative (3)

Yang-Min Ma and his research group reported malformin E, a cyclic peptide isolated from the culture broth of endophytic fungus FR02 from the roots of *Ficus carica*. Malformin E was a cyclic pentapeptide, consisting of leucine, valine, isoleucine and cysteine as shown in **Figure 2.15**. It showed cytotoxic activities against human cancer cell strains MCF-7 and A549 with IC_{50} values of 0.65 and 2.42 μM, respectively and anti-microbial activities against *Bacillus subtilis*, *Staphylococcus aureus*, *Pseudomonas aeruginosa*, *Escherichia coli*, *Penicillium chrysogenum*, *Candida albicans*, and *Fusarium solani* with MIC values of 0.91, 0.45, 1.82, 0.91, 3.62, 7.24, and 7.24 μM, respectively.[36]

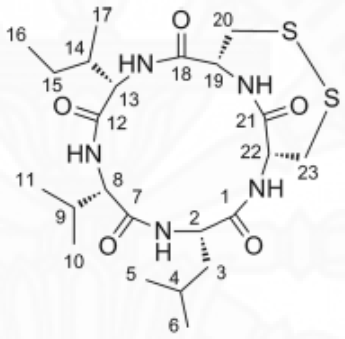

Figure 2.15 A chemical structure of malformin E, cyclic pentapeptide isolated from the culture broth of endophytic fungus FR02 from the roots of *Ficus carica*

Katsuhiko Mitachi and his research group described the synthesis of Muraymycin D1. Muraymycin D1 was an aminoribosyl−uridyl peptides isolated from *Streptomyces spp.* The structure of muraymycin D1 as shown in **Figure 2.16** was consisted of aminoribsyl group, uridyl group and a linear peptide chain, showing an antibiotic activity against *Mycobacterium tuberculosis* with MIC of 1.56μg/mL.[37]

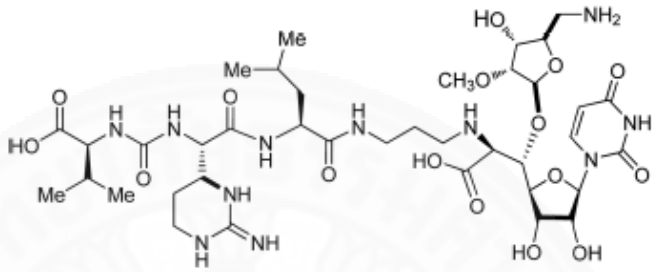

Figure 2.16 The chemical structure of Muraymycin D1, aminoribosyl−uridyl peptides isolated from *Streptomyces* spp.

According to the literature review, it was found that both linear and cyclic peptide showed a very promising antibacterial activity, especially sulfur containing peptides, which demonstrated a potent antibacterial activity against a panel of pathogenic bacteria. This has led us to further study and to discover a novel peptide antibiotics. Lugdunin was a cyclic peptide containing a thiazolidine group that showed a very effective antimicrobial activity against methicillin-resistant *S. aureus*. Therefore, the synthesis of native and mutant lugdunin was very challenging in order to solve the antibiotic resistance problem in the future.

CHAPTER 3
RESEARCH METHODOLOGY

3.1 Chemicals and Instrument

3.1.1 Chemicals

(1) N-(9-Fluorenylmethoxycarbonyl)-L-valine, Fmoc-Val-OH

(2) N-(9-Fluorenylmethoxycarbonyl)-D-valine, Fmoc-D-Val-OH

(3) N-(9-Fluorenylmethoxycarbonyl)-D-Leucine, Fmoc-D-Leu-OH

(4) N_{α}-Fmoc-$N_{(in)}$-Boc-L-tryptophan, Fmoc-Trp(Boc)-OH

(5) 1,1´-Carbonyldiimidazole, CDI

(6) Diisobutylaluminum hydride, DIBAL-H

(7) L-Cysteine methyl ester hydrochloride

(8) N, N′-Dicyclohexylcarbodiimide, DCC

(9) 4-Dimethylaminopyridine, DMAP

(10) Hydroxybenzotriazole, HOBt

(11) 1-[Bis(dimethylamino)methylene]-1H-1,2,3-triazolo[4,5-b]pyridinium 3-oxid hexafluorophosphate, N-[(Dimethylamino)-1H-1,2,3-triazolo-[4,5-b]pyridin-1-ylmethylene]-N-methylmethanaminium hexafluorophosphate N-oxide, HATU

(12) N, N-Diisopropylethylamine, DIPEA

(13) Hydrochloric acid, HCl

(14) L-Cysteine

(15) Sodium bicarbonate, $NaHCO_3$

(16) Trifluoroacetic acid, TFA

(17) Piperidine

(18) 2-chlotrityl chloride resin

(19) Fmoc-Val-Wang resin

(20) Silica gel, 100-200 mesh

(21) Nitrogen gas

(22) Hexane

(23) Ethyl acetate, EtOAc

(24) Dichloromethane, DCM

(25) Methanol, MeOH

(26) Diethyl ether

(27) Tetrahydrofuran, THF

(28) Dimethylformamide, DMF

(29) Methanol HPLC grade

(30) Acetonitrile HPLC grade

(31) Distilled water

(32) Deionized water

3.1.2 Instruments

(1) Laboratory glasswares

(2) Glass chromatography columns

(3) Silica thin layer chromatograhy plates

(4) Glass filtration kit

(5) Syringes and syringe filters

(6) Heating mentle

(7) Magnetic stirrer

(8) Shaker, stuart mini orbital shaker SSM1

(9) Balance 4 digit, METTLER TOLEDO AB304-S

(10) UV lamp

(11) Rotary evaporator, BUCHI vacuum controller V-800 and rotavapor R-205

(12) Vacuum pump, EDWARDS model RV8

(13) Freeze dryer, Flexi-Dry^{TM} MP

(14) Analytical high-performance liquid chromatography, HPLC, SHIMADZU LC20AT

(15) Nuclear magnetic resonance spectrometer (NMR), ultrashield 300 MHz, DPX-300 Bruker Biospin, and 600 MHz, Bruker Avance III HD

(16) Electrospray ionization mass spectrometer, ESI-MS, Thermo Finnigan LCQ Advantage and Finnigan MAT LCQ

(17) Matrix-assisted laser desorption/ionization Time-of-flight mass spectrometry, MALDI-TOF-MS, SHIMADZU Axima performance

(18) Fourier-transform infrared spectroscopy, FTIR, Perkin Elmer infrared spectrophotometer

(20) Ultraviolet–visible spectrophotometer, SHIMADZU UV-1700 Pharma Spec

(21) Preparative high-performance liquid chromatography, Jasco preparative HPLC PU-4086-Binary pump, Jasco UV-4075 UV/Vis Detecter

(22) High-resolution electrospray ionisation mass spectrometry, HR-ESI-MS, SHIMADZU LCMS-IT-TOF

3.2 Experiments

3.2.1 The synthesis of wild type lugdunin

3.2.1.1 Synthesis of an aldehyde precursor (Fmoc-Val-H)

Fmoc-Val-OH (0.500 g, 1.4732 mmol) was added to round bottom flasks (100 mL) which was equipped with a Schlenk adapter, dried under reduced pressure for 2 hours at room temperature and then purged with N_2 gas. To this reaction flask was dissolved by dry CH_2Cl_2 (15 mL), and cooled to 0°C (ice bath). 1,1'-carbonyldiimidazole (CDI, 1.5 eq., 0.3580 g, 2.2098 mmol) dissolved by dry CH_2Cl_2 was subsequently added to the reaction flask and the reaction mixture was allowed to stir for 1 hour under nitrogen atmosphere at 0°C. Then, the reaction mixture was cooled to -78**°C** (CO_2/acetone bath) for 15 minutes. Diisobutylaluminum hydride (DIBAL-H, 5.0 eq., 7.366 mL, 7.366 mmol) was subsequently added to reaction mixture and allowed to stir for 2 hours under nitrogen atmosphere at -78°C. The reaction mixture was quenched by 6 M HCl (20 mL) and warmed to the ambient temperature. The reaction mixture was extracted with CH_2Cl_2 (3×50 mL). The combined organic extracts were washed with H_2O (1 × 200 mL), brine (1 × 200 mL), dried over Na_2SO_4, filtered and concentrated under reduced pressure. The crude product was purified by using flash column chromatography (20% ethyl acetate/hexane) with silica gel as stationary phase to give Fmoc-Val-H (0.2912 mg, 61%). The structure was characterized by ^{1}H-NMR and HR-ESI-MS, respectively. ^{1}H-NMR (600 MHz, $CDCl_3$) δ = 0.94-1.03 (dd, *J* = 10.2, 41.7 Hz, 6H, CH_3-4), 2.28-2.31 (m, *J* = 6.6 Hz, 1H, CH-3), 4.20-4.23 (t, *J* = 10.2 Hz, 1H, CH-8), 4.31-4.34 (q, *J* = 6.0 Hz, 1H, CH-2), 4.39-4.41 (d, *J* = 10.8 Hz, 2H, CH_2-7), 5.34-5.35 (d, *J* = 10.8 Hz, 1H, NH-5), 7.28-7.32 (t, *J* = 11.4 Hz, 2H, Ar'H-11), 7.36-7.40 (t, *J* = 11.4 Hz, 2H, Ar'H-12), 7.57-7.59 (d, *J* = 10.8 Hz, 2H, Ar'H-10), 7.74-7.76 (d, *J* = 10.8 Hz, 2H, Ar'H-13) and 9.64 (s, 1H, COH-1). ^{13}C-NMR (600 MHz, $CDCl_3$) δ = 17.6 (CH_3-4), 29.1 (CH-3), 47.2 (CH-8), 65.0 (CH-2), 67.0 (CH_2-7), 120.0 (ArC-13), 125.0 (ArC-10), 127.1 (ArC-11), 127.7 (ArC-12), 142.0 (ArC-14), 145.0 (ArC-9), 155.0 (CO-6) and 200 (CO-1). Found 346.1408$[M+Na]^+$ and 378.1652 $[M+CH_3OH+Na]^+$; Calculated 323.3864 $[M]^+$.

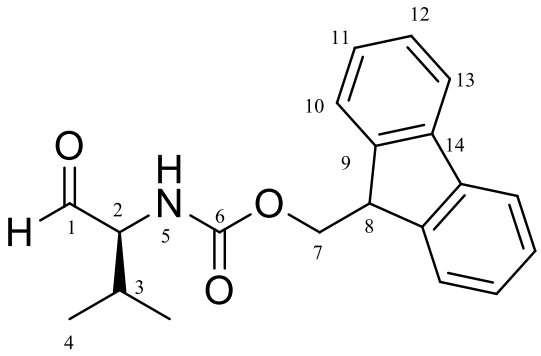

Figure 3.1 Structure of Fmoc-Val-H (**2**)

3.2.1.2 Synthesis of Fmoc-Val-Thiazolidine-OH

Fmoc-Val-H (0.3157 g, 0.9762 mmol) was dissolved by absolute ethanol (15 mL) in round bottom flask (100 mL). Next, cysteine hydrochloride monohydrate (0.2308 g, 0.1464 mmol) dissolved by absolute ethanol (15 mL) was added to the reaction flask. The reaction mixture was allowed to stir overnight. Then, the reaction mixture was evaporated to dryness by using rotary evaporator. The reaction crude was purified by using flash column chromatography (10% methanol/ethyl acetate) with silica gel to afford Fmoc-Val-Thiazolidine-OH (0.3185 g, 38%). The structure was characterized by ^{1}H-NMR and HR-ESI-MS. ^{1}H-NMR (600 MHz, Methanol-D4), δ (ppm): δ = 0.93-1.01 (dd, *J* = 6.7, 38.6 Hz, 6H, CH_3-4), 1.79-1.82 (m, 1H, CH-3), 3.25-3.28 (dd, *J* = 6.4, 9.9 Hz, 2H, CH_2-15), 3.62-3.64 (dd, *J* = 6.5, 9.7 Hz, 1H, CH-16), 3.85-3.87 (dd, *J* = 4.3, 7.6 Hz, 1H, CH-2), 4.26-4.28 (t, *J* = 6.6 Hz, 1H, CH-8), 4.35-4.47 (m, 1H, CH-1), 4.76 (d, *J*=4.2, 2H, CH_2-7), 7.32-7.34 (m, 2H, Ar'H-11), 7.39-7.41 (t, *J* = 7.0 Hz, 2H, Ar'H-12), 7.69-7.73 (m, 2H, Ar'H-10) and 7.81-7.82 (d, *J* = 7.5 Hz, 2H, Ar'H-13). Found 427.8$[M+H]^+$; Calculated 426.5305 $[M]^+$

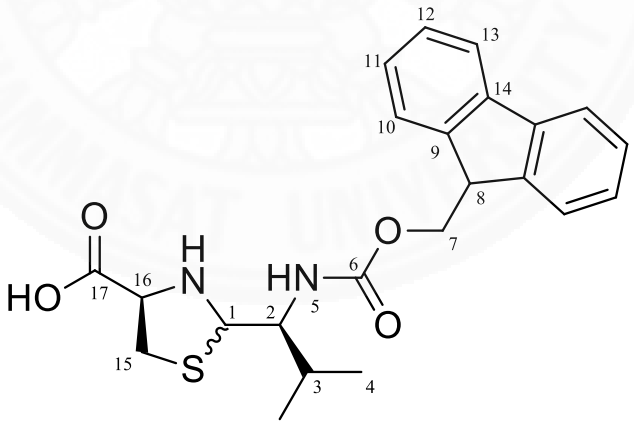

Figure 3.2 Structure of Fmoc-Val-thiazolidine-OH

3.2.1.3 The first amino loading on 2-chlorotrityl chloride resin

2-Chlorotrityl chloride resin (2.0 g, 1.68 mmol) was added to a round bottom flask. To this reaction mixture was added by Fmoc-Val-OH (0.8553 g, 2.52 mmol), DIPEA (2.52 mmol, 0.4286 mL), and DMF (10 mL). The reaction mixture was subsequently shaken for 24 hours. Then, the reaction mixture was filtered and a resin was washed with DMF (3x4 mL), CH_2Cl_2 (3x4 mL), and diethyl ether (3x4 mL) respectively. The first amino acid loading was calculated by using Fmoc test.

3.2.1.4 Fmoc Test

Fmoc-Val-resin (2.0 mg) was added into a small vial. To this vial was added by 20% piperidine/DMF (3 mL), and allowed to shake for 30 minutes. Then, the absorption intensity at 301 nm was measured by using UV-visible spectroscopy, and then calculated the first amino acid loading as follows;

mmol amino acid/g of resin = (Abs.)/(1.65×mg)

% amino loading = [(mmol of amino acid/g of resin)/(mmol/g of loading resin)]×100

3.2.1.5 Solid phase peptide synthesis (SPPS) procedure

(1) Fmoc-Val-2-chlorotrityl resin (0.200 g, 0.1472 mmol) was treated by 20% piperidine in DMF (3 mL) and allowed to shake for 30 minutes at room temperature. Resin was then washed by DMF (3×3 mL).

(2) The resin was coupled by Fmoc-D-Leu-OH (2.0 eq., 0.1039 g, 0.2941 mmol) dissolved in DMF (1 mL) by using DCC (2.0 eq., 0.0607 g, 0.2941 mmol) dissolved in DMF (0.5 mL), DMAP (2.0 eq., 0.0359 g, 0.2941 mmol) dissolved in DMF (0.5 mL) and HOBt (2.0 eq., 0.0498 g, 0.2941 mmol) dissolved in DMF (0.5 mL) as coupling reagents. The reaction mixture was allowed to shake for 60 minutes at room temperature. The resin was subsequently washed by DMF (3×3 mL).

(3) The resin was treated by 20% piperidine in DMF (3 mL) and allowed to shake for 30 minutes at room temperature. The resin was then washed with DMF (3×3 mL).

(4) An amino acid assembly was repeatedly coupled by Fmoc-Trp(Boc)-OH (2.0 eq., 0.1549 g, 0.2941 mmol), Fmoc-D-Val-OH (2.0 eq., 0.0998 g, 0.2941 mmol) and Fmoc-Val-Thiazolidine-OH (2.0 eq., 0.1253 g, 0. 0.2941 mmol), respectively.

(5) The resin was finally coupled with Fmoc-D-Val-OH (2.0 eq., 0.0998 g, 0.2941 mmol) dissolved in DMF (1 mL) by using DCC (2.0 eq., 0.0607 g, 0.2941 mmol) dissolved in DMF (0.5 mL), DMAP (2 eq., 0.0359 g, 0.2941 mmol) dissolved in DMF (0.5 mL) and HOBt (2 eq., 0.0498 g, 0.2941 mmol) dissolved in DMF (0.5 mL) as coupling reagents. The reaction mixture was allowed to shake for 60 minutes at room temperature. Then, the resin was washed with DMF (3×3 mL), CH_2Cl_2 (3×3 mL) and ether (3×3 mL), respectively.

(6) A resin was treated by 20% piperidine in DMF (3 mL) and allowed to shake for 30 minutes at room temperature. Then, the resin was washed with DMF (3×3 mL). Then, the resin was washed with DMF (3×3 mL), CH_2Cl_2 (3×3 mL) and ether (3×3 mL), respectively.

3.2.1.6 The peptide cleavage protocol

The linear peptide chain attached to 2-chlorotrityl resin was treated by using 1% TFA/CH_2Cl_2 (5 mL). The reaction mixture was allowed to shake for 5 minutes. The reaction mixture was evaporated to dryness. The crude product was dried in a desicator over silica gel.

3.2.1.7 Peptide purification

A small sample of crude peptide was analysed by analytical preparative RP-HPLC before purifying by preparative HPLC. The mobile phases contained 0.1 % HPLC grade TFA as an ion pairing agent. Peptide purification was achieved by using preparative reverse-phase HPLC using an ACE 10 C18-AR C18 Column (250 × 4.6 mm). Individual fractions from preparative reverse-phase HPLC were analysed by using analytical reverse-phase HPLC, and pure fractions were combinded and diluted to < 10 % MeCN with deionised water. The peptide was obtained as a white solid after lyophilisation on a Flexi-Dry^{TM} MP freeze dryer. Mass identification by Matrix-Assisted Laser Desorption/Ionisation Time of Flight Mass Spectrometry (MALDI-TOF MS) was performed by using α-cyano-4-hydroxy cinnamic acid as matrix. The following elution methods were used: Method A: 20 to 100% MeCN in H_2O over 45 min. All peptides and reaction mixtures were analysed using Method A unless otherwise specified

3.2.1.8 The peptide cyclization protocol

The fully protected linear lugdunin (0.0203 g, 0.0225 mmol) was subsequently cyclized by using HATU (1.5 eq., 0.0129 g, 0.0338 mmol) and DIPEA (3 eq., 0.0115 mL, 0.0675 mmol) as coupling reagents under a very high dilution condition (1 mg/2 mL). The reaction mixture was allowed to stir overnight at room temperature. Then, the reaction mixture was evaporated to dryness. The resulting crude peptide was treated by 95% TFA in CH_2Cl_2 and subsequently purified by preparative HPLC as described in 3.2.1.7. The synthetic lugdunin was obtained as a yellow solid (48 %, 0.0085 g), and characterized by using ESI-MS spectrometry. Found 993.4 $[M+TFA+2MeOH+Cl]^+$; Calculated 782.45$[M]^+$.

3.2.1.9 The synthesis of mutant lugdunin (a linear scaffold)

The fully protected linear lugdunin (0.0010 g, 0.0011 mmol) was treated by 95% TFA in CH_2Cl_2, and subsequently purified by preparative HPLC as described in details in 3.2.1.7. The synthetic lugdunin was obtained as a white solid (79 %, 0.0007 g), and characterized by using ESI-MS spectrometry Found; 513.9 $[M+2TFA-2H]^+$ and 341.0 $[M+2TFA-3H]^+$; Calculated 801.0535 $[M]^+$.

3.2.2 The synthesis of mutant lugdunins (cysteine linear and cyclic scaffold)

3.2.2.1 Solid phase peptide synthesis (SPPS)

(1) Fmoc-Val-2-chlorotrityl resin (0.200 g, 0.1472 mmol) was treated by 20% piperidine in DMF (3 mL) and allowed to shake for 30 minutes at room temperature. A resin was washed with DMF (3×3 mL).

(2) The resin was coupled by Fmoc-D-Leu-OH (2.0 eq., 0.1039 g, 0.2941 mmol) dissolved in DMF (1 mL) by using DCC (2.0 eq., 0.0607 g, 0.2941 mmol) dissolved in DMF (0.5 mL), DMAP (2.0 eq., 0.0359 g, 0.2941 mmol) dissolved in DMF (0.5 mL) and HOBt (2.0 eq., 0.0498 g, 0.2941 mmol) dissolved in DMF (0.5 mL) as coupling reagents. The reaction mixture was allowed to shake for 60 min at room temperature. The resin was washed with DMF (3×3 mL).

(3) A resin was treated by 20% piperidine in DMF (3 mL) and allowed to shake for 30 minutes at room temperature. The resin was washed with DMF (3×3 mL).

(4) An amino acid assembly was repeatedly coupled by Fmoc-Trp(Boc)-OH (2.0 eq., 0.1549 g, 0.2941 mmol), Fmoc-D-Val-OH (2.0 eq., 0.0998 g, 0.2941 mmol), Fmoc-L-Cys(Trt)-OH (2.0 eq., 0.1723 g, 0.2941 mmol) and Fmoc-L-Val-OH (2.0 eq., 0.0998 g, 0.2941 mmol), respectively.

(5) The resin was finally coupled by Fmoc-D-Val-OH (2.0 eq., 0.0998 g, 0. 0.2941 mmol) dissolved in DMF (1 mL) using DCC (2.0 eq., 0.0607 g, 0.2941 mmol) dissolved in DMF (0.5 mL), DMAP (2 eq., 0.0359 g, 0.2941 mmol) dissolved in DMF (0.5 mL) and HOBt (2 eq., 0.0498 g, 0.2941 mmol) dissolved in DMF (0.5 mL) as coupling reagents. The reaction mixture was allowed to shake for 60 minutes at room temperature. The resin was washed with DMF (3×3 mL), CH_2Cl_2 (3×3 mL) and ether (3×3 mL).

(6) A resin was treated by 20% piperidine in DMF (3 mL) and allowed to shake for 30 minutes at room temperature. Then, the resin was washed with DMF (3×3 mL). Then, the resin was washed with DMF (3×3 mL), CH_2Cl_2 (3×3 mL) and ether (3×3 mL).

3.2.2.2 The peptide cleavage protocol

The linear peptide chain attached to 2-chlorotrityl resin was treated by using 1% TFA/CH_2Cl_2 (5 mL). The reaction mixture was allowed to shake for 5 minutes. The reaction mixture was evaporated to dryness. The crude product was dried in a desiccator over silica gel.

3.2.2.3 Synthesis of mutant linear lugdunin (cysteine)

The crude linear peptide (NH_2-(D)Val-Val-Cys(Trt)-(D)Val-Trp(Boc)-(D)Leu-Val-OH) was treated with 97.5% TFA in CH_2Cl_2 for 1 hour. The reaction mixture was evaporated to dryness and purified with preparative HPLC as described in details (3.2.1.7) to afford a mutant lugdunin (NH_2-(D)Val-Val-Cys-(D)Val-Trp-(D)Leu-Val-OH (59 %, 0.007 g). The molecular weight was verified by using ESI-MS spectrometry**.** Found; 1082.7 $[M+2TFA+K]^+$; Calculated 817.0529 $[M]^+$

3.2.2.4 Synthesis of mutant cyclic lugdunin (cysteine)

The crude linear peptide (NH_2-(D)Val-Val-Cys(Trt)-(D)Val-Trp(Boc)-(D)Leu-Val-OH) (0.0200 g, 0.0145 mmol) was cyclized by using HATU (1.5 eq., 0.0083 g, 0.0280 mmol) and DIPEA (3 eq., 0.0074 mL, 0.0436 mmol) as coupling reagents under a very high dilution condition (1 mg/2 mL). The reaction mixture was allowed to stir overnight at room temperature. The reaction mixture was then evaporated to dryness. Finally, the fully protected cyclic peptide was treated by 97.5% TFA in CH_2Cl_2, and subsequently purified by preparative HPLC as described in details (3.2.1.7) to afford a mutant cyclic lugdunin (26 %, 0.0030 g). The molecular mass of a mutant cyclic lugdunin was verified by using ESI-MS spectrometry. Found; 1063.4 $[M+2TFA+K]^+$ and 1149.2 $[M+2TFA+2ACN+K]^+$; Calculated 799.0376 $[M]^+$

CHAPTER 4
RESULTS AND DISCUSSION

4.1 The synthetic strategy of lugdunin

As mentioned in previous chapter, the structure of lugdunin is a cyclic scaffold, consisting of six amino acid residues, ranging from (D)-Val, Val-Thiazolidine, (D)-Val, Trp, (D)-Leu to Val. This is further included the presence of a thiazolidine moiety. To this research, the synthetic strategy of lugdunin was classified into three important parts; (1) the synthesis of a thiazolidine derivative, (2) an amino acid assembly and (3) a peptide cyclization. The synthesis of a thaizolidine derivative was firstly achieved *via* the condensation between L-cysteine and Fmoc-Val-H as the precursors. While, an amino acid assembly strategy was carried out by using Fmoc based solid phase peptide synthesis (SPPS). Notably, the cyclization of a linear scaffold was performed under a very high dilution condition *via* an intramolecular cyclization.

According to the retro-synthesis of lugdunin (**15**) shown in **Scheme 4.1.** Firstly, the connecting point for the intramolecular peptide cyclization was chosen. In this case, an amide bond between Val^5 and (D)-Val^6 was selected mainly due to the least steric hindrance relative to other bulky amino acids (Tryptophan and Isoleucine), which directly affected to the peptide cyclization efficacy. The orthogonal Boc protecting group was successfully applied for the protection of tryptophan side chain to avoid an unexpected coupling at the tryptophan side chain during an amino acid assembly. Additionally, Fmoc based solid phase peptide synthesis was chosen for an amino acid assembly of a linear lugdunin precursor (compound **11**) mainly owing to a mild condition used for an amino acid assembly when compared to that of the Boc strategy. For instance, TFA has been extensively used in a number steps for the Boc strategy. In contrary to Fmoc strategy, TFA was used only one step for the peptide cleavage. Next, Fmoc-Val-OH was converted to aldehyde *via* a carboxyl activation followed by a selective reduction. Lastly, Fmoc-Val-thiazolidine-OH (**3**) precursor was constructed between Fmoc-Val-H (**2**) and Cysteine.

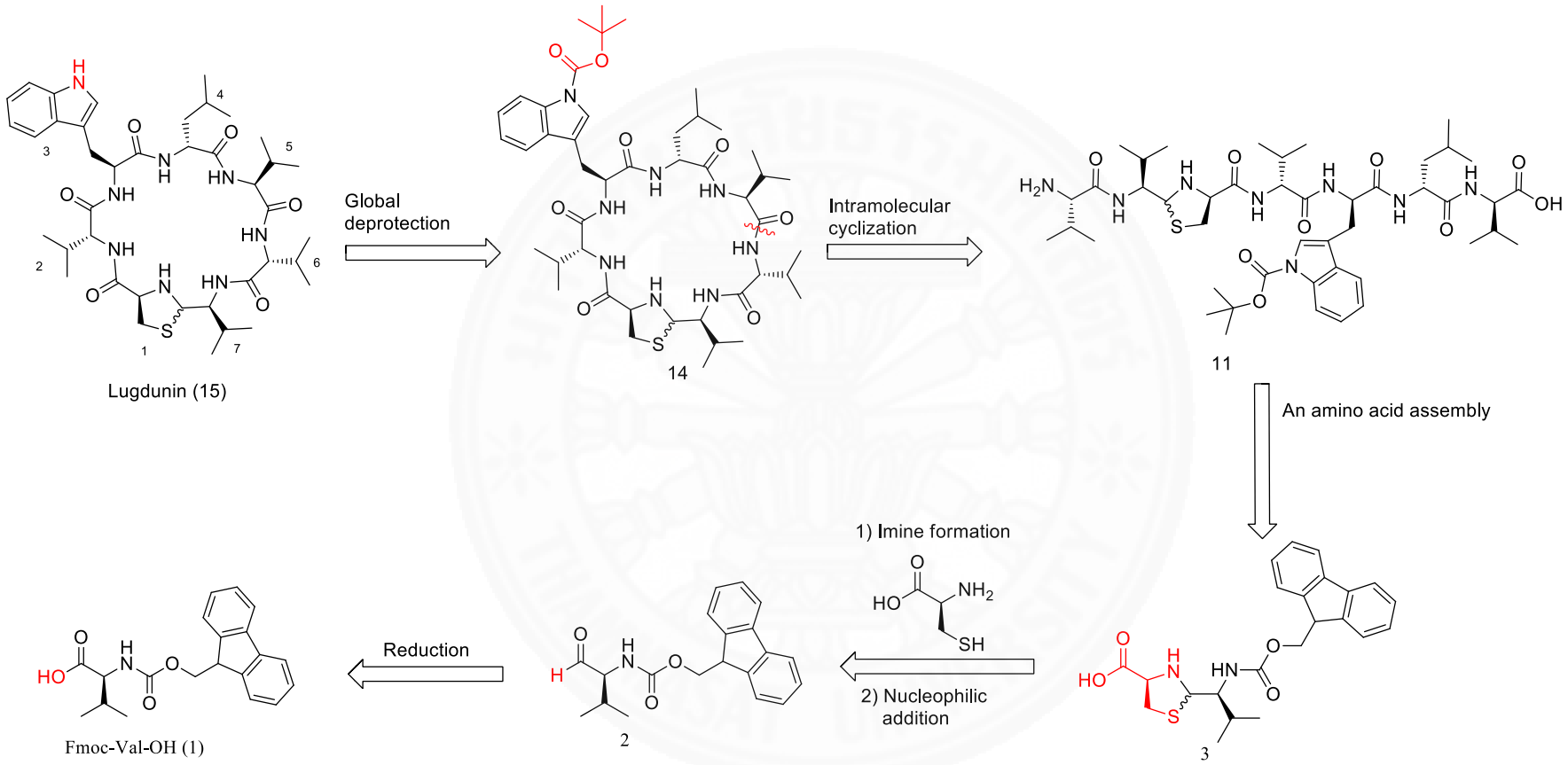

Scheme 4.1 Retro-synthetic analyses of lugdunin

According to the retro-synthetic strategy as shown in **Scheme 4.1**, the synthesis of Fmoc-Val-H as an aldehyde precursor *via* the selective reduction of Fmoc-Val-OH was initially proposed, and the synthetic detail was described in details as follows:

4.2 The synthesis of Fmoc-Val-H

An amino aldehyde (Fmoc-Val-H) was successfully synthesized *via* the reduction of Fmoc-Val-OH in two consecutive steps as shown in **Scheme 4.2**. Firstly, Fmoc-Val-H was synthesized by the carboxyl activation of Fmoc-Val-OH *via* 1,1'-carbonyldiimidazole (CDI) as an activating agent at 0°C, following by a selective reduction by using DIBAL carried out at very low temperature (-78°C) to avoid an over-reduction of Fmoc-Val-OH (**Scheme 4.2**). Additionally, the reduction of Fmoc-Val-OH *via* DIBAL-H was performed under the nitrogen atmosphere to yield Fmoc-Val-H in a moderate yield (61 %). To our study, a varied amount of used DIBAL for the selective reduction of Fmoc-Val-OH was further optimized, and it was found that the reduction of Fmoc-Val-OH with only small amount of DIBAL-H (1 or 2 equivalents) did not take place. This could be ascribed as the result of the unwanted reduction of 1,1'-carbonyldiimidazole, which effectively decreased the received Fmoc-Val-H. In order to solve this problem, an amount of DIBAL-H was increased up to 3.0, 5.0 and 7.0 equivalents, and it was observed that when we increased an amount of DIBAL up to 3.0 equivalents, the amount of Fmoc-Val-H was found to be only 24%. However, when the equivalent of DIBAL-H was escalated to be 5.0 and 7.0 equivalents, respectively as shown in **Table 4.1**, we noticed that the yield of Fmoc-Val-H was found to increase (61%) in the case of 5.0 equivalent. Unfortunately, the over-reduction of Fmoc-Val-OH was markedly observed to give Fmoc-Val-alcohol as the major product in the case of 7.0 equivalent. The results were shown in **Table 4.2**.

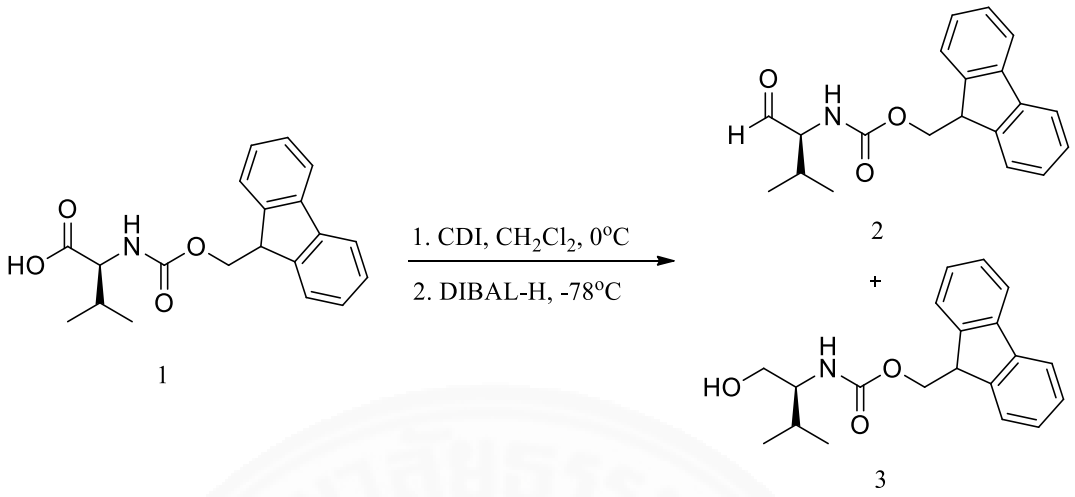

Scheme 4.2 The synthesis of Fmoc-Val-H

Table 4.1 The syntheses of Fmoc-Val-H using the CDI/DIBAL-H

No.	Equivalent of Fmoc-Val-OH	Equivalent of CDI	Equivalent of DIBAL-H	Color	% yield
1	1.0	1.2	1.0	-	-
2	1.0	1.2	2.1	-	-
3	1.0	1.5	3.0	Colorless/oil	24
4	**1.0**	**1.5**	**5.0**	**Colorless/oil**	**61**
5	1.0	1.5	7.0	Colorless/oil	38

The Fmoc-Val-H was subsequently characterized by using ^{1}H-NMR, ^{13}C-NMR, FTIR and ESI-MS spectroscopy as follows:

4.2.1 Characterization of Fmoc-Val-H

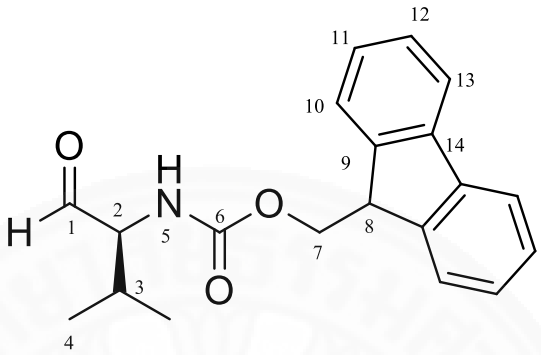

Figure 4.1 Structure of Fmoc-Val-H (**2**)

Name: Fmoc-Val-H (**2**)

Chemical formula: $C_{20}H_{21}NO_3$

ESI-MS: Found 346.1408$[M+Na]^+$ and 378.1652$[M+CH_3OH+Na]^+$; Calculated 323.3864 $[M]^+$

IR (NaCl): ν_{max} 3332, 2926, 1712, 1517, 1450 and 1234 cm^{-1}

^{1}H-NMR (600 MHz, $CDCl_3$), δ = 0.94-1.03 (dd, *J* = 10.2, 41.7 Hz, 6H), 2.28-2.31 (m, *J* = 6.6 Hz, 1H), 4.20-4.23 (t, *J* = 10.2 Hz, 1H), 4.31-4.34 (q, *J* = 6.0 Hz, 1H), 4.39-4.41 (d, *J* = 10.8 Hz, 2H), 5.34-5.35 (d, *J* = 10.8 Hz, 1H), 7.28-7.32 (t, *J* = 11.4 Hz, 2H), 7.36-7.40 (t, *J* = 11.4 Hz, 2H), 7.57-7.59 (d, *J* = 10.8 Hz, 2H), 7.74-7.76 (d, *J* = 10.8 Hz, 2H) and 9.64 (s, 1H).

^{13}C-NMR (150 MHz, $CDCl_3$), δ (ppm): 17.6, 29.1, 47.2, 65.0, 67.0, 120.0, 125.0, 127.1, 127.7, 142.0, 145.0, 155.0 and 200.0.

Table 4.2 ^{1}H-NMR and ^{13}C-NMR of Fmoc-Val-H (**4**)

Position number	Fmoc-Val-H	
	^{1}H-NMR, **δ** (ppm)	^{13}C-NMR, **δ** (ppm)
1	9.64 (s, 1H)	200.0
2	4.31-4.34 (q, *J* = 6.0, 1H)	65.0
3	2.28-2.31 (m, *J* = 6.6, 1H)	29.1
4	0.94-1.03 (dd, *J* = 10.2, 41.7 6H)	17.6
5	5.34-5.35 (d, *J* = 10.8, 1H)	-
6	-	155.0
7	4.39-4.41 (d, *J* = 10.8, 2H)	67.0
8	4.20-4.23 (t, *J* = 10.2, 1H)	47.2
9	-	145.0
10	7.57-7.59 (d, *J* = 10.8, 2H)	125.0
11	7.28-7.32 (t, *J* = 11.4, 2H)	127.1
12	7.36-7.40 (t, *J* = 11.4, 2H)	127.7
13	7.74-7.76 (d, *J* = 10.8, 2H)	120.0
14	-	142.0

According to ^{1}H-NMR spectrum of Fmoc-Val-H, it showed proton signals (δ) at 0.94-1.03 corresponding to the presence of methyl group (C4). The proton signals (δ) at 2.28-2.31 and 4.20-4.23 ppm in ^{1}H-NMR spectrum corresponding to the methine proton at C3 (-CH-) and C8 (-CH-), respectively. The methine proton signal (δ) of C2 (-CH-) and a methylene proton signal (δ) at C7 (-CH_2-) was found at 4.31-4.34 and 3.39-4.41 ppm, respectively. The methine protons of aromatic ring were observed at δ = 7.57-7.59, 7.28-7.32, 7.36-7.40 and 7.74-7.76 ppm, respectively. An aldehyde proton signal (δ) was observed at 9.64 ppm. From the ^{13}C-NMR spectra, the carbonyl group (-CO-) of aldehyde was presented at δ = 200 ppm. The carbon signal (δ) of C2 (-CH-), C3 (-CH-), C4 (-CH_3-) and C6 (-CO_2-) was observed at 65.0, 29.1, 17.6 and 155.0 ppm, respectively. The presence of carbon signal (δ) at 67.0 and 47.2 ppm corresponded to C7 (-CH_2-) and C8 (-CH-), respectively. The aromatic carbon

signal (δ) of Fmoc- group (C9, C10, C11, C12, C13 and C14) was observed at 145.0, 125.0, 127.1, 127.7, 120.0 and 142.0 respectively. According to FTIR results, NH and CH stretching were clearly observed at 3,332 and a strength sharp at 2,926 cm^{-1}. The two peaks of carbonyl stretching were presented with a strength sharp peak at 1712 and 1517 cm^{-1}. According to ESI-MS analyses, it showed the molecular mass adduct at 346.1408 m/z corresponding to $[M+Na]^+$, while, the molecular mass of Fmoc-Val-H was calculated to be 323.3864 m/z. Additionally, the molecular mass signal of methanol adduct $[M+ CH_3OH+Na]^+$ was also observed at 378.1652 m/z. From this result, it clearly indicated that the synthetic compound was confirmed to be Fmoc-Val-H (**2**).

The Fmoc-Val-H was successfully synthesized, and the synthetic strategy of Fmoc-Val-thiazolidine-OH was further proposed. The synthetic pathway of Fmoc-Val-thiazolidine-OH was described as follows.

4.3 The synthesis of Fmoc-Val-thiazolidine-OH

Fmoc-Val-thiazolidine-OH was successfully synthesized *via* an imine formation together with the nucleophilic addition of a sulfur as a nucleophile. The condensation between Cysteine and Fmoc-Val-H was performed, and the reaction mechanism could be described by the formation of an imine which was subsequently attacked by a sulfur nucleophile to generate Fmoc-Val-thiazolidine-OH in a great yield (38%). The mechanism could be described as follows. Firstly, Fmoc-Val-H precursor was condensed with Cysteine in absolute ethanol at ambient temperature as shown in **Table 4.3**. Under this reaction condition, Fmoc-Val-H did not react properly with Cysteine because of the solubility limitation of Cysteine in ethanol. The precipitation of Cysteine was obviously noticeable in ethanol. The sediment of Cysteine was found in the reaction mixture after 2-3 hours after reaction setting up. To overcome the solubility problem, Cysteine was dissolved with a small amount of H_2O and then condensed with Fmoc-Val-H precursor using 50% ethanol/H_2O as an optimized reaction condition. However, the precipitation of Cysteine was also observed under this optimized reaction condition. Therefore, the change of pH was further investigated in the presence of $NaHCO_3$, Na_2CO_3 and NaOH. Firstly, Cysteine was deprotonated by adding $NaHCO_3$, Na_2CO_3 and NaOH respectively to increases the solubility of Cysteine. Unfortunately, Fmoc-Val-thiazolidine-OH did not take place under this studied basic condition as shown in **Table 4.3.** In order to elevate the solubility of Cysteine, Cysteine methyl ester hydrochloride was utilized instead of Cysteine. To this approach, the reaction was allowed to reflux for 1 hour. Under this reaction condition, the resulting product was observed, and subsequently characterized using ^{1}H-NMR, ^{13}C-NMR and ESI-MS. Unfortunately, we clearly identified Fmoc-Val-acetal instead of Fmoc-Val-Thiazolidine under this optimized condition as displayed in **Table 4.3**. Interestingly, we also noticed that when an aldehyde precursor reacted with Cysteine hydrochloride monohydrate using ethanol as solvent, and allowed the reaction

overnight without refluxing leading to the formation of Fmoc-Val-thiazolidine-OH (38%) as shown in **Scheme 4.3**. The structure of Fmoc-Val-Thiazolidine was subsequently confirmed by using ^{1}H-NMR spectroscopy along with ESI-MS spectroscopy.

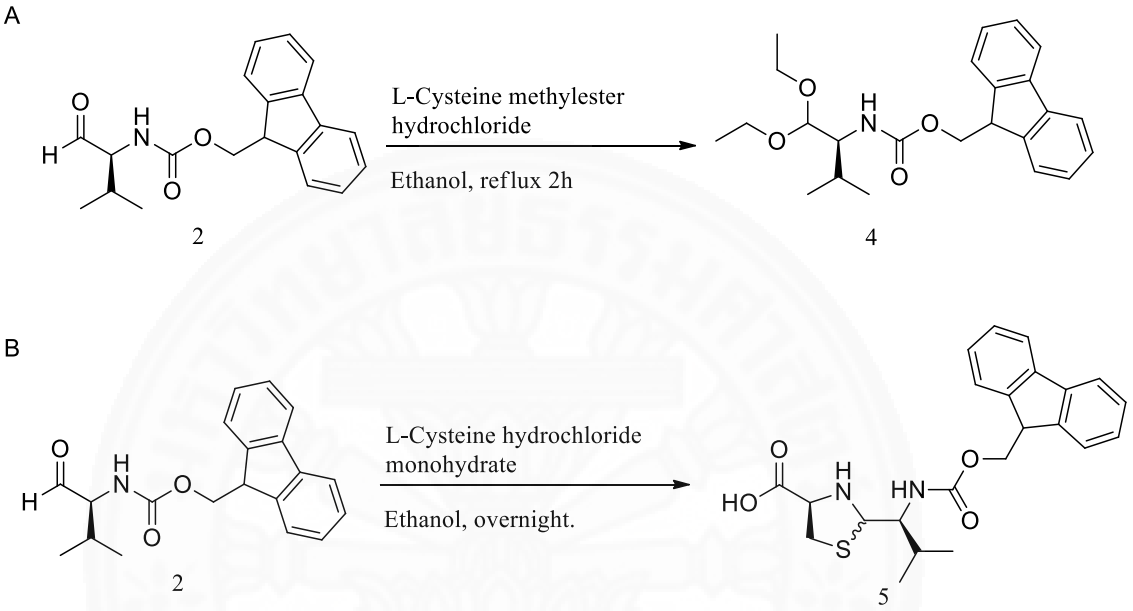

Scheme 4.3 (A) Formation of Fmoc-Val-acetal, (B) synthesis of Fmoc-Val-thiazolidine-OH

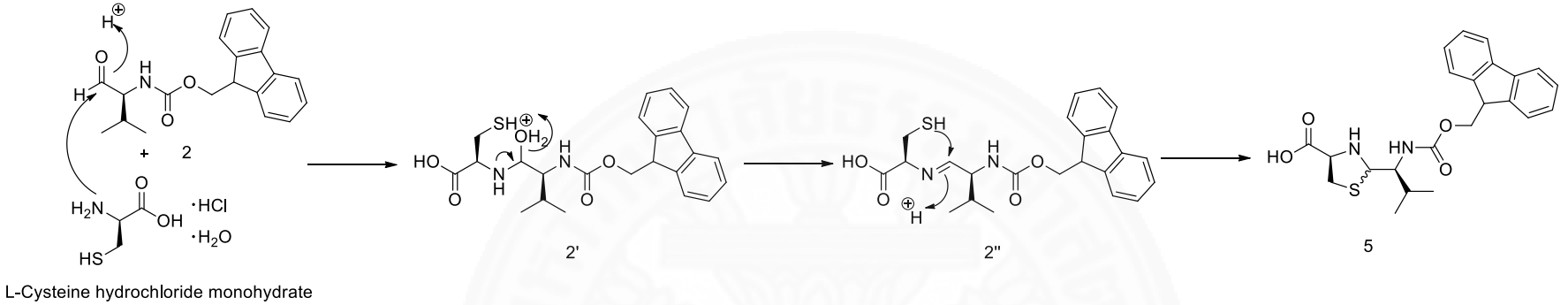

Scheme 4.4 The Fmoc-Val-thiazolidine-OH synthesis mechanism

Table 4.3 Synthesis of Fmoc-Val-thiazolidine-OH

NO.	Fmoc-Val-H (eq.)	L-Cysteine (eq.)	L-Cysteine methyl ester·HCl (eq.)	L-Cysteine hydrochloride monohydrate (eq.)	$NaHCO_3$ (eq.)	Na_2CO_3 (eq.)	NaOH (eq.)	Solvent	% yield
1	1.0	1.0	-	-	-	-	-	Ethanol	-
2	1.0	1.0	-	-	-	-	-	Ethanol/H_2O	-
3	1.0	1.0	-	-	1.0	-	-	Ethanol/H_2O	-
4	1.0	1.0	-	-	-	1.0	-	Ethanol/H_2O	-
5	1.0	1.0	-	-	-	-	1.0	Ethanol/H_2O	-
6	1.0	-	1.0	-	-	-	-	Ethanol	-
7	**1.0**	**-**	**-**	**1.0**	**-**	**-**	**-**	**Ethanol**	**38**

Fmoc-Val-thiazolidine-OH was subsequently characterized by using ^{1}H-NMR, FTIR and mass spectrometry as follows:

4.3.1 Characterization of Fmoc-Val-thiazolidine-OH

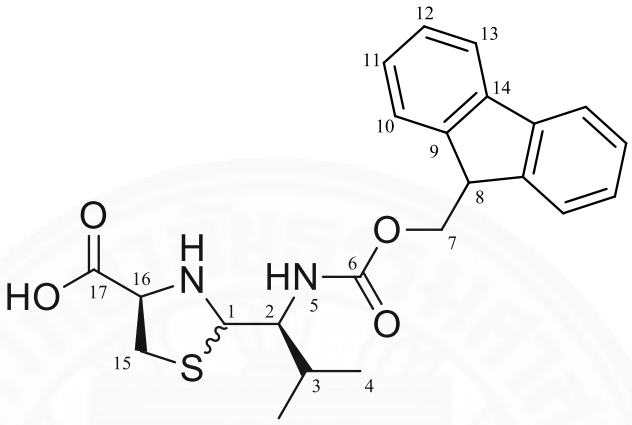

Figure 4.2 Structure of Fmoc-Val-thiazolidine-OH

Name: Fmoc-Val-thiazolidin-OH (**3**)

Chemical formula: $C_{23}H_{26}N_2O_4S$

ESI-MS: Found 427.8$[M+H]^+$; Calculated 426.5305 $[M]^+$

IR (NaCl): ν_{max} 3407, 2927, 1710, 1605 and 1432 cm^{-1}

^{1}H-NMR (600 MHz, methanol-d_4), δ (ppm): δ = 0.93-1.01 (dd, *J* = 6.7, 38.6 Hz, 6H), 1.79-1.82 (m, 1H), 3.25-3.28 (dd, *J* = 6.4, 9.9 Hz, 2H), 3.62-3.64 (dd, *J* = 6.5, 9.7 Hz, 1H), 3.85-3.87 (dd, *J* = 4.3, 7.6 Hz, 1H), 4.26-4.28 (t, *J* = 6.6 Hz, 1H), 4.35-4.47 (m, 1H), 4.76 (d, *J*=4.2, 2H), 7.32-7.34 (m, 2H), 7.39-7.41 (t, *J* = 7.0 Hz, 2H), 7.69-7.73 (m, 2H) and 7.81-7.82 (d, *J* = 7.5 Hz, 2H)

Table 4.4 ^{1}H-NMR and ^{13}C-NMR of Fmoc-Val-thiazolidine-OH (**3**)

Position number	Fmoc-Val-H
	^{1}H-NMR, **δ** (ppm)
1	4.35-4.47 (m, 1H)
2	3.85-3.87 (dd, *J* = 4.3, 7.6 Hz, 1H)
3	1.79-1.82 (m, 1H)
4	0.93-1.01 (dd, *J* = 6.7, 38.6 Hz, 6H)
5	-
6	-
7	4.76 (d, *J*=4.2, 2H)
8	4.26-4.28 (t, *J* = 6.6 Hz, 1H)
9	-
10	7.69-7.73 (m, 2H)
11	7.32-7.34 (m, 2H)
12	7.39-7.41 (t, *J* = 7.0 Hz, 2H)
13	7.81-7.82 (d, *J* = 7.5 Hz, 2H)
14	-
15	3.25-3.28 (dd, *J* = 6.4, 9.9 Hz, 2H)
16	3.62-3.64 (dd, *J* = 6.5, 9.7 Hz, 1H)
17	-
18	-

The proton signals (δ) at 0.93-1.01 and 1.79-1.82 ppm in ^{1}H-NMR spectra corresponded to C3 (-CH_3) and C4 (-CH-) of valine side chain, respectively. The proton signals (δ) of C15 (-CH_2) and C16 (-CH-) of thiazolidine ring were presented at δ = 3.25-3.28 and 3.62-3.64 ppm. The methine proton attached with C1 (-CH-) of thiazolidine ring was observed at 4.35-4.47 ppm. The ^{1}H-NMR signals at δ = 4.76 and 4.26-4.28 ppm were corresponded to C7 (-CH_2-) and C8 (-CH-) respectively. The methine proton signal (δ) at C2 (-CH-) showed at 3.85-3.87 ppm. The proton signals (δ) of aromatic ring of Fmoc region at C10, C11, C12 and C13 were presented

at 7.69-7.73 (-CH-), 7.32-7.34 (-CH-), 7.39-7.41 (-CH-) and 7.81-7.82 (-CH-) respectively. According to the FTIR spectra, it showed a broad peak of -OH at 3,407 cm^{-1}. The IR signal of two carbonyl group was presented a sharp peak at 1710 and 1605 cm^{-1}, respectively. Additionally, the ESI-MS results showed the observed molecular mass (m/z) at 427.8, corresponding to $[M+H]^+$, while the molecular mass was calculated to be 426.5303 amu. According all results, it clearly confirmed the formation of Fmoc-Val-thiazolidine-OH.

4.4 The syntheses of native and mutant lugdunins

4.4.1 Solid phase peptide synthesis (SPPS) of lugdunin

To the amino acid assembly of native and mutant lugdunins by using Fmoc based solid phase peptide synthesis (SPPS) approach, Fmoc-Val-OH was firstly loaded onto 2-chlorotrityl resin to afford Fmoc-Val-O-chlorotrityl resin (**7**). The percent loading of Fmoc-Val-O-2-chlorotrityl resin (**7**) was subsequently measured, and calculated to be 88% based on the Fmoc test as described in detail in **Section 3.2.1.3**. 2-Chlorotrityl resin was applied throughout the experiment mainly owing to their superior intrinsic properties, particularly its acid lability property of this resin which could be selectively cleaved by under mild acid condition (1% TFA/CH_2Cl_2) to obtain a free carboxyl linear peptide chain whereas all protecting groups along the side chain were kept. Next, the Fmoc-Val-O-chlorotrityl resin (**7**) was treated with 20% piperidine/DMF to afford NH_2-Val-O-chlorotrityl resin, which subsequently coupled with Fmoc-D-Leu-OH by using DCC and DMAP as standard coupling agents whereas HOBt was applied as an additive to prevent the racemization, affording the Fmoc-D-Leu-Val-O-chlorotrityl resin (**8**). Then, Fmoc-D-Leu-Val-O-chlorotrityl resin was treated with 20% piperidine/DMF, and subsequently coupled with Fmoc-Trp(Boc)-OH under an optimized condition as previously described to afford Fmoc-Trp(Boc)-D-Leu-Val-O-chlorotrityl resin (**9**). An amino acid assembly was repeatedly performed by the coupling of Fmoc-D-Val-OH, Fmoc-Val-thiazolidine-OH and Fmoc-D-Val-OH, respectively to afford Fmoc-(D)Val-Val-thiazolidine-(D)Val-Trp(Boc)-(D)Leu-Val-O-chlorotrityl resin (**10**). A linear peptide precursor attached to chlorotrityl resin was treated with 20% piperidine/DMF to deprotect an Fmoc- protecting group. Finally, NH_2-(D)Val-Val-thiazolidine-(D)Val-Trp(Boc)-(D)Leu-Val-O-chlorotrityl resin was treated with 1% TFA/CH_2Cl_2 to afford a free carboxyl linear peptide chain of NH_2-(D)Val-Val-thiazolidine-(D)Val-Trp(Boc)-(D)Leu-Val-OH (**11**) with a yield of 33% as shown in **Scheme 4.5**. It is very important to note that an amino acid assembly of Fmoc-Val-thiazolidine-OH was performed by pre-activation of Fmoc-Val-thiazolidine-OH prior to the coupling step in order to enhance the coupling efficacy, mainly due to the steric hindrance of a thiazolidine moiety. In addition, the coupling period was also

doubled. To this synthetic strategy, an aminium based coupling agents were applied for an amino acid assembly to increase the coupling efficacy and to reduce the coupling period. 2-(6-chloro-1H-benzotriazole-1-yl)-1,1,3,3-tetramethylaminium hexafluorophosphate (HCTU) is an example of highly reactive aminium based coupling agents, being used for this amino acid assembly instead of DCC. To the coupling step *via* HCTU, the carboxyl group at an amino terminus was pre-activated by HCTU, and an activation period was allowed for an hour following by the coupling step. Notably, the resulting yield of NH_2-(D)-Val-Val-thiazolidine-(D)-Val-Trp(Boc)-(D)-Leu-Val-OH (**11**) was found to increase with a decreased coupling period when using HCTU as a coupling agent. The HPLC traces of NH_2-(D)Val-Val-thiazolidine-(D)Val-Trp(Boc)-(D)Leu-Val-OH are shown in **Figure 4.3**.

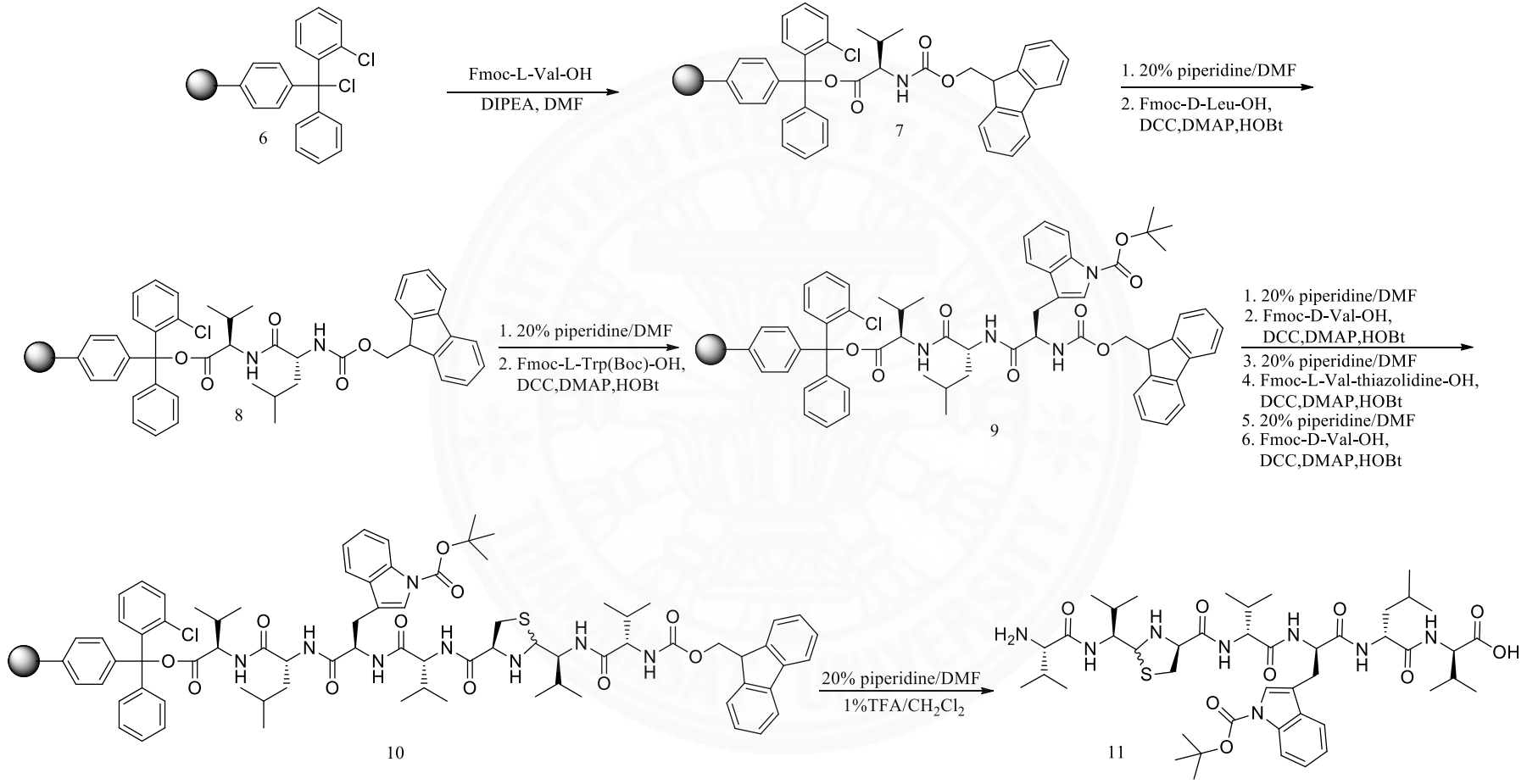

Scheme 4.5 Synthesis of NH_2-(D)Val-Val-Thiazolidine-(D)Val-Trp(Boc)-(D)Leu-Val-OH (**11**)

A

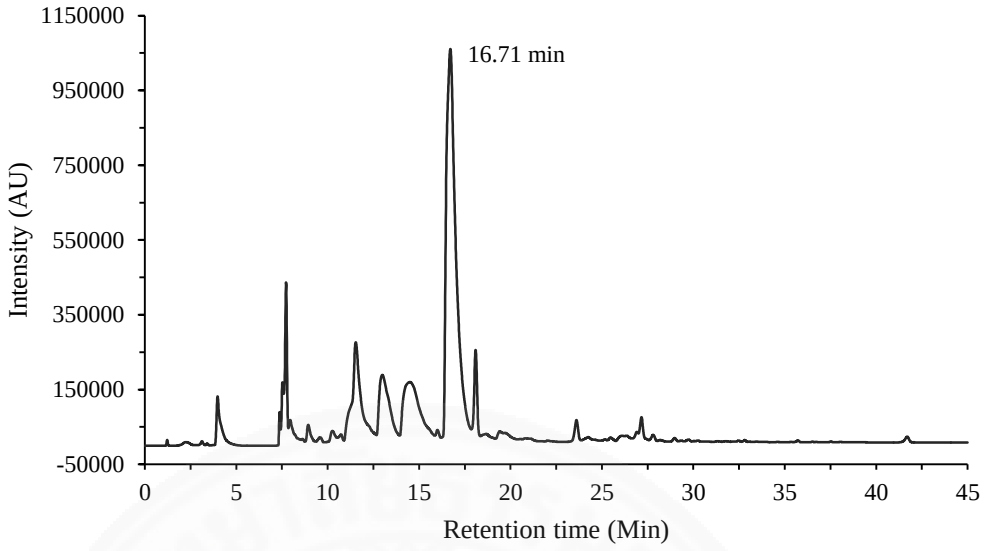

B

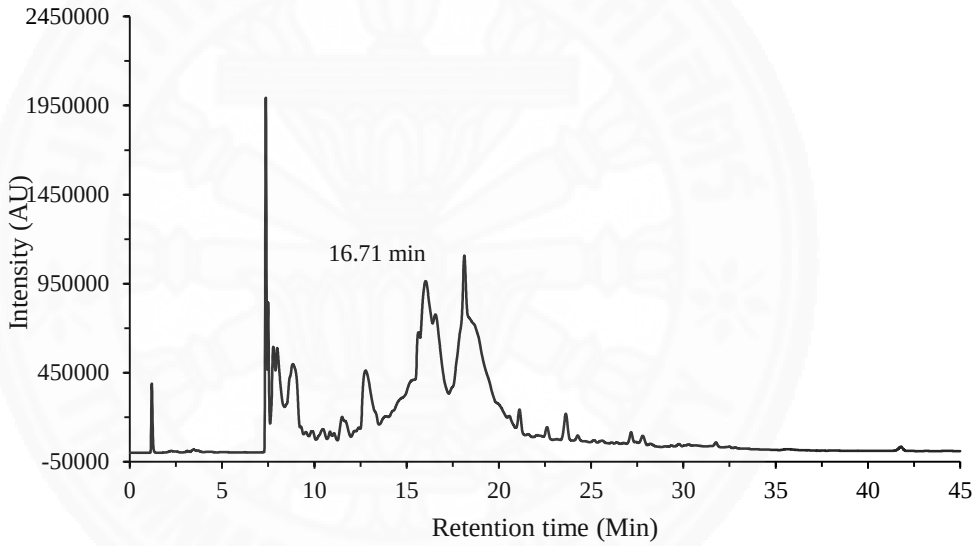

Figure 4.3 HPLC chromatogram of NH_2-(D)Val-Val-thiazolidine-(D)Val-Trp(Boc) -(D)Leu-Val-OH by using DCC (A) and HCTU (B) as a coupling reagent measured at 215 nm

According to the comparison of HPLC chromatogram between the couple *via* DCC and HCTU was presented in **Figure 4.3** A and B respectively. When using HCTU as a coupling agent (30 min), the yield of NH_2-(D)Val-Val-thiazolidine-(D)Val-Trp(Boc)-(D)Leu-Val-OH was found to increase with a short coupling period (30 min), and the purity of NH_2-(D)Val-Val-thiazolidine-(D)Val-Trp(Boc)-(D)Leu-Val-OH was decreased relative to those of products synthesized by using DCC as a

coupling agents. The decrease of purity was ascribed as a result of the solubility limitation of Fmoc-Val-thiazolidine-OH in DMF. However, Fmoc-Val-thiazolidine-OH was found to be well-dissolved in water. As a result, the obtained yield and the purity of NH_2-(D)Val-Val-thiazolidine-(D)Val-Trp(Boc)-(D)Leu-Val-OH coupled by using DCC was relatively high when compared to NH_2-(D)Val-Val-thiazolidine-(D)Val-Trp(Boc)-(D)Leu-Val-OH coupled by using HCTU mainly due to moisture insensitive properties of DCC in the presence of water. Hence, DCC was subsequently selected for an amino acid assembly approach.

It is very important to note that a carboxyl pre-activation of Fmoc-Val-thiazolidine-OH was significantly necessary at an amino acid assembly step. The linear peptide chain without thiazolidine ring (NH_2-(D)Val-(D)Val-Trp(Boc)-(D)Leu-Val-OH) was identified as a major component for an amino acid assembly when no pre-activation of Fmoc-Val-thiazolidine-OH was performed. Then, a linear NH_2-(D)Val-(D)Val-Trp(Boc)-(D)Leu-Val-OH was globally deprotected with 95% TFA in CH_2Cl_2 to afford NH_2-(D)Val-(D)Val-Trp-(D)Leu-Val-OH (**12**) (**Figure 4.4**), which was subsequently characterized by using ESI-MS spectroscopy and the purity was confirmed by using analytical HPLC as shown in **Figure 4.5**.

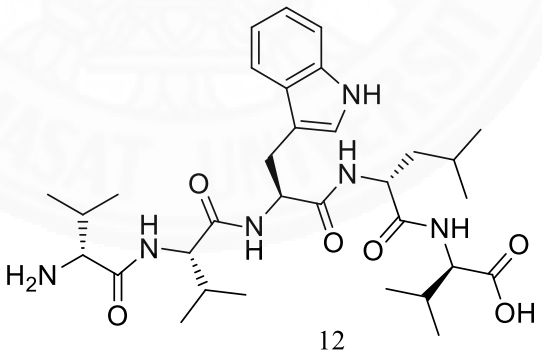

12

Figure 4.4 Chemical structure of NH_2-(D)Val-(D)Val-Trp-(D)Leu-Val-OH (**12**)

Name: NH_2-(D)Val-(D)Val-Trp-(D)Leu-Val-OH (**12**)

Chemical formula: $C_{32}H_{50}N_6O_6$

ESI-MS: Found 615.2 $[M+H]^+$; Calculated 614.7774 $[M]^+$

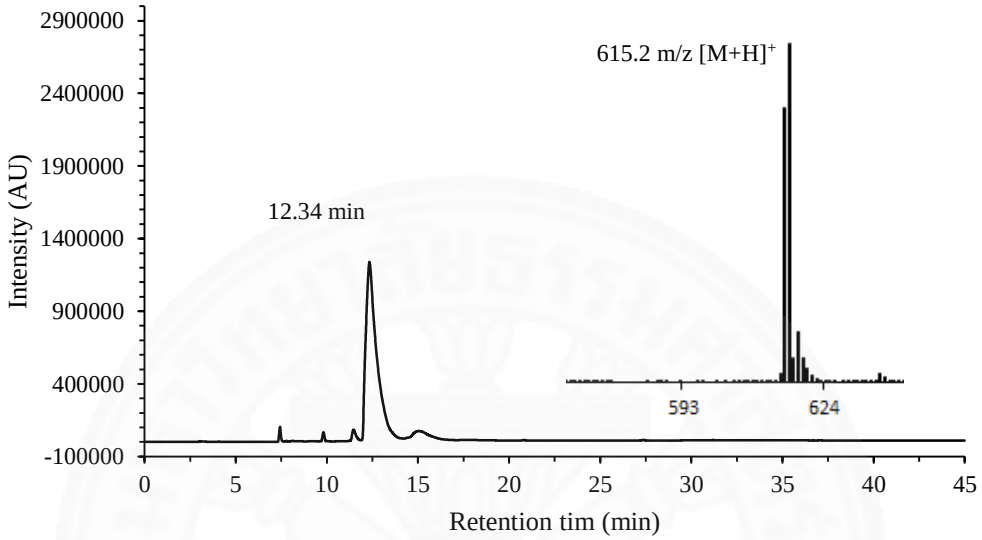

Figure 4.5 HPLC chromatogram and ESI-MS spectra of NH_2-(D)-Val-(D)-Val-Trp-(D)-Leu-Val-OH (**12**)

The ESI-MS spectra of NH_2-(D)Val-(D)Val-Trp-(D)Leu-Val-OH (12) showed the molecular mass adduct $[M+H]^+$ signal at 615.2 amu, when the molecular mass was calculated to be 614.7774 amu. The retention time of NH_2-(D)-Val-(D)-Val-Trp-(D)-Leu-Val-OH (**12**) was presented at 12.3 min. This clearly confirmed that the synthetic peptide was NH_2-(D)Val-(D)Val-Trp-(D)Leu-Val-OH (**12**).

4.4.2 The Synthesis of mutant lugdunin (a linear scaffold)

A mutant lugdunin was successfully synthesized according to Fmoc based SPPS as described previously. The fully protected (NH_2-(D)Val-Val-Thiazolidine-(D)Val-Trp(Boc)-(D)Leu-Val-OH) was globally deprotected by using 95% TFA in CH_2Cl_2, and allowed for an hour to afford NH_2-(D)Val-Val-Thiazolidine-(D)Val-Trp-(D)Leu-Val-OH (**13**) (79%) (**Figure 4.6**) as shown in **Scheme 4.6**. The purity of resulting linear peptide was verified, and characterized by using ESI-MS.

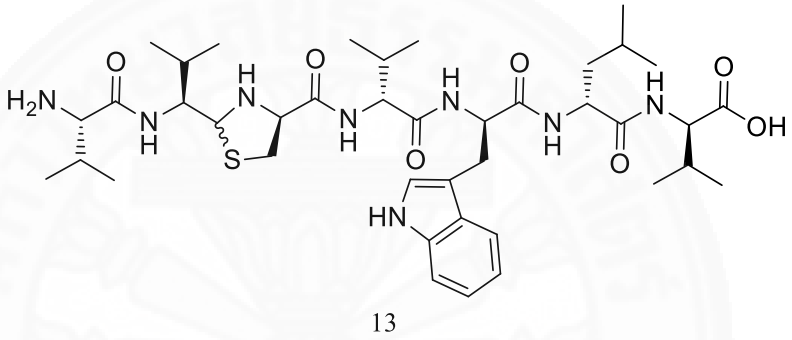

13

Figure 4.6 Structure of NH_2-(D)-Val-Val-Thiazolidine-(D)-Val-Trp-(D)-Leu-Val-OH

NH_2-(D)-Val-Val-Thiazolidine-(D)-Val-Trp-(D)-Leu-Val-OH (**13**):

Chemical formula: $C_{40}H_{64}N_8O_7S$

ESI-MS: Found; 886.4 $[M+2MeOH+Na-2H]^-$, 513.9 $[M+2TFA-2H]^-$ and 341.0 $[M+2TFA-3H]^-$; Calculated 801.0535 $[M]^+$.

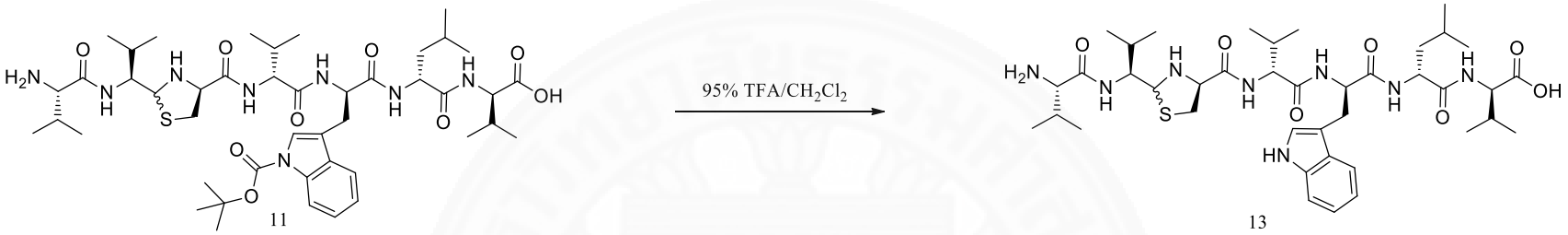

11 13

Scheme 4.6 Synthesis of NH_2-(D)-Val-Val-Thiazolidine-(D)-Val-Trp-(D)-Leu-Val-OH (**13**)

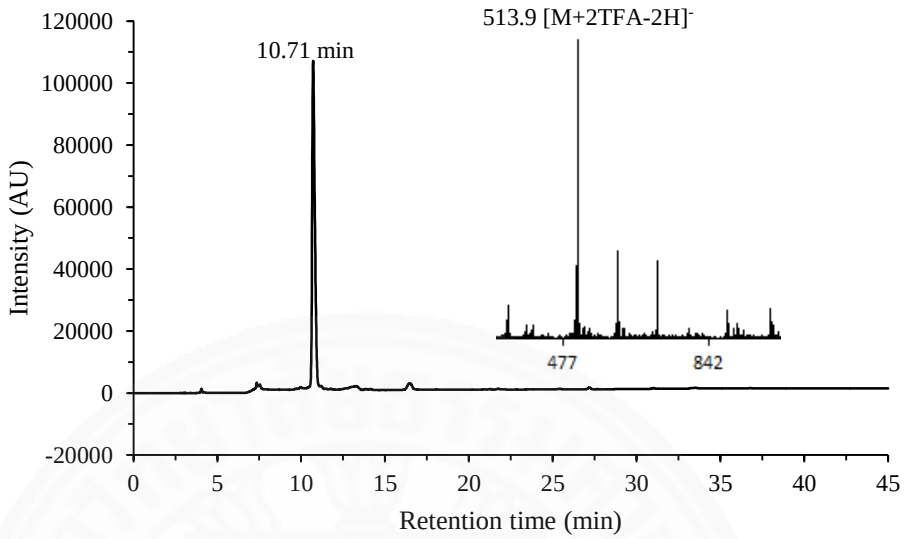

Figure 4.7 The HPLC chromatogram and ESI-MS spectra of NH_2-(D)-Val-Val-Thiazolidine-(D)-Val-Trp-(D)-Leu-Val-OH (**13**)

The purity of NH_2-(D)-Val-Val-Thiazolidine-(D)-Val-Trp-(D)-Leu-Val-OH (**13**) was verified by using analytical HPLC. According to the HPLC chromatogram, it showed the signal at 10.71 min (**Figure 4.7**). The ESI-MS spectrum of NH_2-(D)-Val-Val-Thiazolidine-(D)-Val-Trp-(D)-Leu-Val-OH (**13**) showed the molecular mass adduct $[M+2MeOH+Na-2H]^+$ at 886.4 amu. Also, the molecular mass signal of trifluoroacetic acid adduct $[M+2TFA-2H]^-$ and $[M+2TFA-3H]^-$ was also observed at 513 and 341 amu, respectively (**Figure 4.7**).

4.4.3 The synthesis of native lugdunin

NH_2-(D)Val-Val-Thiazolidine-(D)Val-Trp(Boc)-(D)Leu-Val-OH (**11**) was previously assembled according to Fmoc based SPPS. To the cyclization strategy, HATU was utilized as an effective coupling agent in the presence of DIPEA. HATU was selected for a linear peptide cyclization strategy because HATU was proven to be very efficient in difficult sterically hindered couplings and gave a low level of racemization as examplified by the syntheses of anti-bacterial peptide "cyclo-PLAI" by Inggriani.[38] To our synthetic strategy, the linear peptide precursor (NH_2-(D)Val-Val-Thiazolidine-(D)Val-Trp(Boc)-(D)Leu-Val-OH) (**11**) was successfully cyclized by using HATU and DIPEA as effective coupling agents. The cyclization of the linear precursor (NH_2-(D)Val-Val-Thiazolidine-(D)Val-Trp(Boc)-(D)Leu-Val-OH) was performed under a very high dilution condition (1 mg/2 mL), enabling the prevention of intermolecular dimerization effectively.[39] The resulting native lugdunin was confirmed with analytical HPLC measured at 215 nm as showed in **Figure 4.8**. It was seen that the retention time of the linear precursor (NH_2-(D)Val-Val-Thiazolidine-(D)Val-Trp(Boc)-(D)Leu-Val-OH) (**11**) and the protected cyclic lugdunin (**14**) were showed at 16.7 min and 30.9 min, respectively. This clearly indicated that the cyclization of the linear precursor (NH_2-(D)Val-Val-Thiazolidine-(D)Val-Trp(Boc)-(D)Leu-Val-OH) (**11**) was successful. Lastly, the fully protected lugdunin was globally deprotected using 95% TFA in CH_2Cl_2 to afford the native lugdunin (**15**) (48%). Next, the crude native lugdunin was subsequently purified using a preparative HPLC. The molecular mass of native lugdunin was verified using ESI-MS spectroscopy.

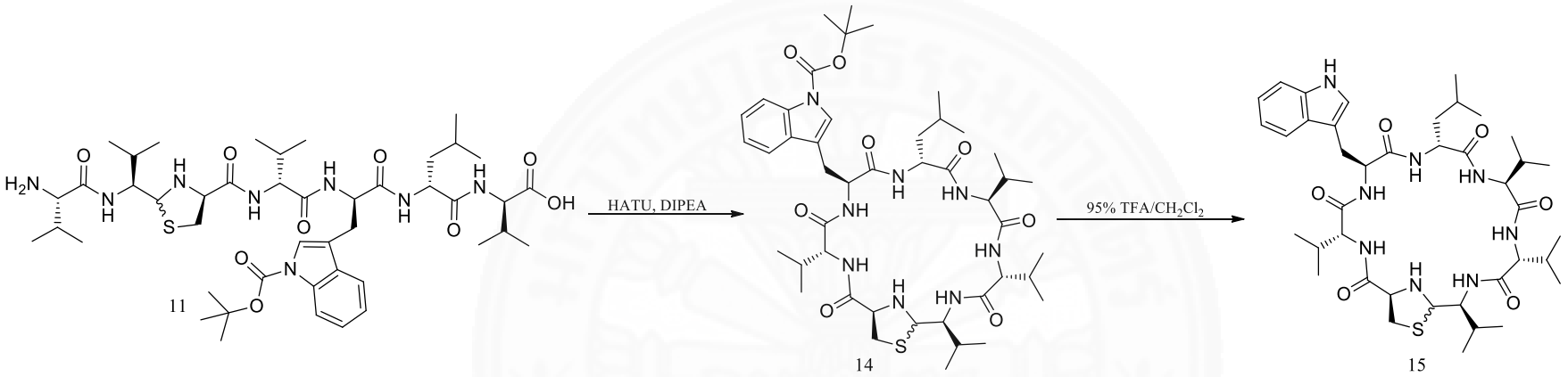

Scheme 4.7 The synthesis of native lugdunin (**15**)

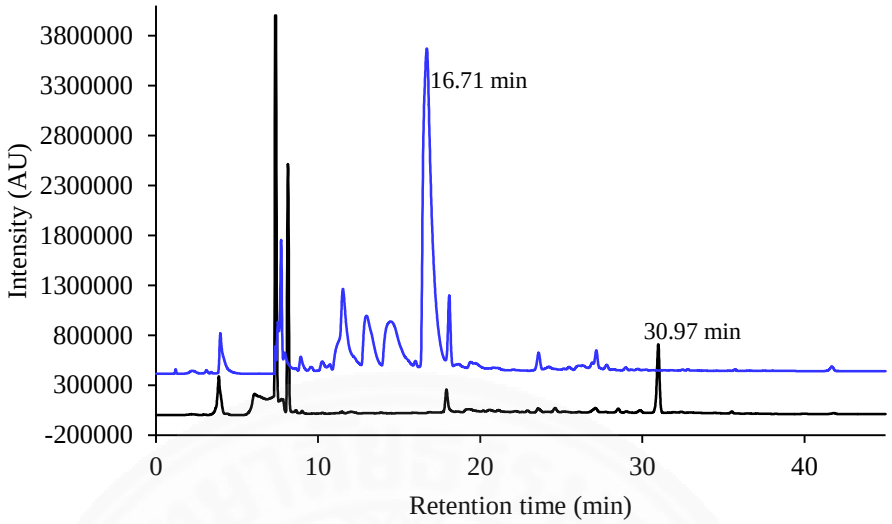

Figure 4.8 HPLC chromatogram of the protected linear peptide **11** (blue line) and cyclization reaction of lugdunin (black line)

4.4.3.1 Characterization of synthetic lugdunin

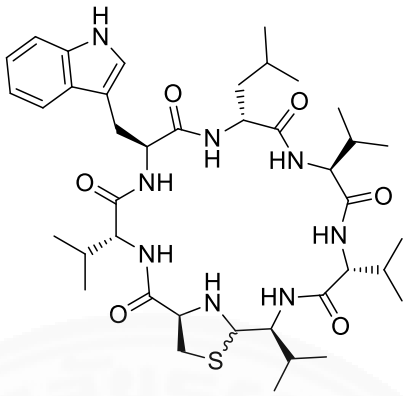

15

Figure 4.9 Structure of synthetic native lugdunin

Name: synthetic native lugdunin (**15**):

Chemical formula: $C_{40}H_{62}N_8O_6S$

ESI-MS: Found; 993.9 $[M+TFA+2MeOH+Cl]^-$; Calculated 783.0382 $[M]^+$

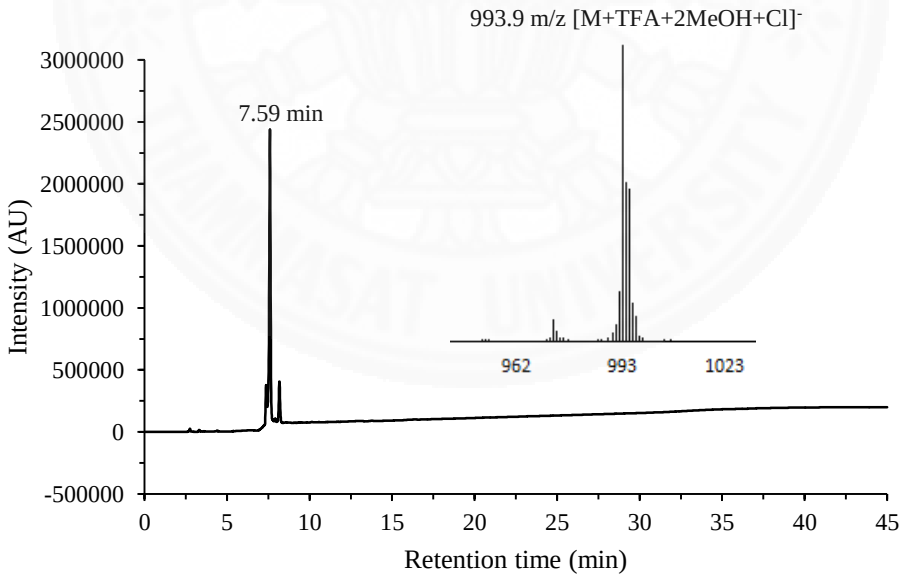

Figure 4.10 The HPLC chromatogram and ESI-MS spectrum of synthetic native lugdunin (**15**)

According to ESI-MS spectrum of native lugdunin, it demonstrated the molecular mass of trifluoroacetic acid and chloride adduct at 993.9 amu, corresponding to $[M+TFA+2MeOH+Cl]^+$ whereas the molecular mass $[M]^+$ was calculated to be 783.0382 amu.. The purity of native lugdunin was assessed by analytical HPLC, showing the signal at 7.59 min. From this result, this clearly indicated that native lugdunin (**15**) was successfully synthesized.

Additionally, the fully protected linear peptide (NH_2-(D)-Val-(D)-Val-Trp(Boc)-(D)-Leu-Val-OH) as previously assembled in 4.4.1 was successfully cyclized according to our developed condition (using HATU and DIPEA as coupling reagents). The cyclization of a fully protected linear peptide (NH_2-(D)Val-(D)Val-Trp(Boc)-(D)Leu-Val-OH) was greatly achieved under the similar optimized condition as seen in **Section 4.4.3**. However, the intermolecular dimerization was favorably achieved as a major product under this condition as shown in **Figure 4.12**, and the proposed mechanism is illustrated in **Scheme 4.8**. The formation of a fully protected intermolecular dimerization product could be ascribed as follows; (1) The fully protected linear peptide (NH_2-(D)Val-(D)Val-Trp(Boc)-(D)Leu-Val-OH) was intermolecular coupled with the other molecule of NH_2-(D)Val-(D)Val-Trp(Boc)-(D)Leu-Val-OH to afford the fully protected dimerized linear peptide (NH_2-(D)Val-(D)Val-Trp(Boc)-(D)Leu-Val-(D)Val-(D)Val-Trp(Boc)-(D)Leu-Val-OH) (**16**). (2) The fully protected dimer linear peptide was intramolecularly cyclized to afford a fully protected cyclo-dimerized peptide (D)Val-(D)Val-Trp(Boc)-(D)Leu-Val (**17**).

Surprisingly, the fully protected cyclo-dimerized peptide was found to be the major product under this optimized condition. The failure of a thiazolidine coupling at an amino acid assembly was mainly due to the steric hindrance encountered, affecting to the cyclization efficacy. Next, the resulting fully protected cyclo-dimerized peptide ((D)Val-(D)Val-Trp(Boc)-(D)Leu-Val) (**17**) was globally deprotected using 95% TFA in CH_2Cl_2 to afford the fully deprotected cyclo-dimerized(D)Val-(D)Val-Trp-(D)Leu-Val (**18**), and was purified using HPLC, and characterized by using ESI-MS spectrometry.

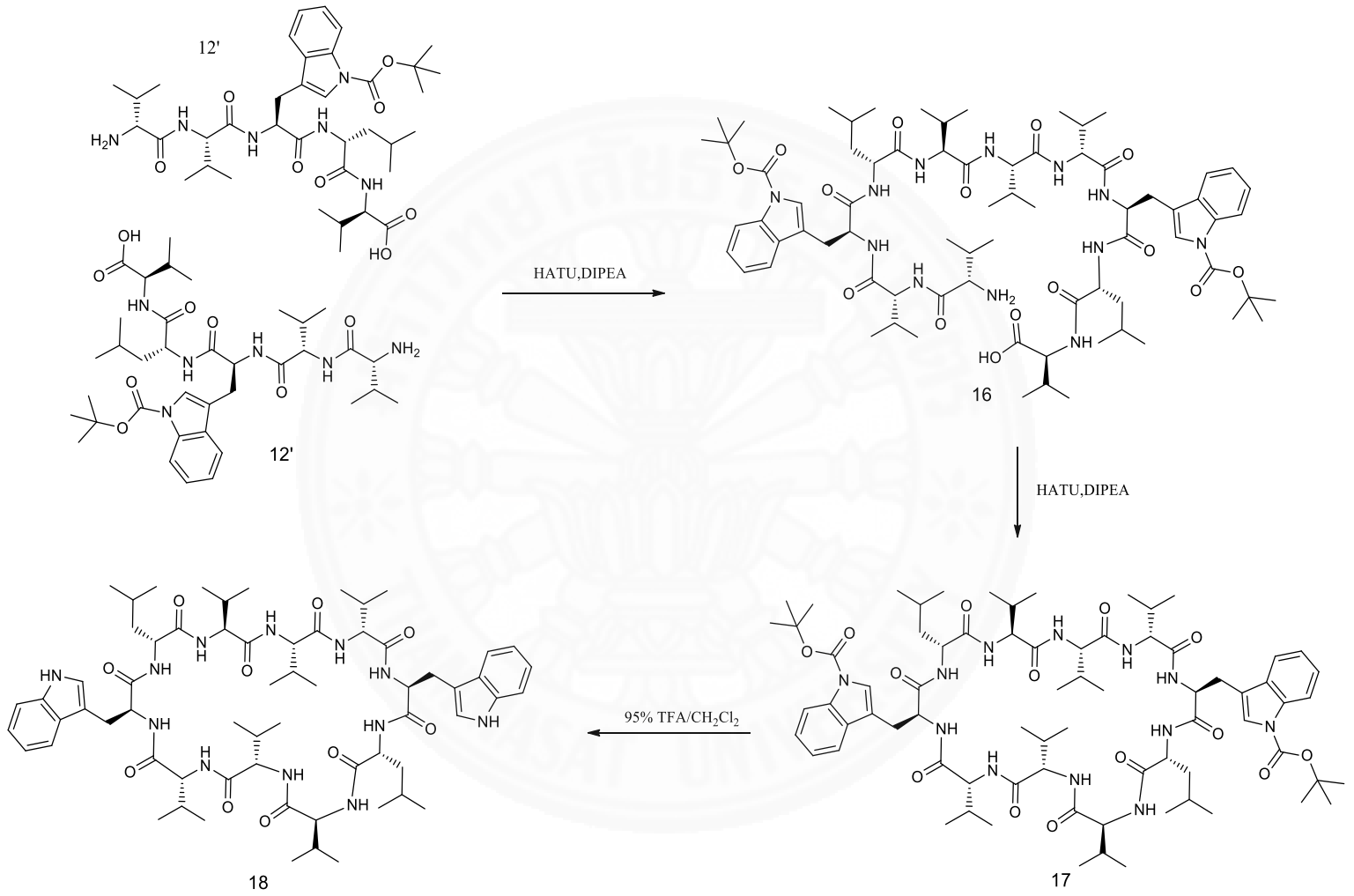

Scheme 4.8 Formation of fully deprotected cyclo-dimerized peptide (D)Val-(D)Val-Trp(Boc)-(D)Leu-Val (**18**) mechanism

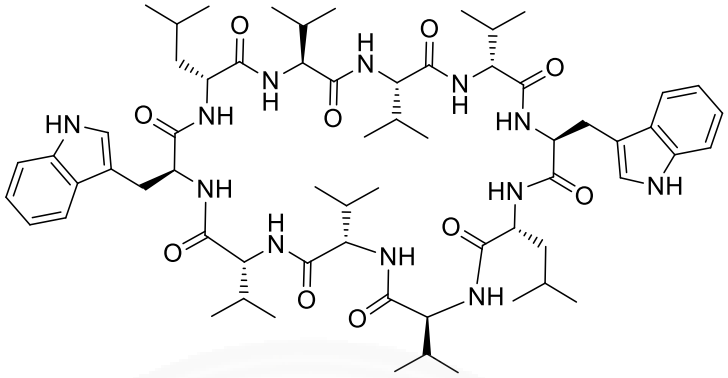

18

Figure 4.11 Structure of deprotected cyclic-dimerized-(D)Val-(D)Val-Trp-(D)Leu-Val

Name: Deprotected cyclo-dimerized-(D)Val-(D)Val-Trp-(D)Leu-Val

Chemical formula: $C_{64}H_{96}N_{12}O_{10}$

ESI-MS: Found; 1218.4 $[M+Na]^+$; Calculated 1193.5243 $[M]^+$

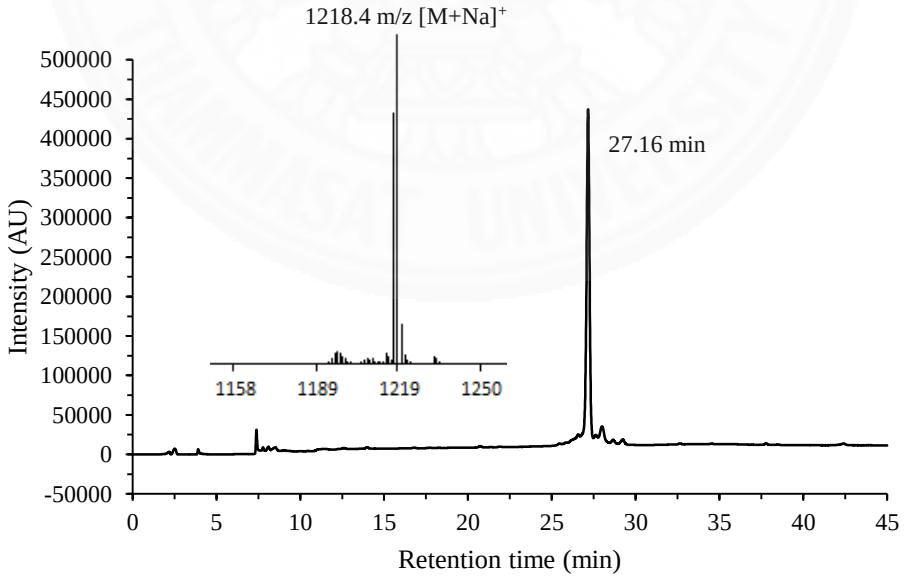

Figure 4.12 HPLC chromatogram and ESI-MS spectrum of deprotected cyclo-dimerized-(D)-Val-(D)-Val-Trp-(D)-Leu-Val

According to the ESI-MS spectrum of deprotected cyclo-dimerized-(D)-Val-(D)-Val-Trp-(D)-Leu-Val, it clearly showed the molecular mass at 1218.4 amu, corresponding to $[M+Na]^+$, and the molecular mass was calculated to be 1193.5243 $[M]^+$. The purity of deprotected cyclo-dimerized (D)Val-(D)Val-Trp-(D)Leu-Val was verified using HPLC, showing an obvious signal at 27.16 min. From this result, this clearly indicated that the synthetic deprotected cyclo-dimerized (D)Val-(D)Val-Trp-(D)Leu-Val was successfully synthesized as shown in **Figure 4.12**.

4.5 The Synthesis of mutant ludunin (cysteine)

4.5.1 The synthesis of a fully protected mutant lugdunin (cysteine)

A fully protected mutant lugdunin (cysteine) was successfully synthesized *via* solid phase peptide synthesis (SPPS) according to Fmoc-based SPPS. Notably, an amino acid assembly was carried out under the similar manner as previously described in **Section 4.4.1**. The details were illustrated as following; (1). The Fmoc-Val-OH was firstly loaded into 2-chlorotrityl resin in the presence of DIPEA to afford Fmoc-Val-O-chlorotrityl resin (**7**). Next, Fmoc-Val-O-2-chlorotrityl resin (**7**) was treated with 20% piperidine in DMF to afford NH_2-Val-O-2-chlorotrityl resin, which subsequently coupled with Fmoc-D-Leu-OH using DCC and DMAP as standard coupling agents whereas HOBt was employed as an additive to prevent the racemization, finally affording the Fmoc-D-Leu-Val-O-chlorotrityl resin (**8**). Then, Fmoc-D-Leu-Val-O-chlorotrityl resin was treated with 20% piperidine/DMF, and subsequently coupled with Fmoc-Trp(Boc)-OH under an optimized condition as previously described in **Section 4.4.1** to afford Fmoc-Trp(Boc)-D-Leu-Val-O-chlorotrityl resin (**9**). An amino acid assembly was repeatedly performed by the coupling of Fmoc-D-Val-OH, Fmoc-Cys(Trt)-OH, Fmoc-Val-OH and Fmoc-D-Val-OH, respectively to afford NH_2-(D)Val-Val-Cys(Trt)-(D)Val-Trp(Boc)-(D)Leu-Val-O-chlorotrityl resin (**19**). Finally, NH_2-(D)Val-Val-Cys(Trt)-(D)Val-Trp(Boc)-(D)Leu-Val-O-2-chlorotrityl resin (**19**) was treated with 1% TFA/CH_2Cl_2 to afford a free carboxyl terminus linear peptide of NH_2-(D)Val-Val-Cys(Trt)-(D)Val-Trp(Boc)-(D)Leu-Val-OH (**20**) with a yield of 90%. The HPLC chromatogram of NH_2-(D)Val-Val-Cys(Trt)-(D)Val-Trp(Boc)-(D)Leu-Val-OH was shown in **Figure 4.13**. The fully protected linear NH_2-(D)Val-Val-Cys(Trt)-(D)Val-Trp(Boc)-(D)Leu-Val-OH (**20**) was further utilized in the next step without purification.

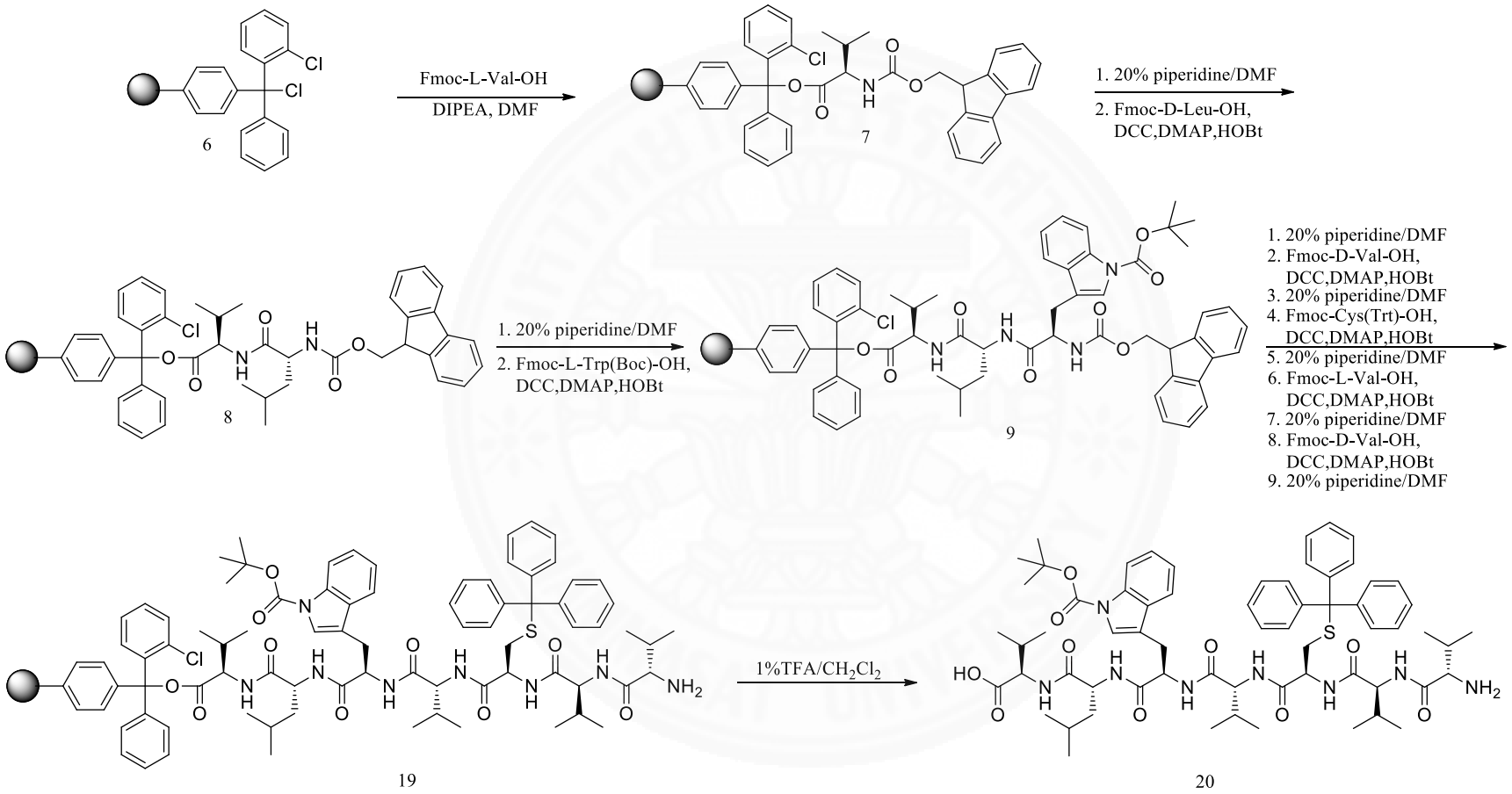

Scheme 4.9 Synthesis of NH_2-(D)Val-Val-Cys(Trt)-(D)Val-Trp(Boc)-(D)Leu-Val-OH (**20**)

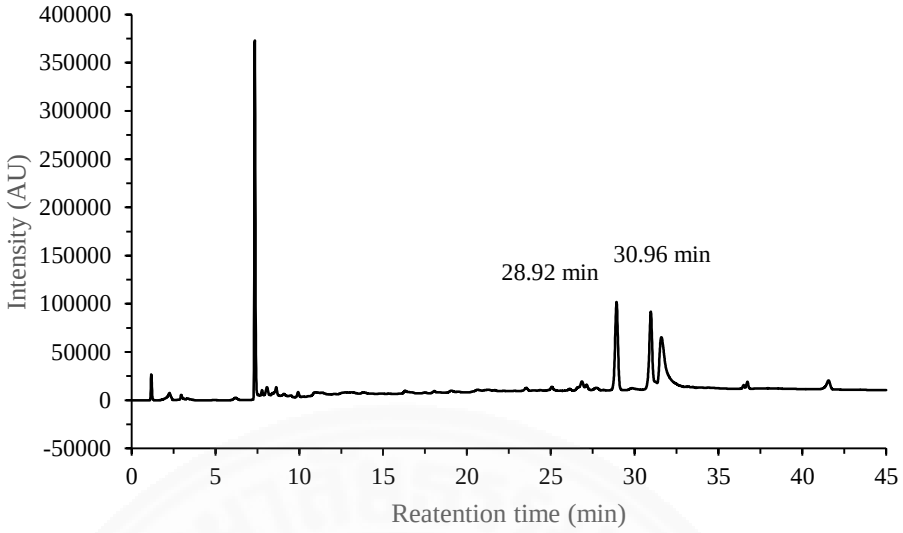

Figure 4.13 HPLC chromatogram of NH_2-(D)Val-Val-Cys(Trt)-(D)Val-Trp(Boc)-(D)Leu-Val-OH crude (**20**)

4.5.2 The synthesis of mutant linear lugdunin (cysteine)

A mutant lugdunin (cysteine) was successfully synthesized using a fully protected mutant lugdunin (cysteine) linear scaffold (**20**) which was previously described in **Section 4.4.3**, and then was globally deprotected by using 95% TFA in CH_2Cl_2 for 1 hr to afford a mutant linear lugdunin (cysteine) (**21**) with a yield of 59%. The resulting reaction was purified using preparative HPLC. The purity was verified by using analytical HPLC and ESI-MS spectrometry, respectively.

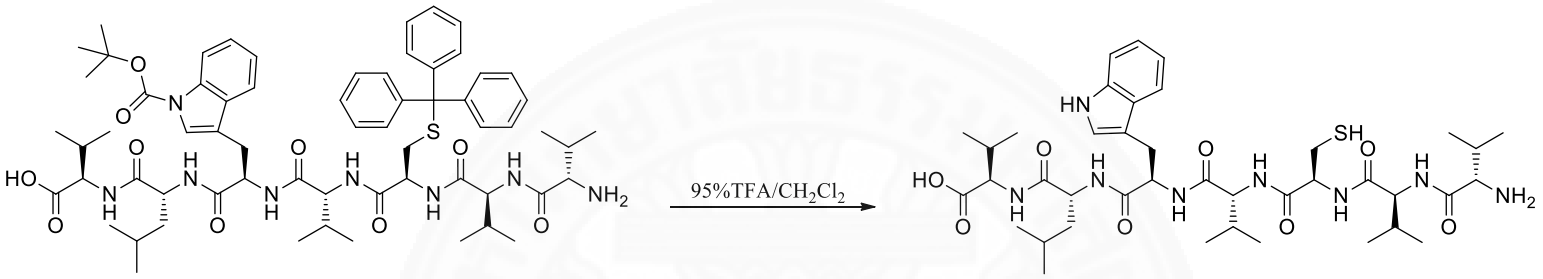

20 21

Scheme 4.10 Synthesis of mutant linear lugdunin (cysteine) (**21**)

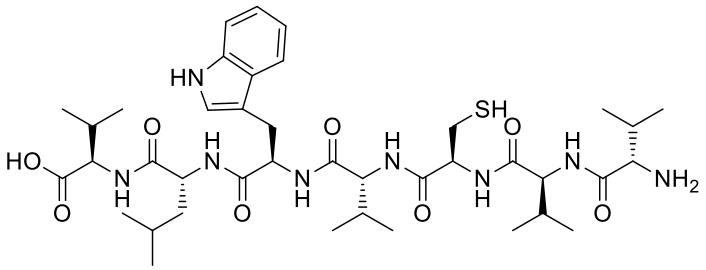

21

Figure 4.14 Structure of mutant linear lugdunin (cysteine) (**21**)

Name: Mutant linear lugdunin (cysteine)

Chemical formula: $C_{40}H_{64}N_8O_8S$

ESI-MS result: Found; 1082.7 $[M+2TFA+K]^+$; Calculated 817.0529 $[M]^+$

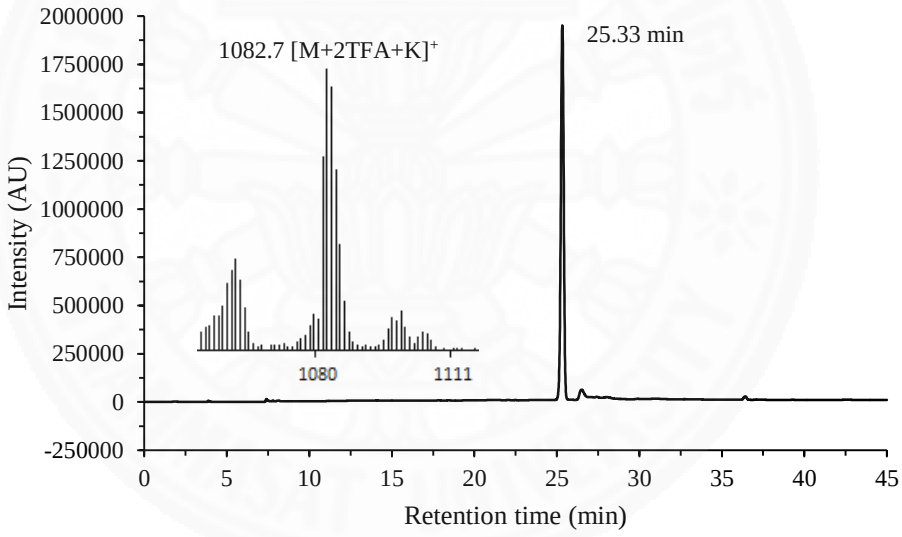

Figure 4.15 HPLC chromatogram and ESI-MS spectrum of mutant linear lugdunin (cysteine) (**21**)

The purity of mutant linear lugdunin (cysteine) was verified using analytical HPLC. The signal of mutant linear lugdunin (cysteine) was presented at 25.33 min. Additionally, ESI-MS spectrum showed the molecular mass at 1082.7 amu, corresponding to $[M+2TFA+K]^+$, and the molecular mass was calculated to be 817.0529 $[M]^+$. Therefore, this clearly indicated that the mutant linear lugdunin (cysteine) was synthesized.

4.5.3 The synthesis of mutant cyclic lugdunin (cysteine)

The fully protected mutant lugdunin (cysteine) (NH_2-(D)Val-Val-Cys(Trt)-(D)Val-Trp(Boc)-(D)Leu-Val-OH) (**20**) as previously assembled in **Section 4.5.1** was successfully cyclized according to our developed condition (using HATU and DIPEA as a coupling reagent). The cyclization of a fully protected mutant lugdunin (cysteine) (NH_2-(D)Val-Val-Cys(Trt)-(D)Val-Trp(Boc)-(D)Leu-Val-OH) was greatly achieved under the similar optimized condition as seen in **Section 4.4.3**, and then was globally deprotected by using 95% TFA in CH_2Cl_2 for 1 hr to afford a mutant cyclic lugdunin (cysteine) (**23**) with a yield of 26%. The resulting reaction was purified using preparative HPLC, and the molecular mass was verified by using ESI-MS spectrometry.

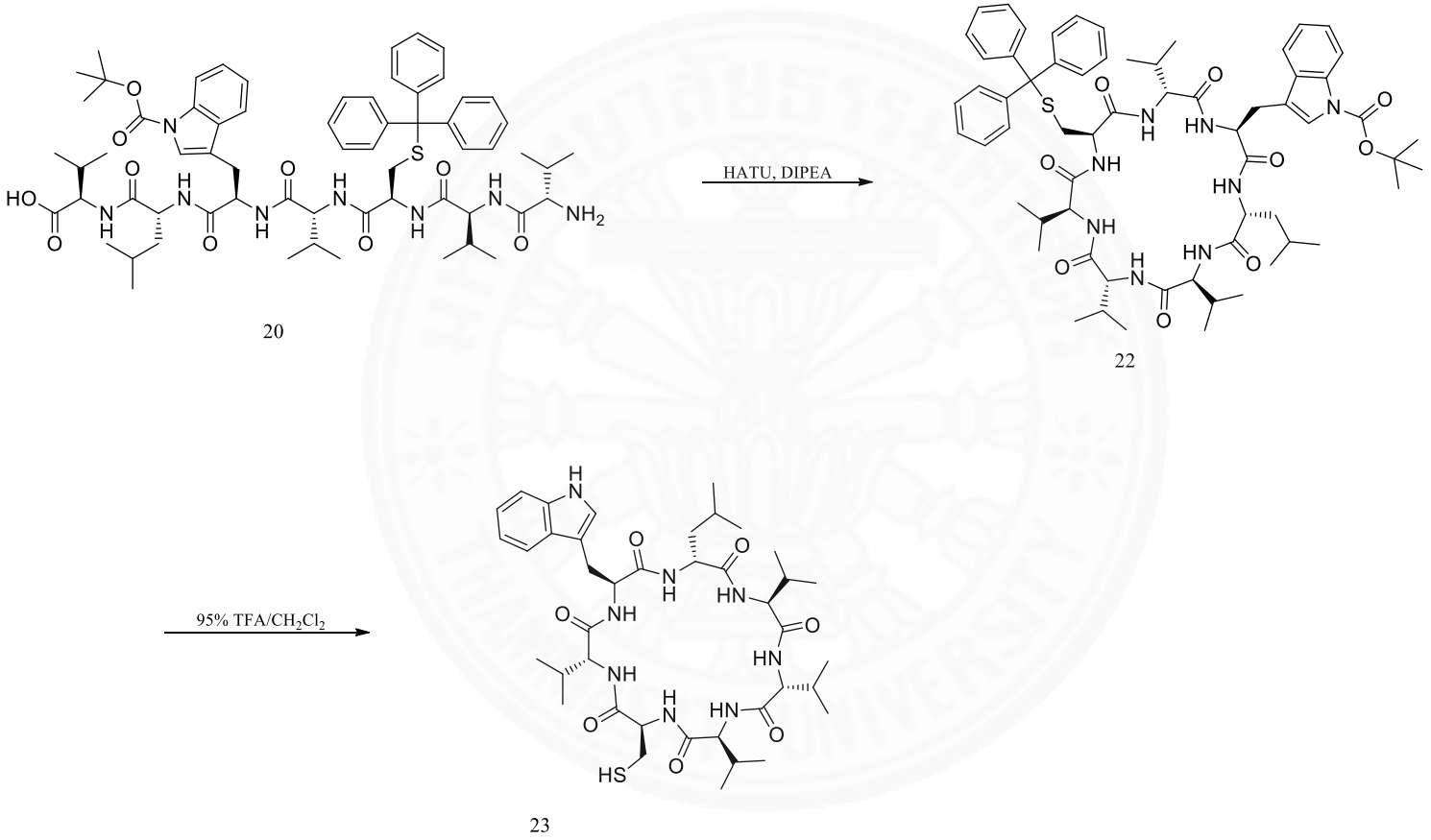

20

22

23

Scheme 4.11 Synthesis of mutant cyclic cysteins lugdunin (**23**)

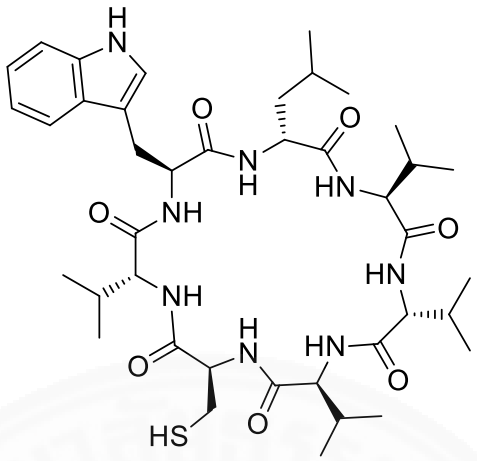

23

Figure 4.16 Chemical structure of mutant cyclic lugdunin (cysteine) (**23**)

Name: Mutant cyclic lugdunin (cysteine)

Chemical formula: $C_{40}H_{62}N_8O_7S$

ESI-MS result: Found; 1063.4 $[M+2TFA+K]^+$ and 1149.2 $[M+2TFA+3ACN]^+$; Calculated 799.0376 $[M]^+$

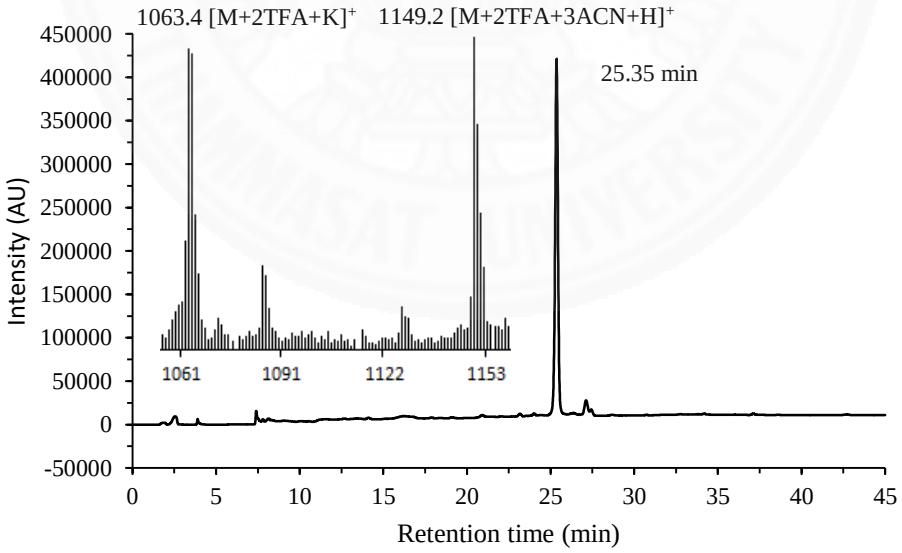

Figure 4.17 HPLC chromatogram and ESI-MS result of mutant cyclic lugdunin (cysteine)

According to the ESI-MS spectrum (**Figure 4.17**), it clearly showed the signal of the trifluoroacetic acid adduct of mutant cyclic lugdunin (cysteine) at 1063.4 amu, corresponding to $[M+2TFA+K]^+$ whereas the molecular mass was calculated to be 799.0376 $[M]^+$. Additionally, the formation of mutant cyclic lugdunin (cysteine), acetonitrile and trifluoroacetic acid adduct was also observed at 1149.2 amu, corresponding to $[M+2TFA+2ACN+K]^+$. The purity of mutant cyclic lugdunin (cysteine) was verified using analytical HPLC. The signal of mutant cyclic lugdunin (cysteine) presented at 25.35 min (**Figure 4.17**). From the result, it clearly indicated that the mutant cyclic lugdunin (cysteine) was successfully synthesized.

Herein, we summarized that syntheses and characterization of six types of lugdunin was accomplished. The structures were different in terms of sequences and the scaffold. . All six derivatives of lugdunin were NH_2-(D)Val-Val-Thiazolidine-(D)Val-Trp-(D)Leu-Val-OH (**13**), native lugdunin (**15**), NH_2-(D)Val-(D)Val-Trp-(D)Leu-Val-OH (**12**), deprotected cyclo-dimerized(D)Val-(D)Val-Trp-(D)Leu-Val (**18**), mutant linear lugdunin (cysteine) (**21**) and mutant cyclic lugdunin (cysteine) (**23**) as showed in **Figure 4.18**. Importantly, all synthesized lugdunin derivatives will be further evaluated anti-bacterial activities against a panel of multidrug resistant bacteria, such as Methicillin-resistance *Staphylococcus aureus*, Vancomycin-resistant *Enterococcus faecium*, Cephalosporin-resistant *Neisseria gonorrhoeae* and etc.

.

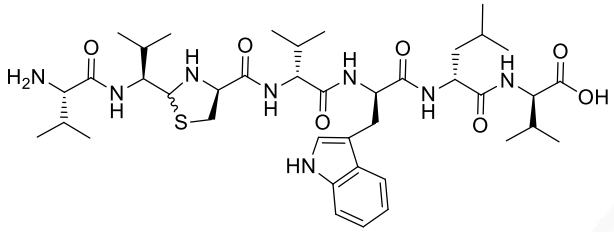

NH_2-(D)Val-Val-Thiazolidine-(D)Val-Trp-(D)Leu-Val-OH (13)

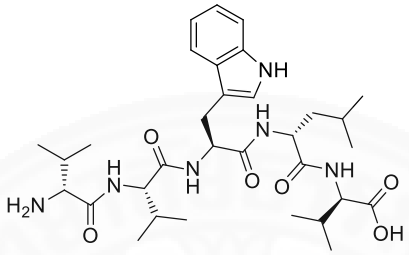

NH_2-(D)Val-(D)Val-Trp-(D)Leu-Val-OH (12)

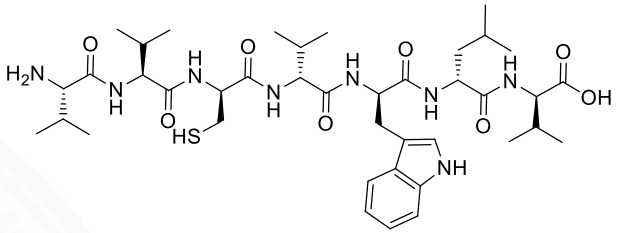

Mutant linear lugdunin (cysteine) (21)

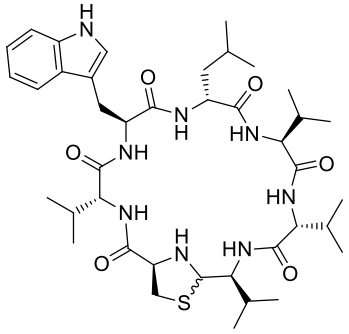

Synthetic native lugdunin (15)

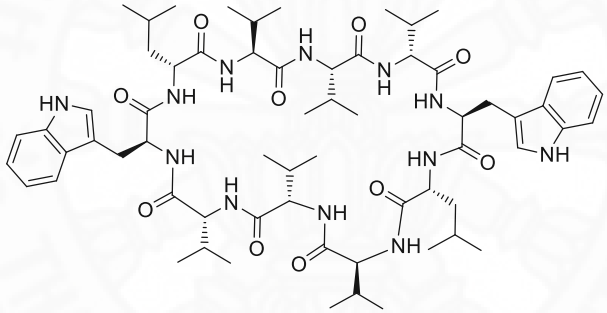

Deprotected cyclo-dimerized(D)Val-(D)Val-Trp-(D)Leu-Val (18)

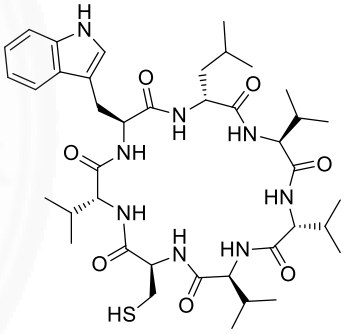

Mutant cyclic lugdunin (cysteine) (23)

Figure 4.18 Chemical structures of all synthetic compounds

CHAPTER 5
CONCLUSIONS

Synthetic native lugdunin and mutant lugdunins were designed and successfully synthesized *via* solid phase peptide synthesis (SPPS) to afford six resulting peptides based on the lugdunin scaffold. All six types of lugdunin both mutant and wildtype lugdunins were NH_2-(D)Val-Val-Thiazolidine-(D)Val-Trp-(D)Leu-Val-OH (**13**), native lugdunin (**15**), NH_2-(D)Val-(D)Val-Trp-(D)Leu-Val-OH (**12**), cyclo-dimerized(D)Val-(D)Val-Trp-(D)Leu-Val (**18**), mutant linear lugdunin (cysteine) (**21**) and mutant cyclic lugdunin (cysteine) (**23**) as showed in **Figure 4.18**.

The synthetic strategies of native lugdunin (**15**) and mutant linear lugdunin (NH_2-(D)Val-Val-Thiazolidine-(D)Val-Trp-(D)Leu-Val-OH (**13**)) were classified into three important parts. Firstly, the synthesis of an amino aldehyde (Fmoc-Val-H) by using the activation of a carboxyl moiety *via* CDI activation, and a selective reduction, respectively to afford an amino aldehyde (Fmoc-Val-H), which subsequently reacted with cysteine to afford Fmoc-Val-thiazolidine-OH. Secondly, an amino acid assembly of NH_2-(D)Val-Val-thiazolidine-(D)Val-Trp(Boc)-(D)Leu-Val-O-2-chlorotrityl resin was performed under a standard Fmoc strategy. To this approach, the pre-activation of Fmoc-Val-thiazolidine-OH was firstly performed prior to the coupling step in order to increase the coupling efficacy. Finally, the cyclization of NH_2-(D)Val-Val-thiazolidine-(D)Val-Trp(Boc)-(D)Leu-Val-OH was carried out by using HATU as an effective coupling agent to yield a synthetic native lugdunin (**15**). A linear NH_2-(D)Val-Val-thiazolidine-(D)Val-Trp(Boc)-(D)Leu-Val-OH was globally deprotected to afford a mutant linear lugdunin (NH_2-(D)Val-Val-Thiazolidine-(D)Val-Trp-(D)Leu-Val-OH (13)). Moreover, the fully protected linear peptide (NH_2-(D)Val-(D)Val-Trp(Boc)-(D)Leu-Val-OH), a minor product at an amino assembly step of NH_2-(D)Val-Val-thiazolidine-(D)Val-Trp(Boc)-(D)Leu-Val-OH, was identified, and subsequently deprotected to afford NH_2-(D)Val-(D)Val-Trp-(D)Leu-Val-OH (**12**). Additionally, a cyclo-dimerized (D)Val-(D)Val-Trp-(D)Leu-Val (**18**) was also identified which was successfully synthesized *via* an intermolecular dimerization and followed by the global deprotection, respectively.

The mutant linear lugdunin (cysteine) (**21**) and mutant cyclic lugdunin (cysteine) (**23**) were synthesized *via* solid phase peptide synthesis (SPPS). The all mutant lugdunins (cysteine) were performed under a standard Fmoc strategy to afford NH_2-(D)Val-Val-Cys(Trt)-(D)Val-Trp(Boc)-(D)Leu-Val-OH which was globally deprotected to yield a mutant linear lugdunin (cysteine) (**21**). Additionally, NH_2-(D)Val-Val-Cys(Trt)-(D)Val-Trp(Boc)-(D)Leu-Val-OH was successfully cyclized by using our developed condition to afford a mutant cyclic lugdunin (cysteine) (**23**). The molecular masses and purity were confirmed by using ESI-MS and HPLC, respectively.

All synthetic native lugdunin and mutant lugdunins will be further evaluated anti-bacterial activities against a panel of multidrug resistant bacteria, such as Methicillin-resistance *Staphylococcus aureus*, Vancomycin-resistant *Enterococcus faecium*, Cephalosporin-resistant *Neisseria gonorrhoeae* and etc.

REFERENCES

1. Van Boeckel TP, Gandra S, Ashok A, Caudron Q, Grenfell BT, Levin SA, et al. Global antibiotic consumption 2000 to 2010: an analysis of national pharmaceutical sales data. The Lancet Infectious Diseases. 2014;14(8):742-50.

2. Schilling NA, Berscheid A, Schumacher J, Saur JS, Konnerth MC, Wirtz SN, et al. Synthetic Lugdunin Analogues Reveal Essential Structural Motifs for Antimicrobial Action and Proton Translocation Capability. Angewandte Chemie International Edition. 2019;58(27):9234-8.

3. Ivkovic J, Lembacher-Fadum C, Breinbauer R. A rapid and efficient one-pot method for the reduction of N-protected α-amino acids to chiral α-amino aldehydes using CDI/DIBAL-H. Org Biomol Chem. 2015;13(42):10456-60.

4. Bisht R, Katiyar A, Singh R, Mittal P. Antibiotic resistance - A global issue of concern2009. 34-9 p.

5. Ventola CL. The antibiotic resistance crisis: part 1: causes and threats. P & T : a peer-reviewed journal for formulary management. 2015;40(4):277-83.

6. Cooper MA, Shlaes D. Fix the antibiotics pipeline. Nature (London, U K). 2011;472(7341):32.

7. Anonymous. The antibiotic alarm. Nature. 2013;495(7440):141.

8. Chamoun K, Farah M, Araj G, Daoud Z, Moghnieh R, Salameh P, et al. Surveillance of antimicrobial resistance in Lebanese hospitals: retrospective nationwide compiled data. Int J Infect Dis. 2016;46:64-70.

9. McGann P, Snesrud E, Maybank R, Corey B, Ong AC, Clifford R, et al. Escherichia coli harboring mcr-1 and blaCTX-M on a novel IncF plasmid: first report of mcr-1 in the United States. Antimicrob Agents Chemother. 2016;60(7):4420-1.

10. Zipperer A, Konnerth MC, Laux C, Berscheid A, Janek D, Weidenmaier C, et al. Human commensals producing a novel antibiotic impair pathogen colonization. Nature. 2016;535(7613):511-6.

11. Al-Warhi TI, Al-Hazimi HMA, El-Faham A. Recent development in peptide coupling reagents. Journal of Saudi Chemical Society. 2012;16(2):97-116.

12. A. G. N. Montalbetti C, Falque V. Amide Bond Formation and Peptide Coupling2005. 10827-52 p.

13. Valeur E, Bradley M. Amide bond formation: beyond the myth of coupling reagents. Chemical Society Reviews. 2009;38(2):606-31.

14. Palomo JM. Solid-phase peptide synthesis: an overview focused on the preparation of biologically relevant peptides. RSC Advances. 2014;4(62):32658-72.

15. Isidro-Llobet A, Álvarez M, Albericio F. Amino Acid-Protecting Groups. Chemical Reviews. 2009;109(6):2455-504.

16. Luly JR, Dellaria JF, Plattner JJ, Soderquist JL, Yi N. A synthesis of protected aminoalkyl epoxides from .alpha.-amino acids. The Journal of Organic Chemistry. 1987;52(8):1487-92.

17. Gołębiowski A, Jurczak J, Jacobsson U. High pressure approach to the total synthesis of 6-EPI-d-purpurosamine b. Tetrahedron. 1987;43(13):3063-6.

18. Falorni M, Giacomelli G, Porcheddu A, Taddei M. A Simple Method for the Reduction of Carboxylic Acids to Aldehydes or Alcohols Using H2 and Pd/C. The Journal of Organic Chemistry. 1999;64(24):8962-4.

19. Ocejo M, Vicario J, Badia D, Carrillo L, Reyes E. A Direct and Efficient Stereoconservative Procedure for the Selective Oxidation of N-Protected β-Amino Alcohols2006.

20. Sergeev M, Pronin VB, Voyushina TL. Procedure for the Oxidation of β-Amino Alcohols to α-Amino Aldehydes2005. 2802-4 p.

21. Soto-Cairoli B, Justo de Pomar J, Soderquist JA. Enantiomerically Pure α-Amino Aldehydes from Silylated α-Amino Acids. Organic Letters. 2008;10(2):333-6.

22. Prashantha Kumar BR, Basu P, Adhikary L, Nanjan MJ. Efficient Conversion of N-Terminal of L-Tyrosine, DL-Phenyl Alanine, and Glycine to Substituted 2-Thioxo-thiazolidine-4-ones: A Stereospecific Synthesis. Synthetic Communications. 2012;42(20):3089-96.

23. Ratner S, Clarke HT. The Action of Formaldehyde upon Cysteine. Journal of the American Chemical Society. 1937;59(1):200-6.

24. Esra Önen F, Boum Y, Jacquement C, Spanedda MV, Jaber N, Scherman D, et al. Design, synthesis and evaluation of potent thymidylate synthase X inhibitors. Bioorganic & Medicinal Chemistry Letters. 2008;18(12):3628-31.

25. Liu Y, Jing F, Xu Y, Xie Y, Shi F, Fang H, et al. Design, synthesis and biological activity of thiazolidine-4-carboxylic acid derivatives as novel influenza neuraminidase inhibitors. Bioorganic & Medicinal Chemistry. 2011;19(7):2342-8.

26. Onen-Bayram FE, Buran K, Durmaz I, Berk B, Cetin-Atalay R. 3-Propionyl-thiazolidine-4-carboxylic acid ethyl esters: a family of antiproliferative thiazolidines. MedChemComm. 2015;6(1):90-3.

27. Yuan C, Williams RM. Total Synthesis of the Anti Methicillin-Resistant Staphylococcus aureus Peptide Antibiotics TAN-1057A-D. J Am Chem Soc. 1997;119(49):11777-84.

28. Vijaya KEK, Kenia J, Mukhopadhyay T, Nadkarni SR. Methylsulfomycin I, a new cyclic peptide antibiotic from a Streptomyces sp. HIL Y-9420704. J Nat Prod. 1999;62(11):1562-4.

29. Barsby T, Kelly MT, Gagne SM, Andersen RJ. Bogorol A produced in culture by a marine Bacillus sp. reveals a novel template for cationic peptide antibiotics. Org Lett. 2001;3(3):437-40.

30. Hughes RA, Thompson SP, Alcaraz L, Moody CJ. Total Synthesis of the Thiopeptide Antibiotic Amythiamicin D. J Am Chem Soc. 2005;127(44):15644-51.

31. Wohlrab A, Lamer R, VanNieuwenhze MS. Total synthesis of plusbacin A3: a depsipeptide antibiotic active against vancomycin-resistant bacteria. J Am Chem Soc. 2007;129(14):4175-7.

32. Desjardine K, Pereira A, Wright H, Matainaho T, Kelly M, Andersen RJ. Tauramamide, a lipopeptide antibiotic produced in culture by Brevibacillus laterosporus isolated from a marine habitat: structure elucidation and synthesis. J Nat Prod. 2007;70(12):1850-3.

33. Hu H, Xue J, Swarts BM, Wang Q, Wu Q, Guo Z. Synthesis and Antibacterial Activities of N-Glycosylated Derivatives of Tyrocidine A, a Macrocyclic Peptide Antibiotic. J Med Chem. 2009;52(7):2052-9.

34. Zhang C, Herath K, Jayasuriya H, Ondeyka JG, Zink DL, Occi J, et al. Thiazomycins, thiazolyl peptide antibiotics from Amycolatopsis fastidiosa. J Nat Prod. 2009;72(5):841-7.

35. LaMarche MJ, Leeds JA, Dzink-Fox J, Gangl E, Krastel P, Neckermann G, et al. Antibiotic optimization and chemical structure stabilization of thiomuracin A. J Med Chem. 2012;55(15):6934-41.

36. Ma YM, Liang XA, Zhang HC, Liu R. Cytotoxic and Antibiotic Cyclic Pentapeptide from an Endophytic Aspergillus tamarii of Ficus carica. J Agric Food Chem. 2016;64(19):3789-93.

37. Mitachi K, Aleiwi BA, Schneider CM, Siricilla S, Kurosu M. Stereocontrolled Total Synthesis of Muraymycin D1 Having a Dual Mode of Action against Mycobacterium tuberculosis. J Am Chem Soc. 2016;138(39):12975-80.

38. Napitupulu O, Sumiarsa D, Subroto T, Nurlelasari N, Harneti D, Supratman U, et al. Synthesis of cyclo-PLAI using a combination of solid- and solution-phase methods. Synthetic Communications. 2019;49:1-8.

39. Davies JS. The cyclization of peptides and depsipeptides. Journal of Peptide Science. 2003;9(8):471-501.

APPENDICES

APPENDIX A

Sample Preparation for Analysis

- NMR sample preparation

The sample compound (5-25 mg) was dried under vacuum for 30-60 minute and dissolved with deuterated solvent such as chloroform-d, methanol-d_4, acetone-d_6 and DMSO-d_6. The sample solution was transferred to NMR tube and submitted for analyses.

- Mass spectrometry sample preparation

The sample compound was dissolved by HPLC grade solvent such as methanol HPLC grade and acetonitrile HPLC grade. The sample solution was filtered by using 0.22 µm syringe filter and submitted for analyses.

- High performance liquid chromatography sample preparation and HPLC method

The sample compound was dissolved with HPLC grade solvent and filtered with 0.45 or 0.22 µm syringe filter. The sample solution was analysed by using 4.6x250 mm ACE-C_{18} column, 20 µL injection volume, 1.0 mL/min flow rate, 45.0 run time, 20-100 in 45.0 min gradient, A: DI-water and B: acetonitrile mobile phase and detected at 215 & 280 nm.

APPENDIX B

Nuclear magnetic resonance spectrum

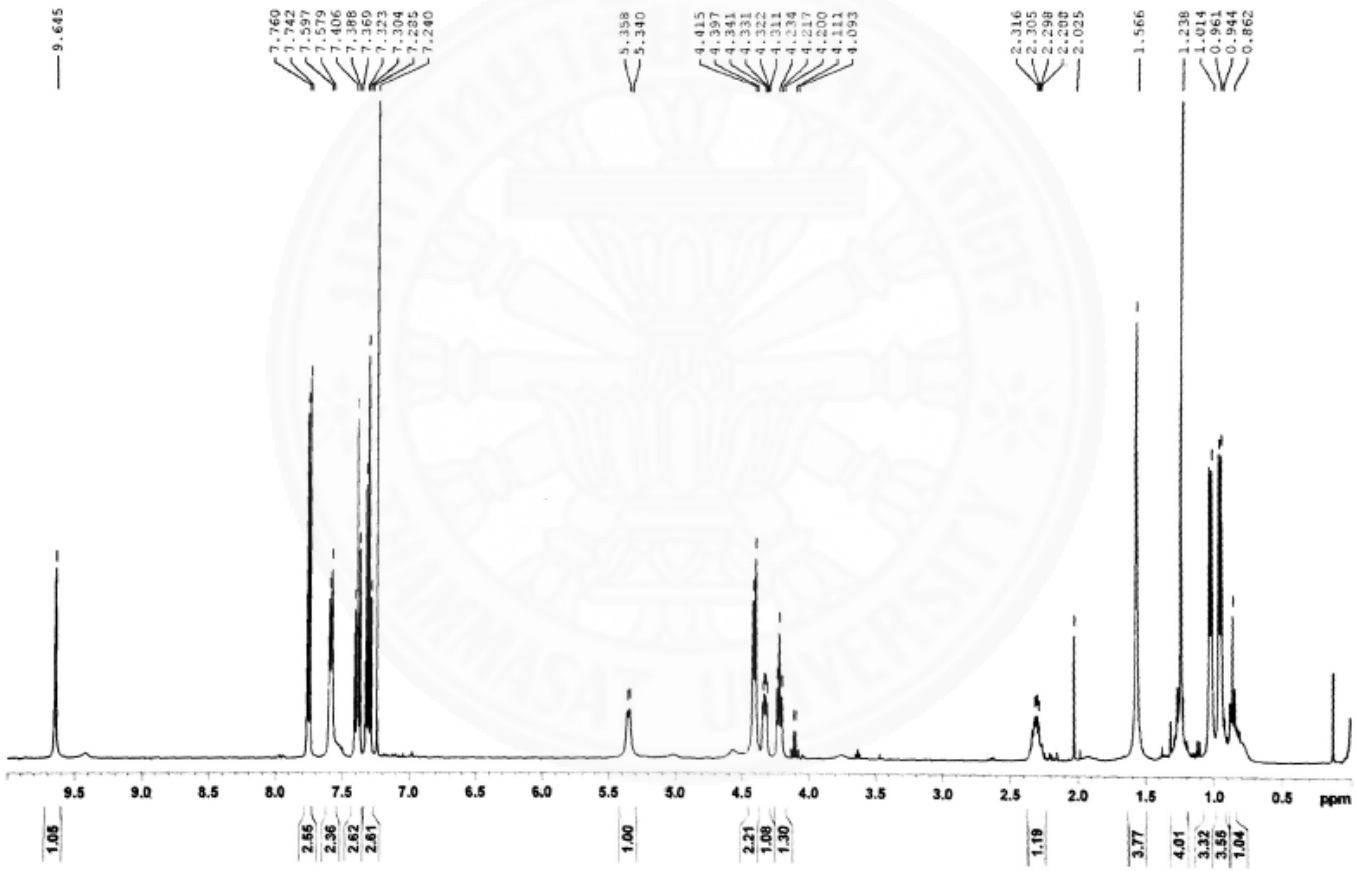

Figure B.1 ^{1}H-NMR spectrum (600 MHz, $CDCl_3$) of Fmoc-Val-H

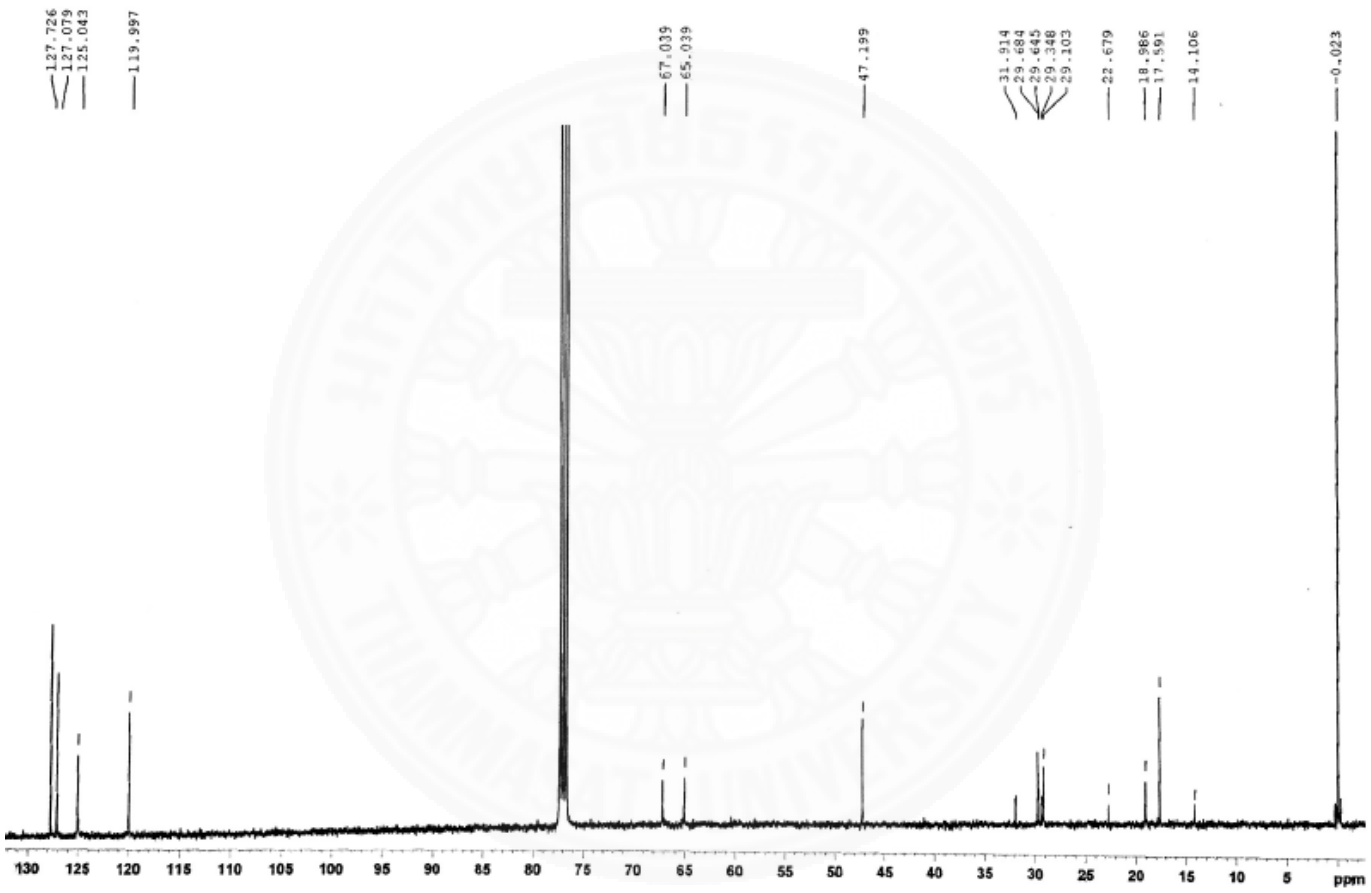

Figure B.2 ^{13}C-NMR spectrum (150 MHz, $CDCl_3$) of Fmoc-Val-H

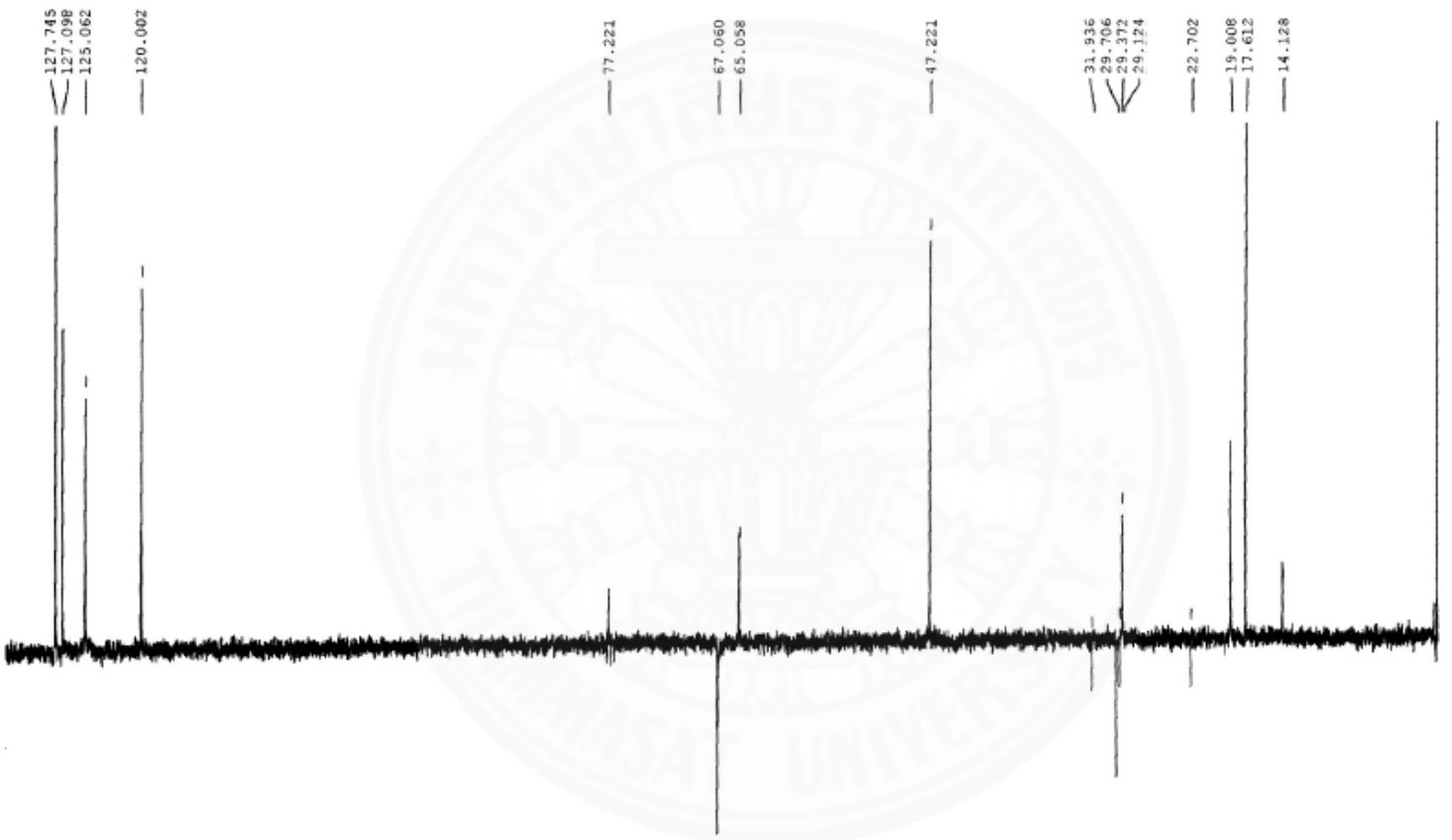

Figure B.3 DEPT 135 spectrum (600 MHz, $CDCl_3$) of Fmoc-Val-H

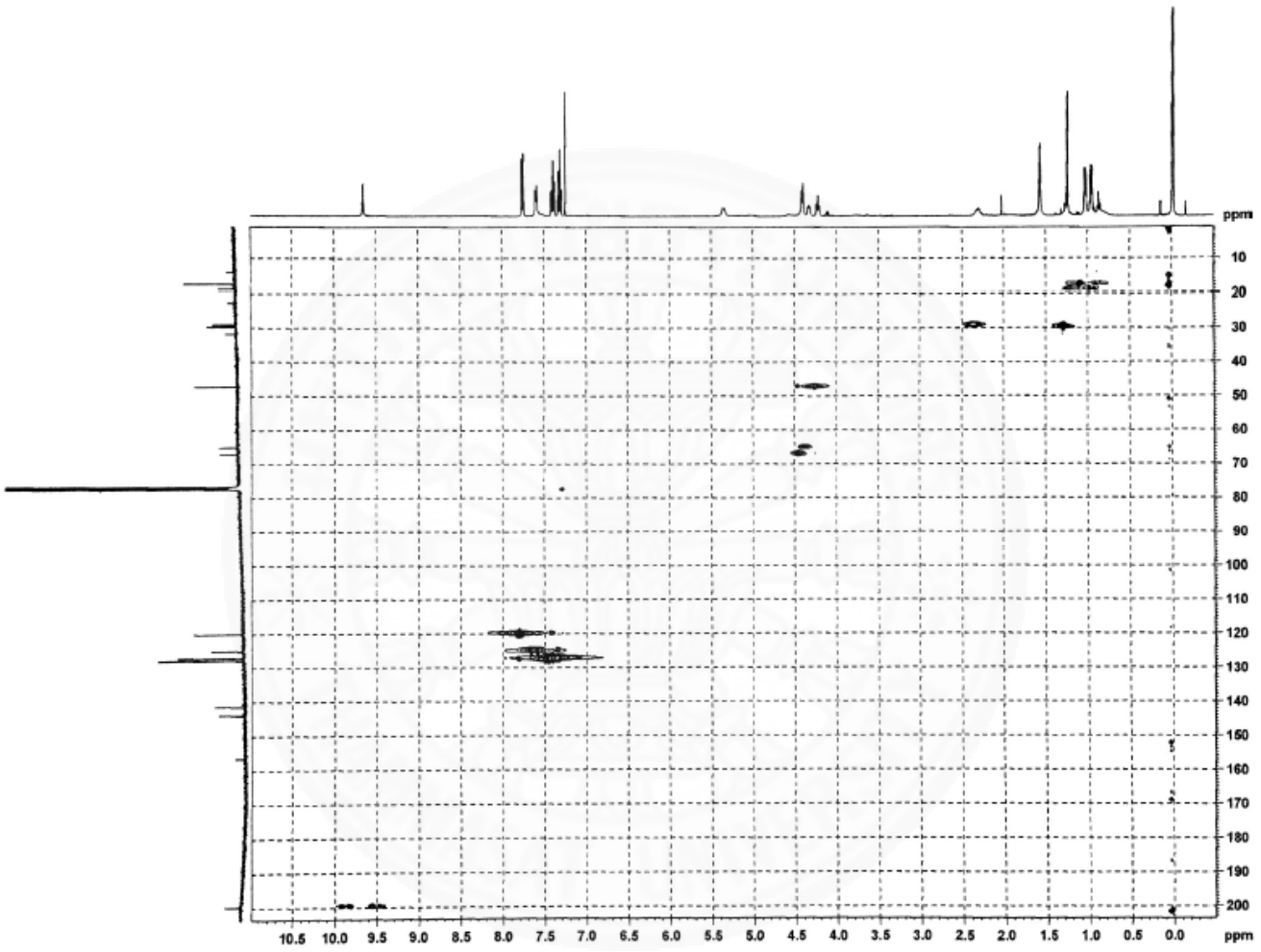

Figure B.4 HSQC spectrum (600 MHz, $CDCl_3$) of Fmoc-Val-H

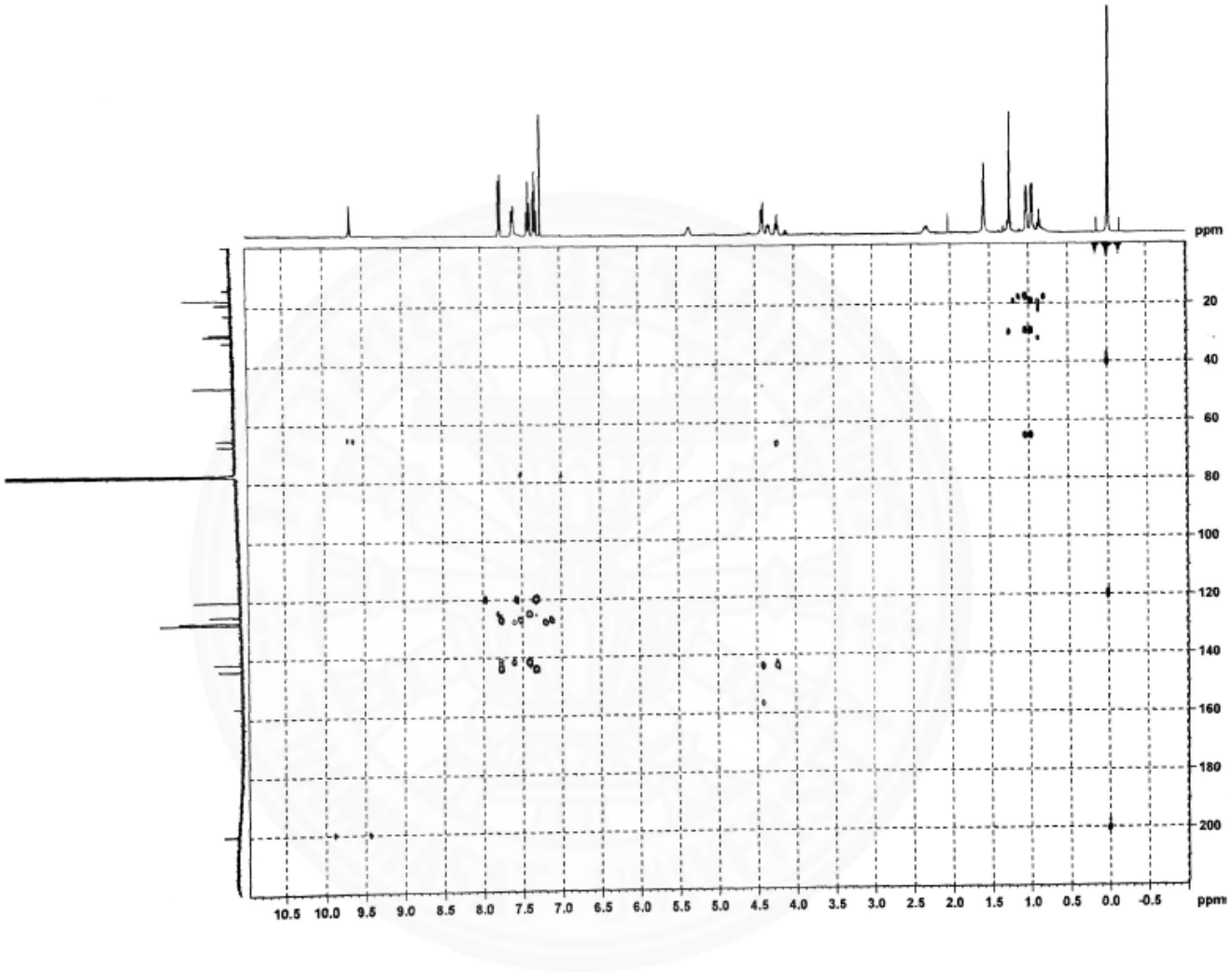

Figure B.5 HMBC spectrum (600 MHz, $CDCl_3$) of Fmoc-Val-H

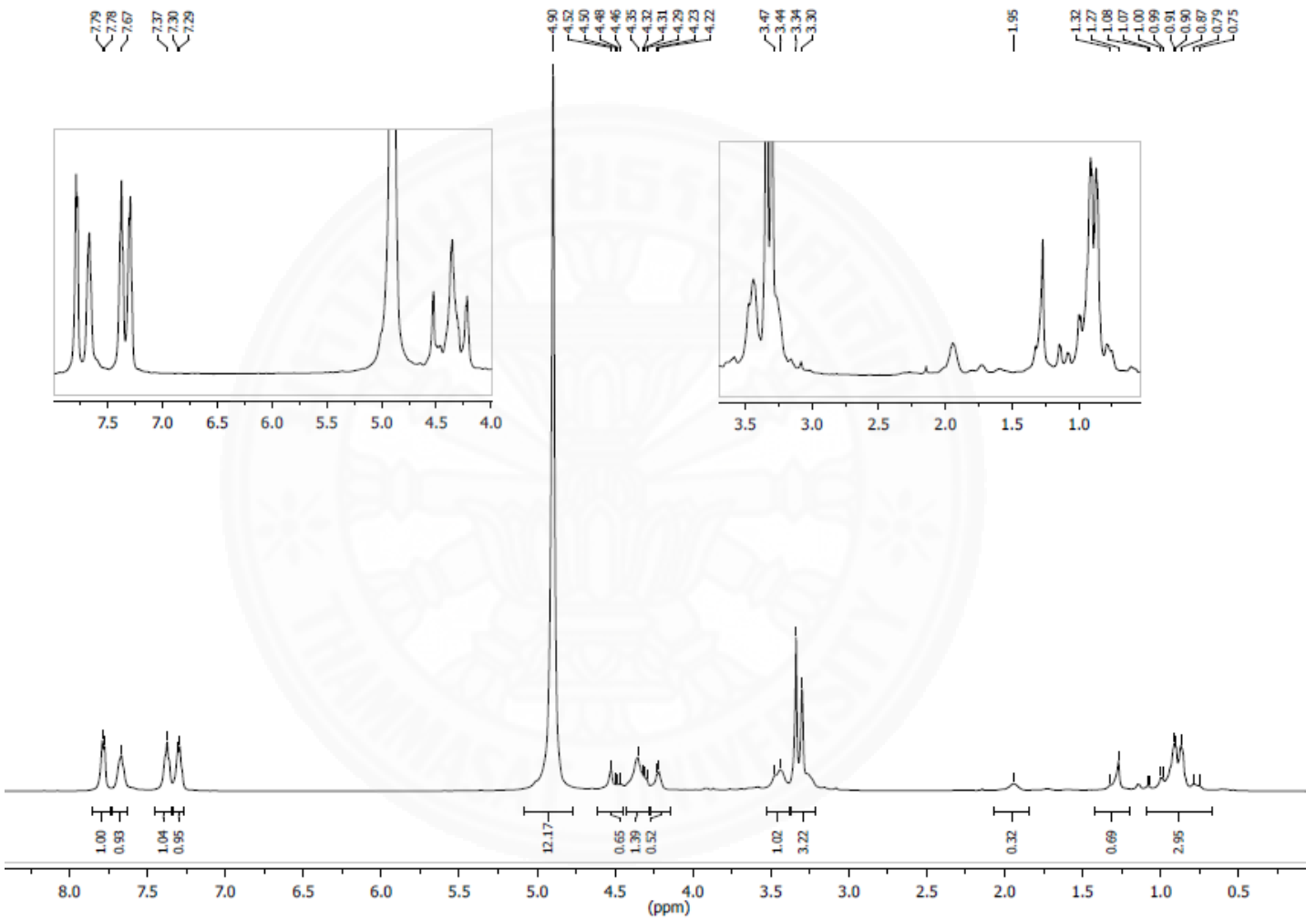

Figure B.6 ^{1}H-NMR spectrum (300 MHz, methanol-d_4) of Fmoc-Val-thiazolidine-OH

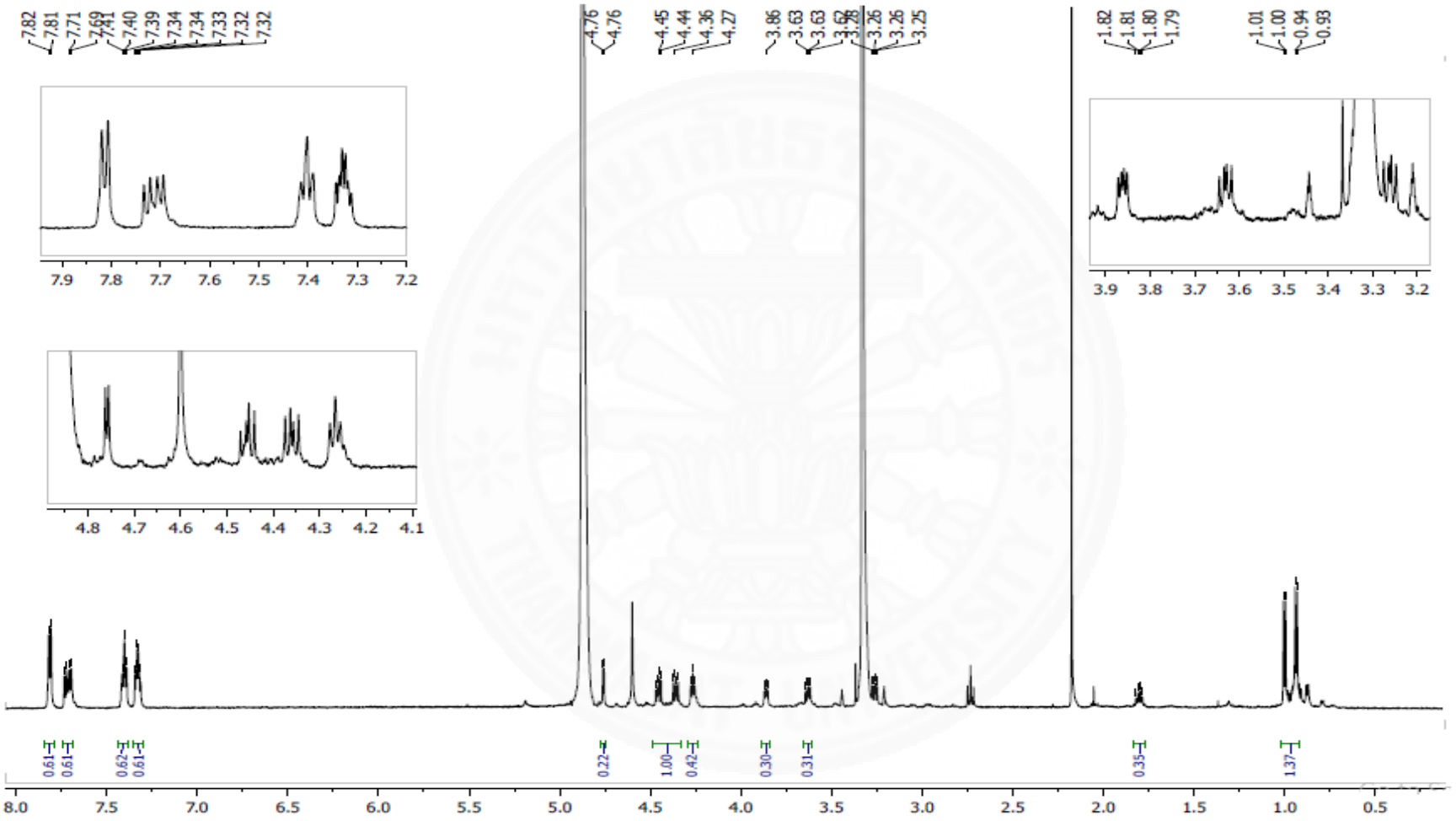

Figure B.7 ^{1}H-NMR spectrum (600 MHz, methanol-d_4) of Fmoc-Val-thiazolidine-OH

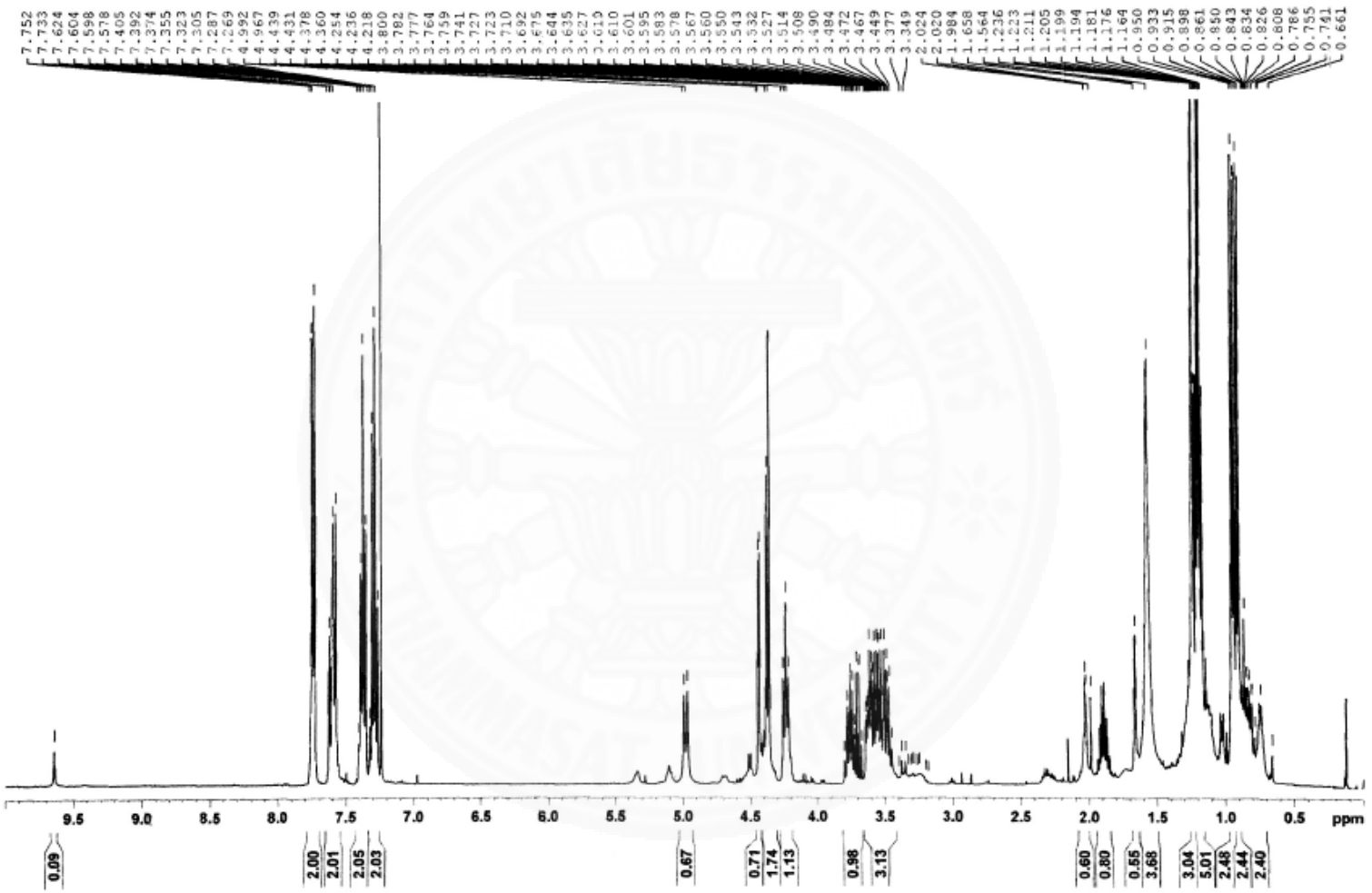

Figure B.8 ^{1}H-NMR spectrum (600 MHz, $CDCl_3$) of Fmoc-Val-Acetal

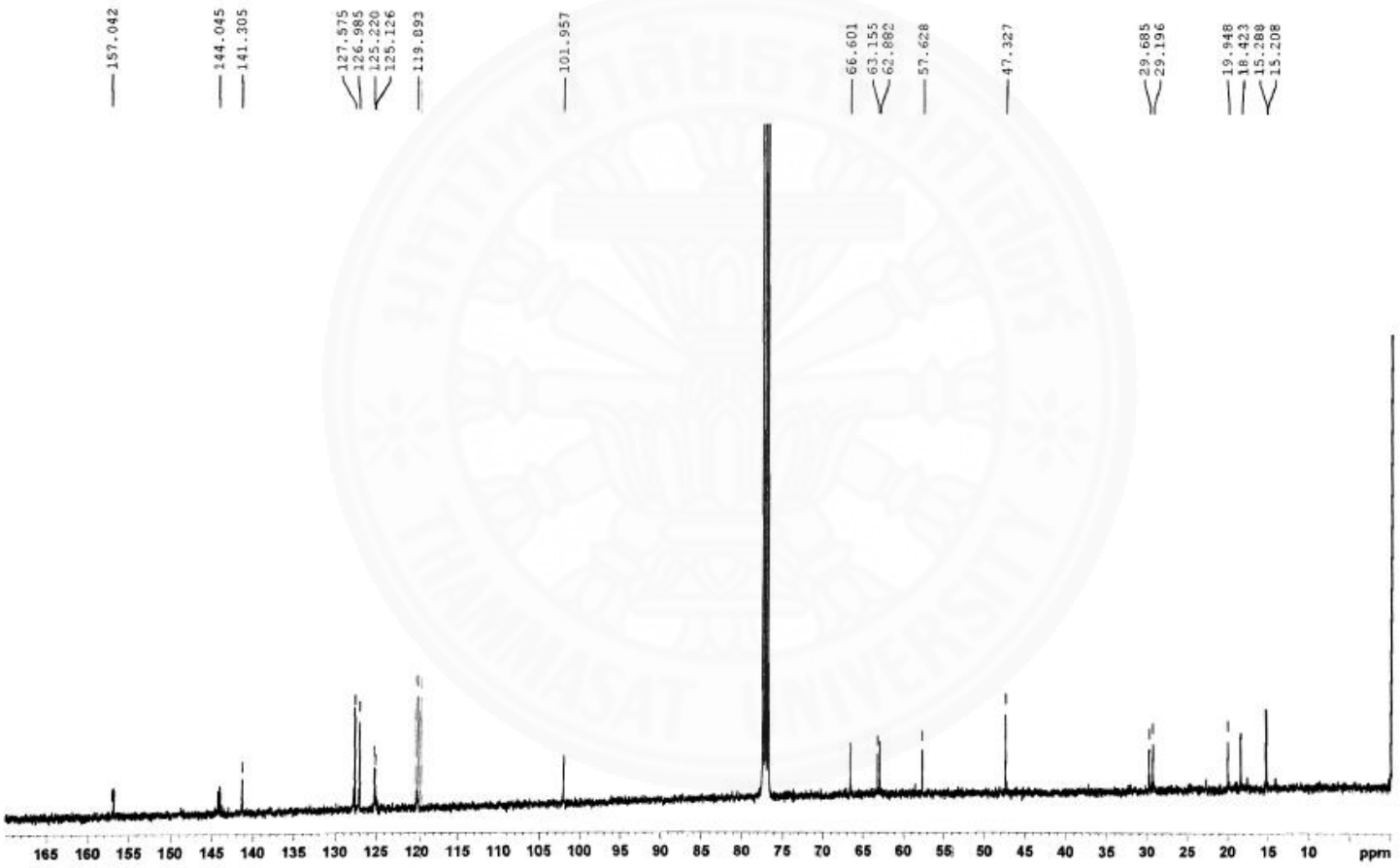

Figure B.9 ^{13}C-NMR spectrum (150 MHz, $CDCl_3$) of Fmoc-Val-Acetal

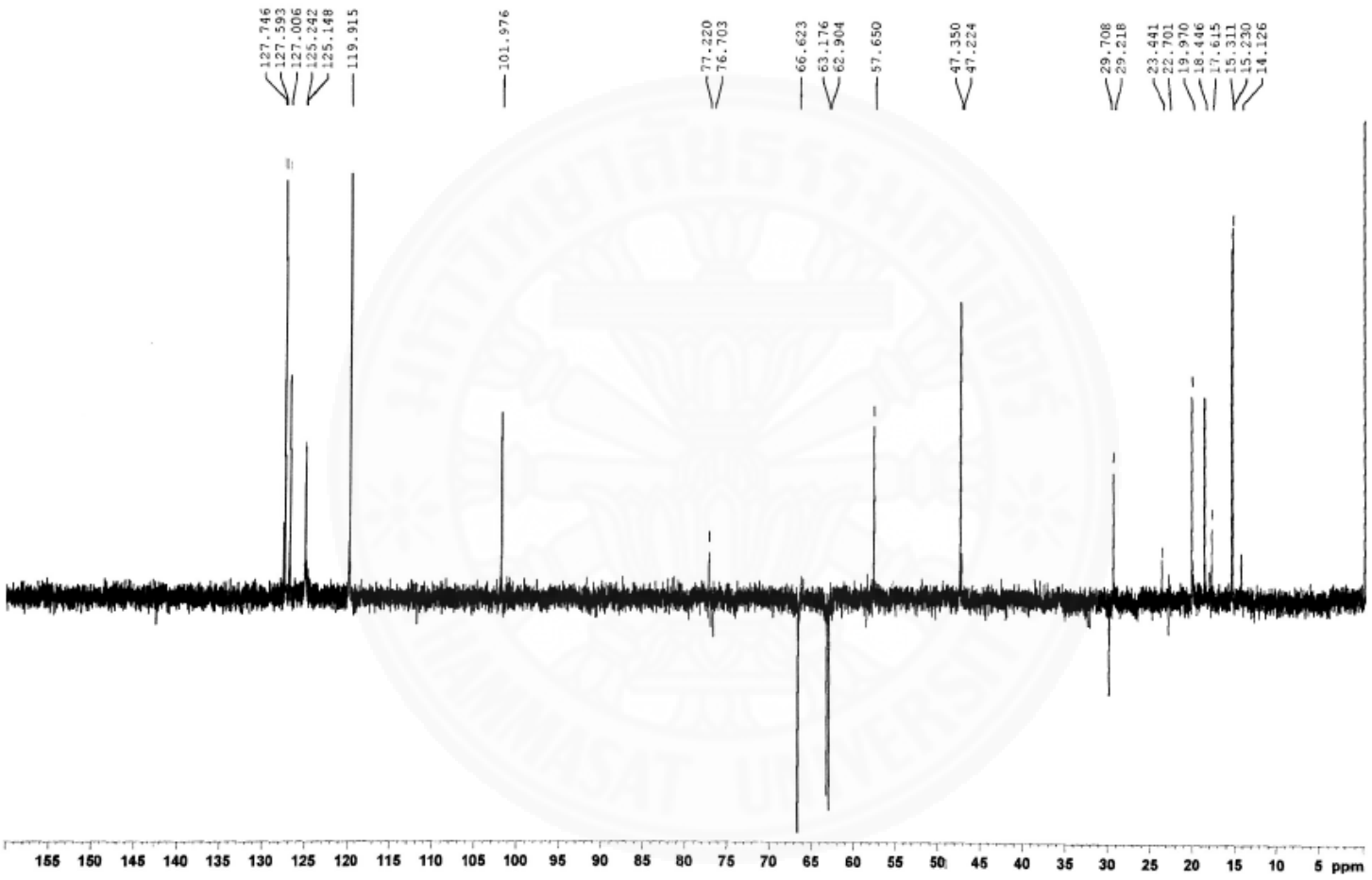

Figure B.10 DEPT 135 spectrum (600 MHz, $CDCl_3$) of Fmoc-Val-Acetal

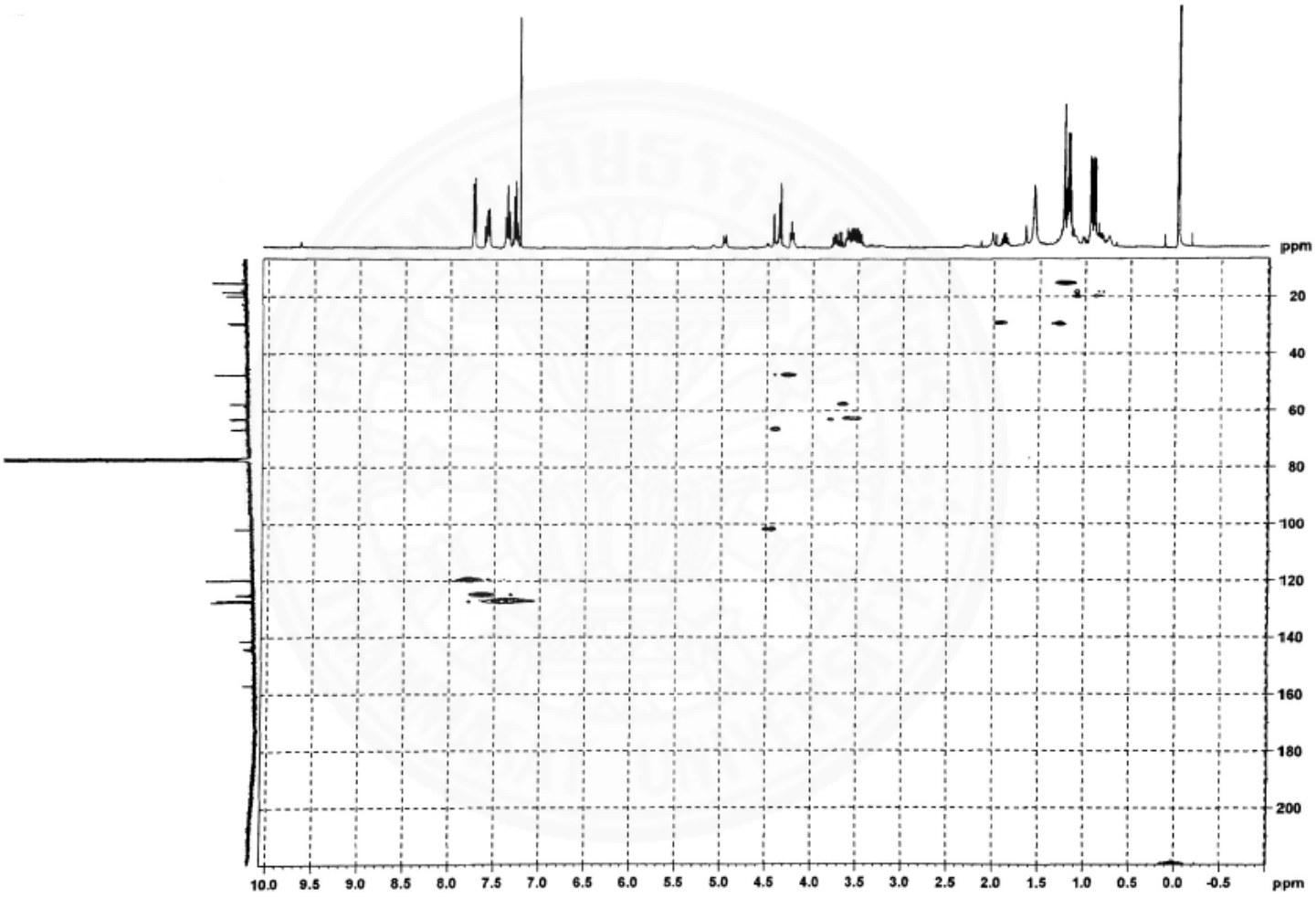

Figure B.11 HSQC spectrum (600 MHz, $CDCl_3$) of Fmoc-Val-Acetal

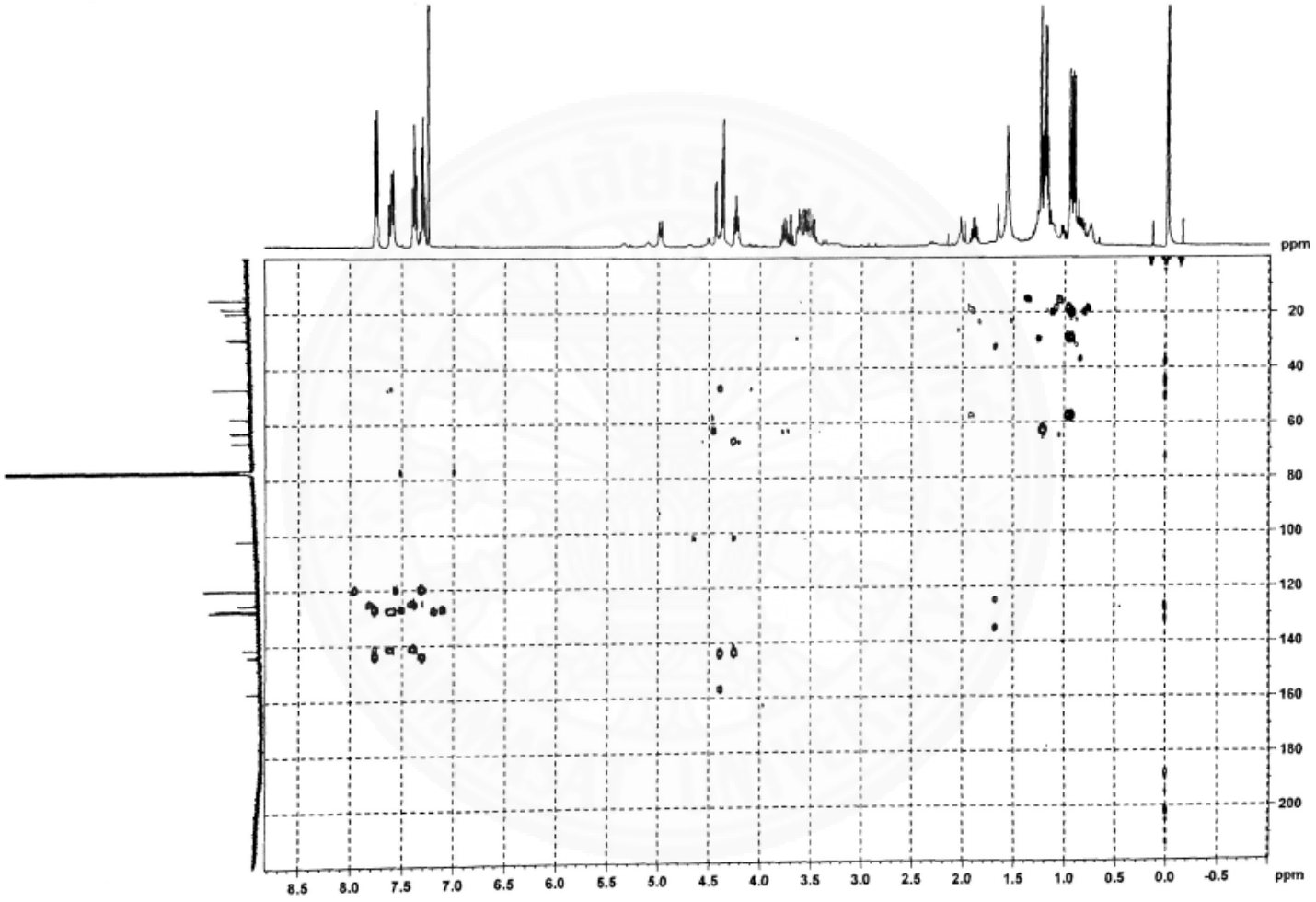

Figure B.12 HMBC spectrum (600 MHz, $CDCl_3$) of Fmoc-Val-Acetal

APPENDIX C

Mass spectrum

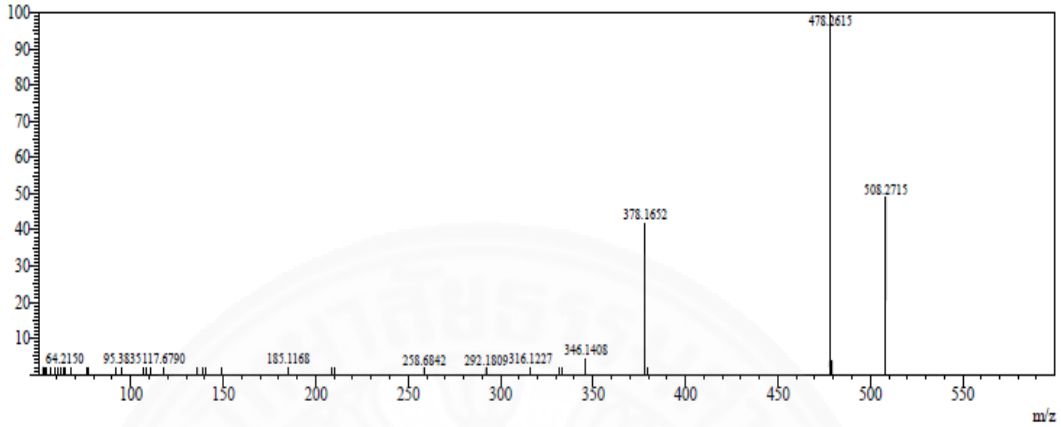

Figure C.1 Positive mode mass spectrum of Fmoc-Val-H (Found; 346.1408$[M+Na]^+$ and 378.1652$[M+CH_3OH+Na]^+$; Calculated 323.3864 $[M]^+$)

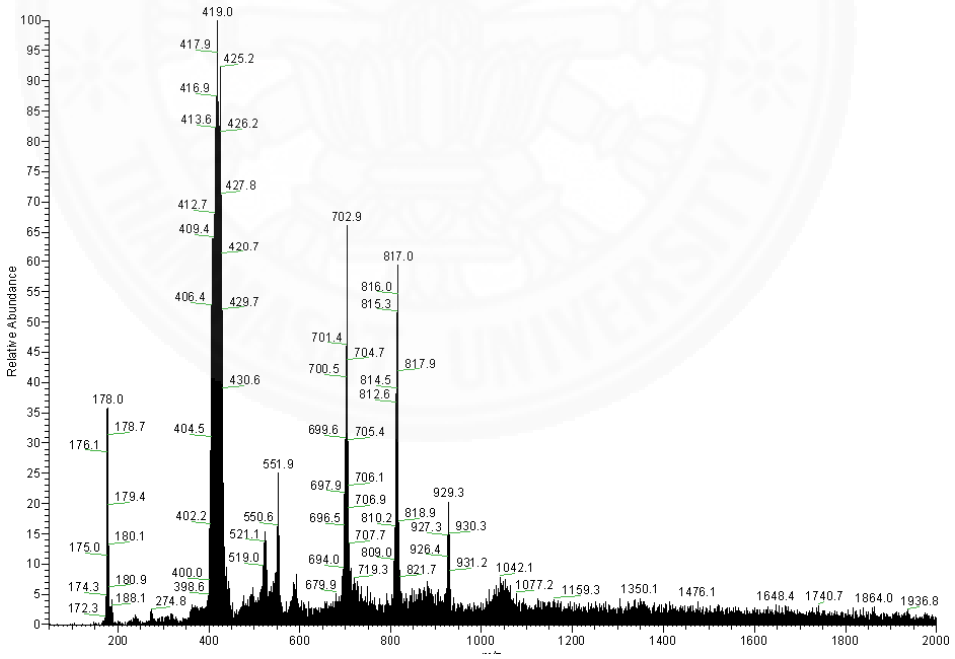

Figure C.2 Positive mode mass spectrum of Fmoc-Val-thiazolidine-OH (Found; 427.8$[M+H]^+$; Calculated 426.5305 $[M]^+$)

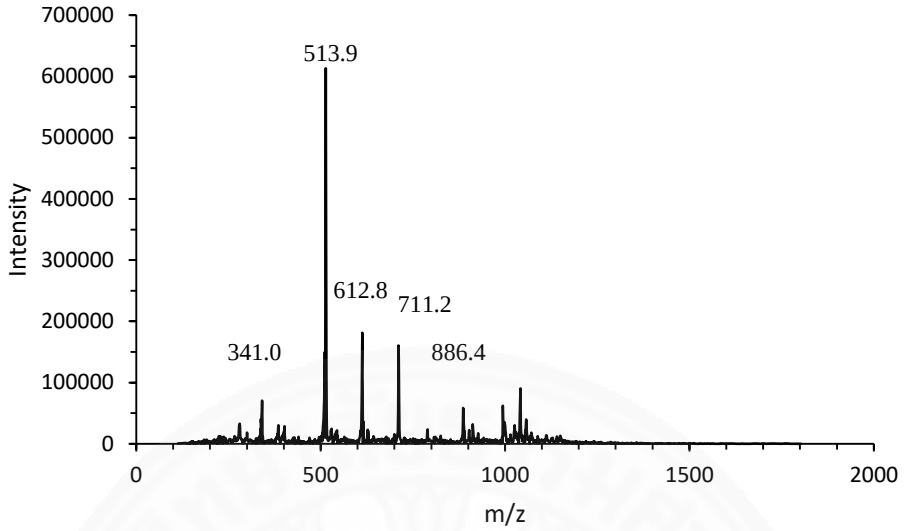

Figure C.3 Negative mode mass spectrum of NH_2-(D)Val-Val-Thiazolidine-(D)Val-Trp-(D)Leu-Val-OH (**13**) (Found; 886.4 $[M+2MeOH+Na-2H]^+$, 513.9 $[M+2TFA-2H]^+$ and 341.0 $[M+2TFA-3H]^+$; Calculated 801.0535 $[M]^+$

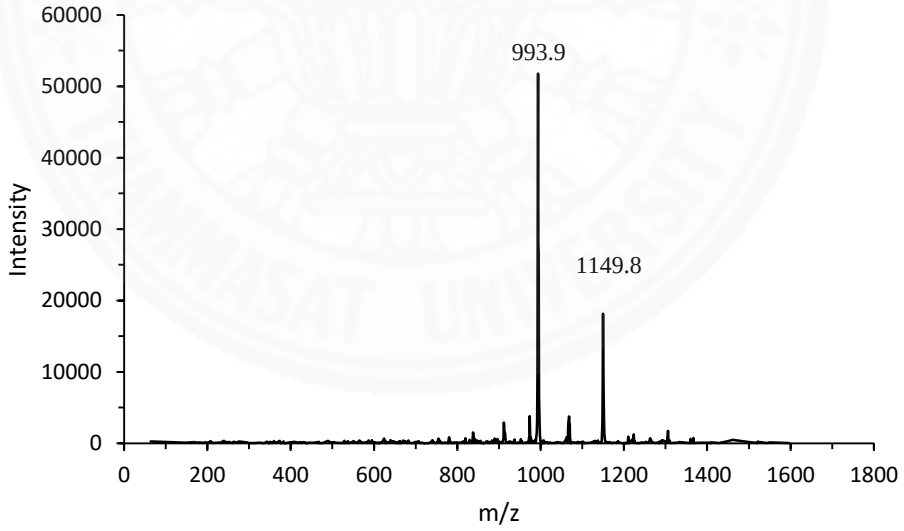

Figure C.4 Negative mode mass spectrum of synthetic native lugdunin (**15**) (Found; 993.9 $[M+TFA+2MeOH+Cl]^+$ or $[M+TFA+ACN+H_2O+K-2H]^+$ Calculated 783.0382 $[M]^+$)

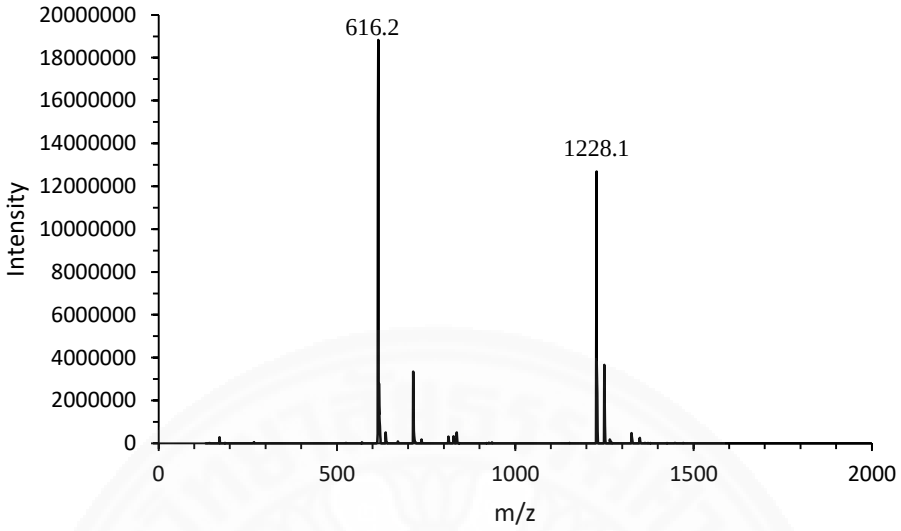

Figure C.5 Positive mode mass spectrum of synthetic NH_2-(D)Val-(D)Val-Trp-(D)Leu-Val-OH (**12**) (Found; 616.2 $[M+H]^+$; Calculated 614.7774 $[M]^+$)

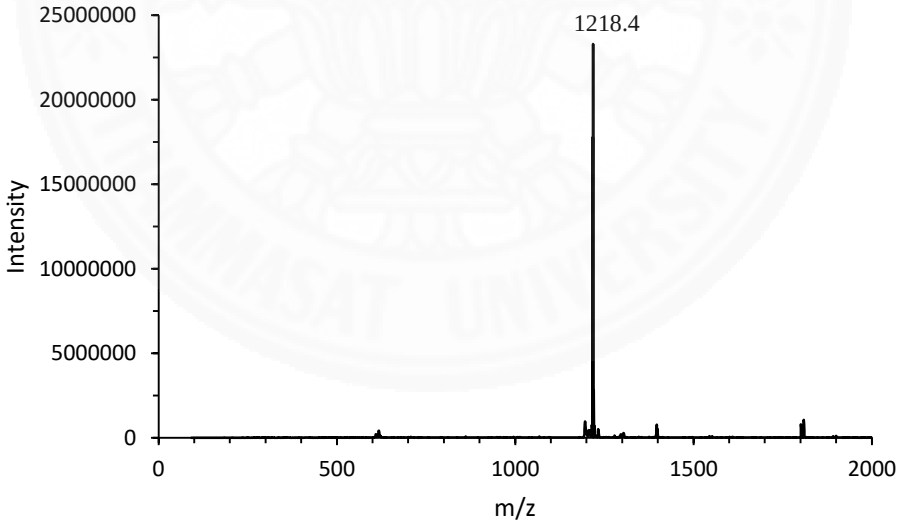

Figure C.6 Positive mode mass spectrum of deprotected cyclo-dimerized(D)Val-(D)Val-Trp-(D)Leu-Val (**18**) (Found; 1218.4 $[M+Na]^+$; Calculated 1193.5243 $[M]^+$)

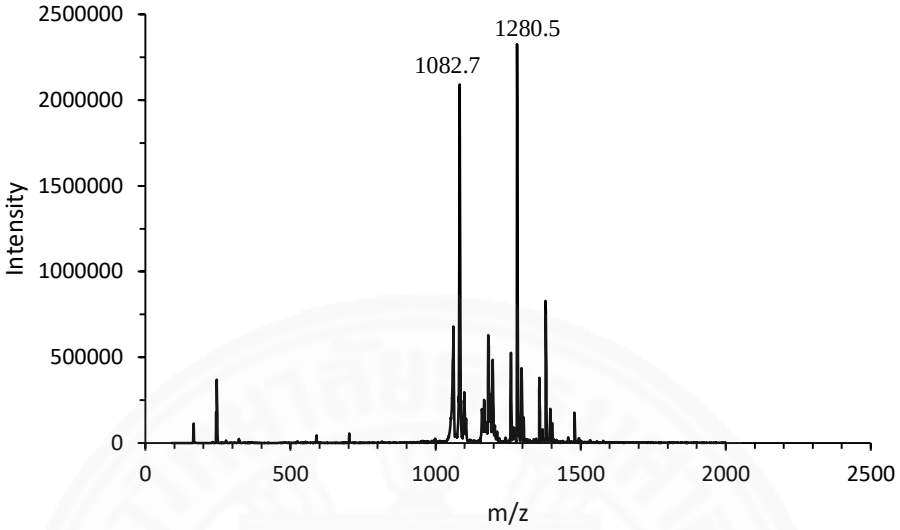

Figure C.7 Positive mode mass spectrum of mutant linear lugdunin (cysteine) (**21**) (Found; 1082.7 $[M+2TFA+K]^+$ and 1280 $[M+3TFA+2ACN+K]^+$; Calculated 817.0529 $[M]^+$)

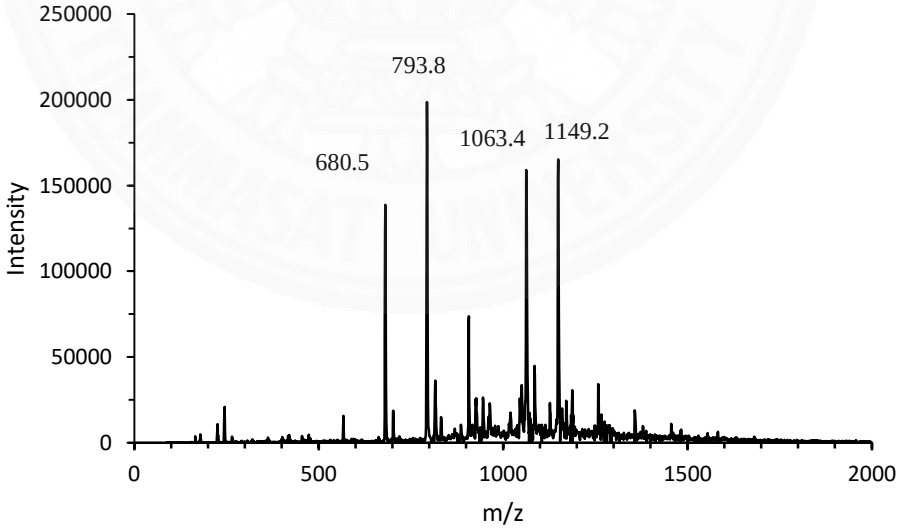

Figure C.8 Positive mode mass spectrum of mutant cyclic lugdunin (cysteine) (**23**) (Found; 1063.4 $[M+2TFA+K]^+$ and 1149.2 $[M+2TFA+2ACN+K]^+$; Calculated 799.0376 $[M]^+$)

APPENDIX D

High performance liquid chromatography chromatogram

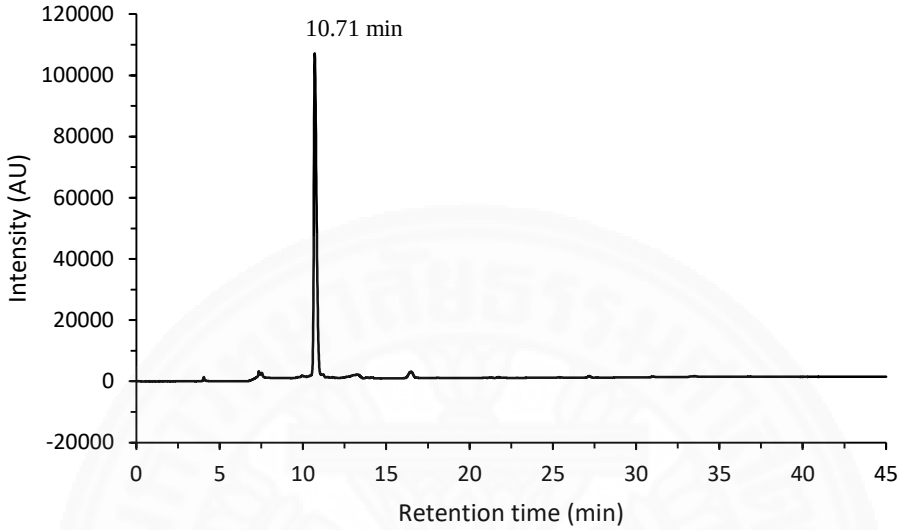

Figure D.1 HPLC chromatogram of NH_2-(D)Val-Val-Thiazolidine-(D)Val-Trp-(D)Leu-Val-OH (**13**)

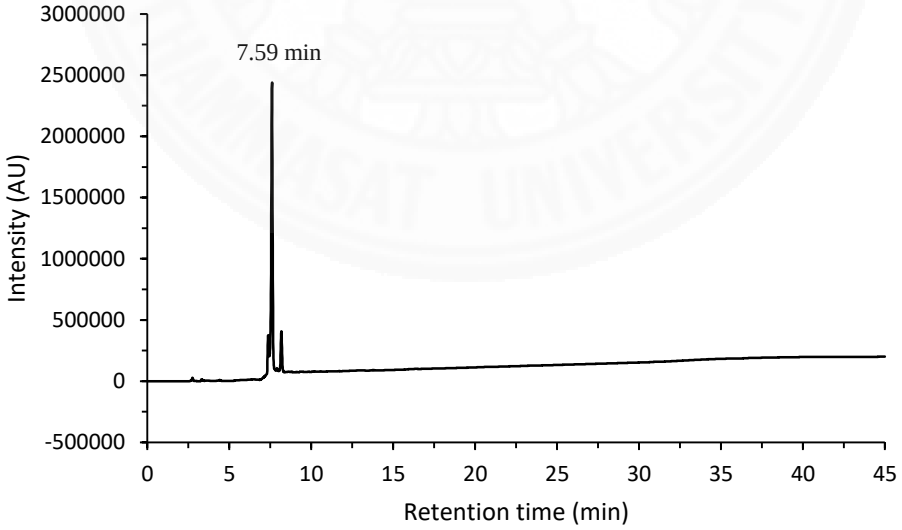

Figure D.2 HPLC chromatogram of synthetic native lugdunin (**15**)

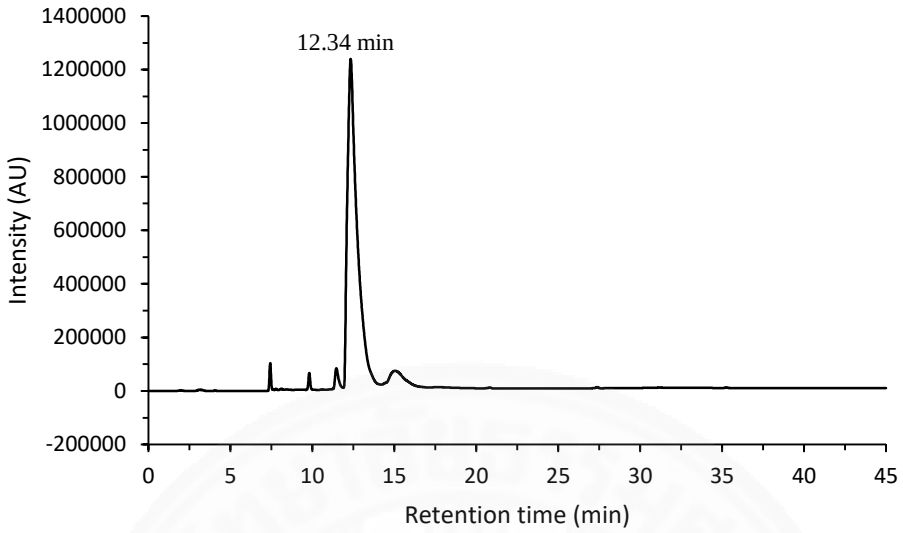

Figure D.3 HPLC chromatogram of NH_2-(D)Val-(D)Val-Trp-(D)Leu-Val-OH (**12**)

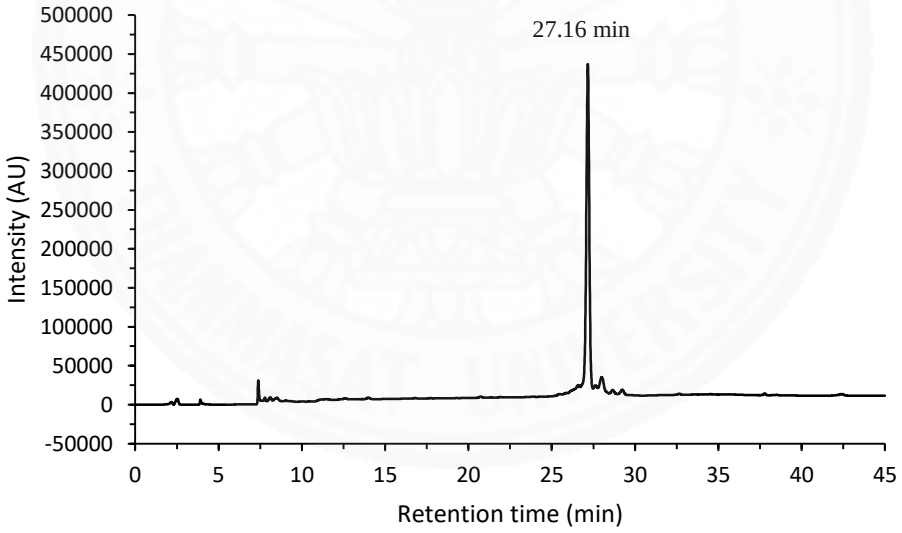

Figure D.4 HPLC chromatogram of deprotected cyclo-dimerized(D)Val-(D)Val-Trp-(D)Leu-Val (**18**)

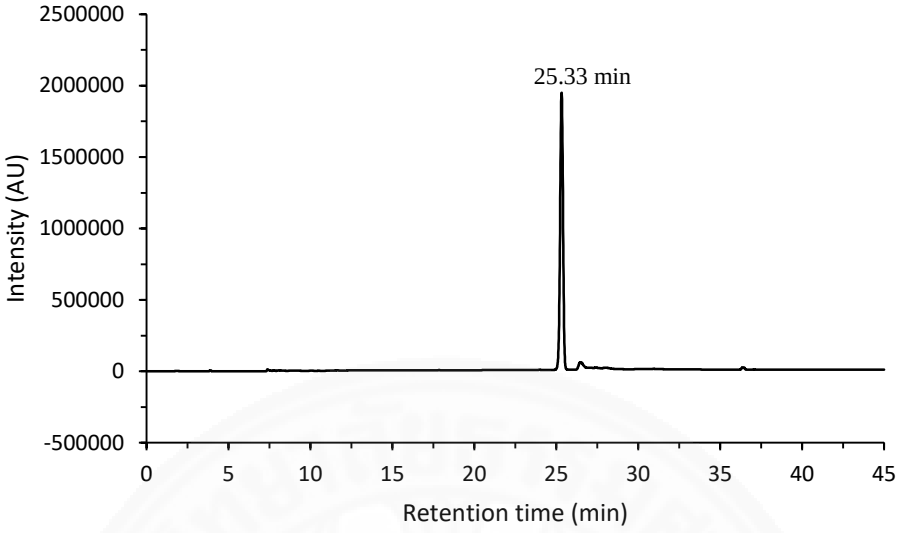

Figure D.5 HPLC chromatogram of mutant linear lugdunin (cysteine) (**21**)

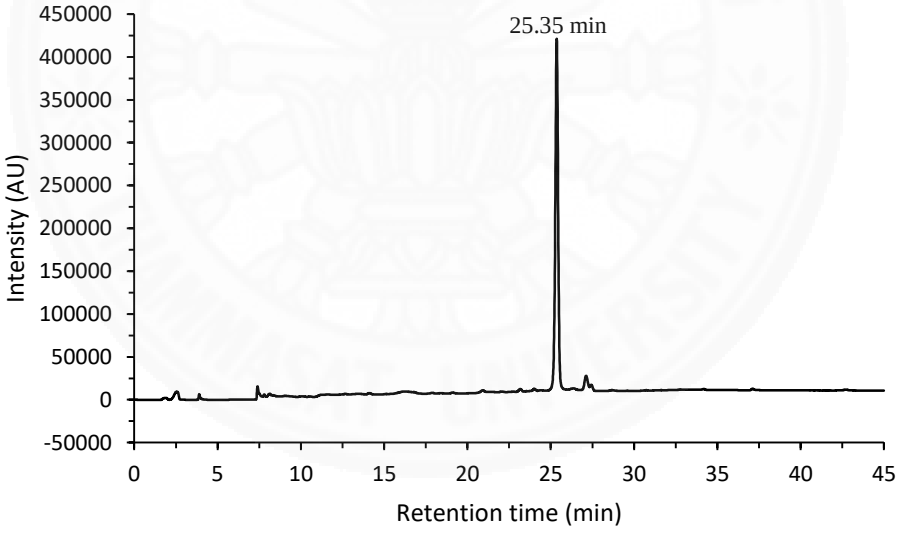

Figure D.6 HPLC chromatogram of mutant cyclic lugdunin (cysteine) (**23**)

APPENDIX E

Infrared spectrum

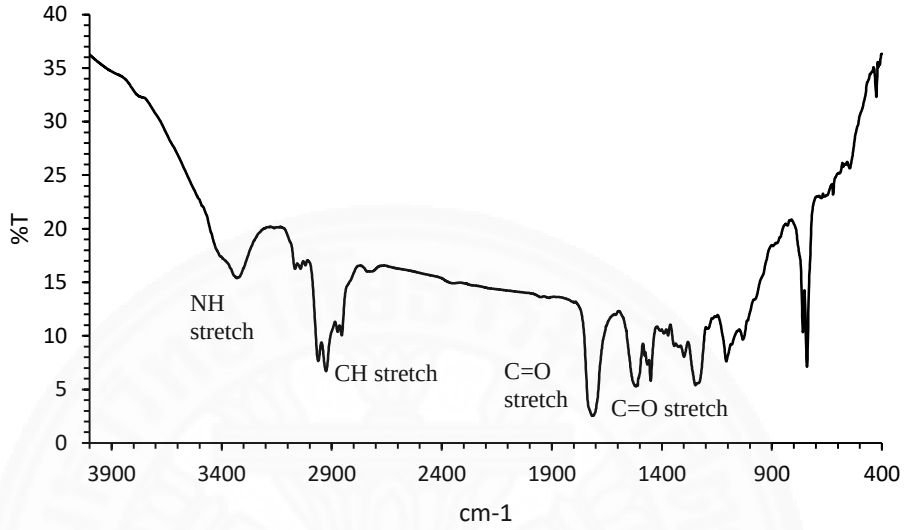

Figure E.1 IR spectrum of Fmoc-Val-H (**2**)

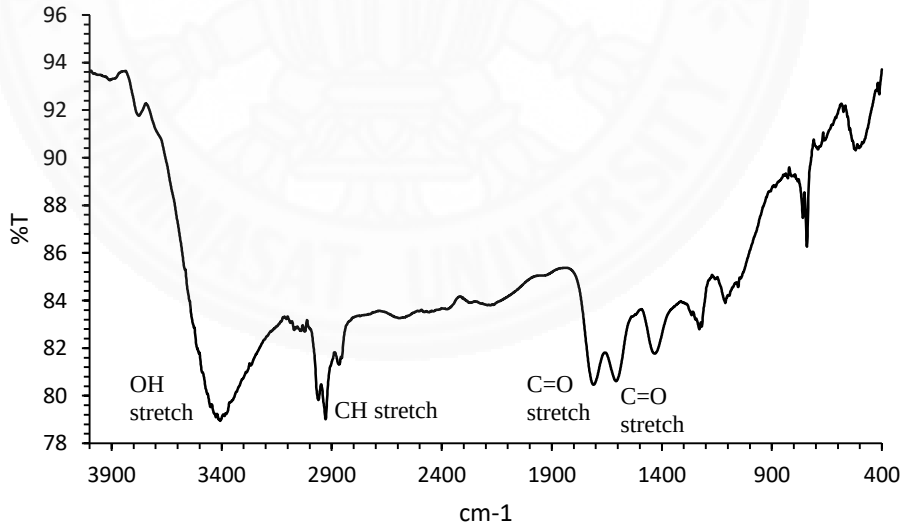

Figure E.2 IR spectrum of Fmoc-Val-thiazolidine-OH

BIOGRAPHY

Name	Mr. Pakonsiri Sontisiri
Date of Birth	August 5, 1993
Educational Attainment	2015: B.Sc. (Chemistry) Department of Chemistry, Faculty of Science and Technology, Thammasat University
Scholarship	2018: National Research Council of Thailand "FY2018 Thesis Grant for master degree student"

Publications

- Pakonsiri Sontisiri, Dumrongkiet Arthan, and Panumart Thongyoo. The total synthesis of lugdunin. Proceeding The 13th International Symposium of the Protein Society of Thailand. 2018:178-185.

Work Experiences	2016-2019: Teaching assistant at Department of Chemistry, Faculty of Science and technology, Thammasat University